



University  
of Exeter

## Cyber-Natural Control Systems

Submitted by

Mohammed Alsubhi

to the University of Exeter as a thesis for the degree of Doctor of Philosophy in Mathematics.

March 2023.

This thesis is available for Library use on the understanding that it is copyright material and that no quotation from the thesis may be published without proper acknowledgement.

I certify that all material in this thesis which is not my own work has been identified and that any material that has previously been submitted and approved for the award of a degree by this or any other University has been acknowledged.

Signature: ..... Mohammed Alsubhi.....

## Abstract

The thesis explores complex dynamics at the interface of natural systems and control systems. It is divided into three main parts. The first part considers adaptive stabilisation and destabilisation for continuous-time systems. Here a Byrnes-Willems high-gain adaptive controller is revisited for classes of positive systems that arise in a context of population dynamics. We show that the convergent adaptive, positive high-gain, Byrnes-Willems controller results in convergence of the gain to a stabilising gain — so that the adaptive controller learns to stabilise. We then develop a convergent, adaptive destabilising controller for the same class of systems but with adaptive negative high gain. In this case, the resulting convergent gain is destabilising — so that the adaptive controller learns to destabilise. We then show that when the two adaptation algorithms are combined, then the resulting convergent gain is the critical gain — so that a bifurcation between stable and unstable behaviour is learnt. In the second part, we develop similar results for discrete-time systems that arise in a context of population protection matrix models. We construct adaptive stabilising and destabilising controllers which converge to stabilising and destabilising controllers, respectively. When the stabilising and destabilising adaptation algorithms are combined, we find more complicated outcomes than in the continuous-time case — a so called arms race ensues. Sometimes the arms race converges, and a concord is reached. But other times, the arms race is divergent. These results are explored in a number of simulations for 1, 2 and 3-dimensional systems. In the third part we consider the competitive exclusion principle for two populations in competition. For certain ranges of the species interaction parameters and their respective carrying capacities competitive exclusion occurs — either one or the other species persists and the other dies out. We show that if the carrying capacities are not constant, but instead adapt to the prevailing population abundances — with relatively more of one species causing its own carry capacity to decrease (degrade) and the others to increase (re-

new) — then competitive co-existence is reached. All the results are illustrated with numerous examples throughout.

## **Dedication**

*This work is dedicated to the soul of my father may Allah Almighty bless him.*

# Acknowledgement

First of all, I would like to thank Allah for His mercy, blessings, and granting me the ability to accomplish this research. Moreover, I am deeply grateful for the situations that have strengthened my faith 'Iman' and allowed me to successfully complete this work.

I would like to express my gratitude to Prof. Stuart Townley, my supervisor, for his outstanding mentorship during my PhD program. He has consistently provided me with insightful feedback and guidance whenever required, for which I am truly grateful. My research would not have been possible without the guidance and support of my supervisor. It was a privilege to work with him, and I hold his attitude and approach to mentorship in high regard.

I would like to express my heartfelt gratitude to my mother, brothers, and sisters for their exceptional support and encouragement. Their unwavering support and encouragement have been instrumental in helping me achieve my goals. I am so thankful to my friends Ibrahim and Faisal for their support during my studies. Lastly, I would like to acknowledge and thank the Royal Embassy of Saudi Arabia Cultural Bureau and Taibah University for their invaluable financial assistance during my PhD studies. Their support has enabled me to focus on my research and academic pursuits without financial constraints.

# Contents

<b>Acknowledgements</b>	<b>iv</b>
<b>1 Introduction</b>	<b>1</b>
1.1 Complex dynamics – towards a framework for cyber natural systems . . . . .	2
1.2 Main contributions of the thesis . . . . .	3
1.3 Publications . . . . .	6
<b>2 Population Dynamics</b>	<b>7</b>
2.1 Interacting populations – predator-prey dynamics, competition and mutualism .	8
2.2 Predator prey systems and evolution . . . . .	19
2.3 Structured population models . . . . .	23
2.4 Conclusion . . . . .	27
<b>3 Adaptive Control</b>	<b>29</b>
3.1 Adaptive control . . . . .	29
3.2 Indirect vs. Direct Adaptive Control – An example . . . . .	30
3.3 Byrnes-Willems direct adaptive control . . . . .	33
3.4 Adaptive control and pest management . . . . .	35

3.5	Adaptive destabilization and persistence . . . . .	37
3.6	Do adaptive controllers learn to stabilise? . . . . .	39
3.7	Conclusion . . . . .	41
<b>4</b>	<b>A Bifurcation Learning Algorithm</b>	<b>42</b>
4.1	Byrnes-Willems adaptive control with a stabilising limit gain . . . . .	43
4.2	Byrnes-Willems style adaptive destabilisation with a destabilising limit gain . . . . .	47
4.3	Byrnes-Willems style bifurcation–learning adaptive algorithm . . . . .	51
4.4	Bifurcation learning – simulation examples . . . . .	59
4.5	Set point control with a proportional controller . . . . .	66
4.6	Conclusion . . . . .	71
<b>5</b>	<b>Adaptive Stabilisation and Destabilisation and an Adaptive "Arms Race"</b>	<b>72</b>
5.1	Adaptive stabilisation of discrete-time populations . . . . .	74
5.2	Adaptive Destabilisation of Discrete-time Populations . . . . .	80
5.3	An adaptive arms race . . . . .	85
5.4	Conclusion . . . . .	107
<b>6</b>	<b>Adaptive Control Inspired Habitat Renewal</b>	<b>109</b>
6.1	Habitat renewal and interspecific competition model . . . . .	111
6.2	A habitat-population feedback mechanism for habitat renewal . . . . .	113
6.3	Habitat-population feedback and competitive co-existence . . . . .	114
6.4	Examples . . . . .	117
6.5	Conclusion . . . . .	127
<b>7</b>	<b>Conclusion</b>	<b>128</b>

<b>A Preliminaries</b>	<b>129</b>
A.1 Continuous vs. discrete time systems . . . . .	129
A.2 Pest Management . . . . .	131
A.2.1 What is a pest? . . . . .	131
A.2.2 What is a pesticide? . . . . .	131
A.3 Linearisation . . . . .	132
A.4 High dimensional simulation For Bifurcation algorithms . . . . .	136
 <b>Bibliography</b>	 <b>139</b>

# List of Figures

1.1	A schematic idea of cyber-natural systems. . . . .	3
2.1	The evolution of (2.1) on two different scenarios . . . . .	10
2.2	Simulation of system (2.1)min case (iv). Left plot. Density of predator and prey against time; Right plot. Predator-prey cycle in phase space. . . . .	10
2.3	The zero isoclines that are produced by the competitive exclusion equation (2.2). The left diagram (2.3a) indicates the zero isocline for $N_1$ ; the right diagram (2.3b) explains the zero isocline for $N_2$ . . . . .	13
2.4	The four potential findings of the Interspecific Competition model (2.2). . . . .	15
2.5	Phase plane for the Mutual system (2.9). . . . .	18
2.6	Experiment 1 : Simulating Schreiber et al's Model (2.10); The initial conditions are $N_1 = 120, N_2 = 80, P = 30$ and $X = -0.04$ and the parameters are $\sigma = 0.01$ and $h = 0.25$ . . . . .	21
2.7	Experiment 2 :Simulating Schreiber et al's model (2.10) with (2.11); The initial conditions are $N_1 = 120, N_2 = 80, P = 30$ and $X = -0.02$ , and the parameters are $\sigma = 0.01$ and $h = 0.25$ . . . . .	21
2.8	Experiment 3 : Simulating Schreiber et al's model (2.10) with (2.11); The initial conditions are $N_1 = 5, N_2 = 120, P = 20$ and $X = 0.2$ , and the parameters are $\sigma = 0.01$ and $h = 0.02$ . . . . .	22

2.9	Experiment 4 : Simulating Schreiber et al's model (2.10) with (2.11).; The initial conditions are $N_1 = 0.00009$ , $N_2 = 120.1$ , $P = 2.9$ and $X = 0.1900009$ , and the parameters are $\sigma = 0.04$ and $h = 0.025$ . . . . .	22
2.10	The cycle of life of 3 stages population. . . . .	23
2.11	The evolution of the population (2.14). . . . .	26
2.12	The evolution of the population (2.15). . . . .	27
4.1	3-dimensional simulation with $A$ matrix given by $M_3$ in (4.16) for the three adaptive controllers: $A$ and $B$ for controller (4.3); $C$ and $D$ for controller 4.6; $E$ and $F$ for controller (4.12). . . . .	61
4.2	4-dimensional simulation with $A$ matrix given by $M_4$ in (4.16) for the three adaptive controllers: $A$ and $B$ for controller (4.3); $C$ and $D$ for controller 4.6; $E$ and $F$ for controller (4.12). . . . .	62
4.3	6-dimensional simulation with $A$ matrix given by $M_6$ in (4.16) for the three adaptive controllers: $A$ and $B$ for controller (4.3); $C$ and $D$ for controller 4.6; $E$ and $F$ for controller (4.12). . . . .	63
4.4	8-dimensional simulation with $A$ matrix given by $M_8$ in (4.16) for the three adaptive controllers: $A$ and $B$ for controller (4.3); $C$ and $D$ for controller 4.6; $E$ and $F$ for controller (4.12). . . . .	64
4.5	Top left and right: Simulations of output and gain for the bifurcation learning algorithm (4.19); Bottom left and right: Simulations for the adaptive integral control algorithm (4.18). . . . .	70
5.1	Adaptive Stabilisation (5.2) for system (5.3). Left plot: Convergent gain $v(t)$ . Right plot: Stage structures $x(t)$ converging to zero. . . . .	78

5.2	Adaptive Stabilisation (5.2) for system (5.4). Left plot: Convergent gain $v(t)$ . Right plot: Stage structures $x(t)$ converging to zero. . . . .	79
5.3	Adaptive Destabilisation (population persistence) (5.16). Left plot. Convergent gain $r(t)$ . Right plot. Divergent (persistent) stage structures $x(t)$ . . . . .	83
5.4	Adaptive Destabilisation (population persistence) (5.16). Left plot. Convergent gain $r(t)$ . Right plot. Divergent (persistent) stage structures $x(t)$ . . . . .	84
5.5	Arms race simulation: Left plot – population abundance; Right plot - volume $v(t)$ and resistance $r(t)$ . . . . .	87
5.6	Arms race simulation: $e(t) = v(t) - r(t)$ . . . . .	88
5.7	Arms race simulation: Left plot – population abundance; Right plot - volume $v(t)$ and resistance $r(t)$ . . . . .	89
5.8	Arms race simulation (5.10): $e(t) = v(t) - r(t)$ . . . . .	90
5.9	Arms race simulation, case 1 + 1 : Left plot – population abundance; Right plot - volume $v(t)$ and resistance $r(t)$ . . . . .	93
5.10	Phase plane of (5.14). The black arrows indicate the trajectories direction. . . . .	94
5.11	Arms race simulation for system (5.16) in 2 dimensions . . . . .	95
5.12	Arms race simulation (5.16): $e(t) = v(t) - r(t)$ . . . . .	96
5.13	Arms race simulation for system (5.16) in 2 dimensions. . . . .	97
5.14	Arms race simulation (5.16): $e(t) = v(t) - r(t)$ . . . . .	98
5.15	Some Simulations for the above calculation while Convergence "green" as well when is Divergence "blue" with a size step =0.001. . . . .	106
6.1	Competitive exclusion when $K_2 > \frac{K_1}{b_{12}}$ and $K_1 > \frac{K_2}{b_{21}}$ in (6.1). . . . .	112
6.2	A cartoon explaining the sensitivity process; with respect to the timing $t_S$ , of which population is excluded. . . . .	116

6.3	Simulation results for habitat renewal (6.4) using the parameters 6.1. . . . .	120
6.4	Simulation results for habitat renewal (6.4) using the parameters 6.2. . . . .	122
6.5	Simulation results for habitat renewal (6.4) using the parameters 6.3. . . . .	125
A.1	The difference among the ODE of the logistic growth model. . . . .	130
A.2	individuals resistance Pesticide Credit <a href="https://upload.wikimedia.org/wikipedia/commons/8/85/Pesticide_resistance.svg">https://upload.wikimedia.org/wikipedia/commons/8/85/Pesticide_resistance.svg</a> . . . . .	132
A.3	An explanation about the phase plane analysis within the linearisation shows above. . . . .	135
A.4	9 -dimensional simulation for the adaptive controllers 4.4, A and B, 4.8, C and D,4.13, E and F. A matrix given by $M_9$ in (4.16). . . . .	138
A.5	13 -dimensional simulation for the adaptive controllers 4.4, A and B, 4.8, C and D,4.13, E and F. A matrix given by $M_{13}$ in (4.16). . . . .	138
A.6	15 -dimensional simulation for the adaptive controllers 4.4, A and B, 4.8, C and D,4.13, E and F. A matrix given by $M_{15}$ in (A.5). . . . .	139

# List of Tables

2.1	Definitions of variables and parameters for the Schreiber et al. model (2.10) with (2.11). . . . .	20
2.2	Types of structured population models . . . . .	23
4.1	The values of $k_\infty(x_0)$ , $-g_\infty(x_0)$ , $q_\infty(x_0)$ and $k_c$ for Simulation Result 4.17. . . . .	64
5.1	The Parameter values for Example (a). . . . .	87
5.2	The Parameter values for Example (b). . . . .	88
5.3	The Parameter values for Example (a). . . . .	95
5.4	The Parameter values for Example (a). . . . .	96
6.1	The Parameter values for Example 1. . . . .	117
6.2	The Parameter values for Example 2. . . . .	121
6.3	The Parameter values for Example 3. . . . .	123
A.1	The values of $k_\infty(x_0)$ , $-g_\infty(x_0)$ , $q_\infty(x_0)$ and $k_c$ . Resulting of 4.17. . . . .	139

# Chapter 1

## Introduction

The thesis is rooted in two parallel developments. First it builds on adaptive control theory and its recent application in a context of pest management [1]. Second, it draws inspiration from the natural systems that have the capacity to evolve [2]. This leads naturally on to interactions between feedback control (cyber) and populations (natural) and an overarching aim towards developing a theory for cyber-natural systems. This cyber-natural idea is explored in two separate studies. The first considers an arms race that emerges when an adaptive feedback control is applied in a context of pest management wherein the pest may evolve resistance. In the second, we consider how, in a competitive interaction, the species may degrade or enhance their habitat. One highlight of the thesis was discovered somewhat accidentally – within this cyber-natural systems thinking we found (or constructed) an arms-race like adaptive controller which learns a bifurcation. This bifurcation learning controller, in turn, leads to a powerful new way of solving the classical and well-known set-point control problem. Within this cyber-natural thinking, we also develop a simple model of a mechanism for habitat renewal which forces a system in to co-existence when otherwise competitive exclusion would prevail.

## **1.1 Complex dynamics – towards a framework for cyber natural systems**

My PhD project is open-ended and ideas driven. It aims to explore complex dynamics at the interface of natural systems and control systems. In control systems, one way to handle uncertainty in the to-be-controlled system is to use adaptive control. Here parameters adapt continuously, or in a switched manner, in response to how the controller is performing. The paper 'Robust model reference adaptive control' [3] explains some of the ideas behind adaptive control. Natural systems are inherently adaptive and evolve in response to selection pressures. The ideas behind adaptive/evolving natural systems is explored in numerous papers and is at the heart of evolution theory. In a specific context of predator-prey dynamics, these ideas are in [4, 5]. Comparing natural and man-made systems we can contrast two modes of adaptation: in control, adaptation is often direct (and designed) whereas in natural systems adaptation is more implicit and undirected. My thesis will explore the resulting complex dynamics when these two adaptive mechanisms are combined in to what we might call “cyber-natural systems”. Such cyber-natural systems arise, for example, in management of pesticides where amount of pesticide applied may increase and where its efficacy may decrease because of resistance acquired by the pests. Alternatively, in treating bacterial diseases, harmful bacteria may develop resistance to the applied anti-biotics which are used in increasing amounts.

The overall cyber-natural system is a combination of designed and natural interactions in which the system and the controller adapt in response to each other. Importantly, the mechanisms of adaptation are different: the designed adaptations are direct, the natural adaptations are implicit. One may seek to minimise a cost function, the other to maximise population fitness.

Some illustrative examples of cyber-natural systems:

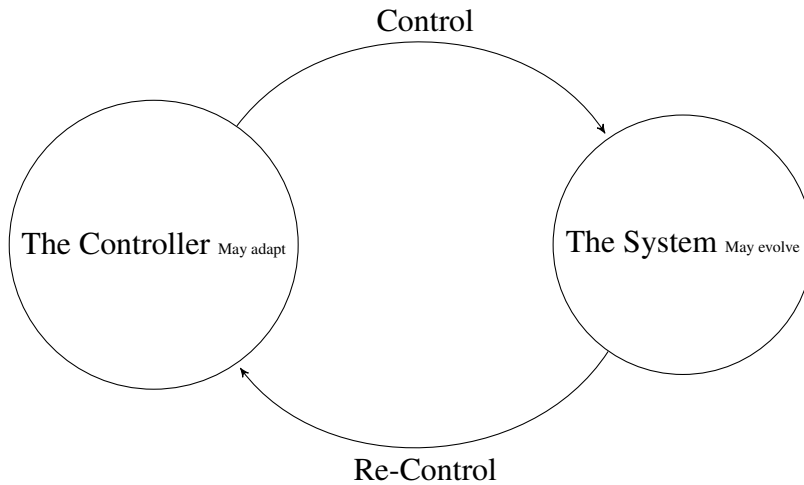


Figure 1.1: A schematic idea of cyber-natural systems.

- Taxation policies and society response (cyber-social systems) [6].
- Controlling disease in a context of anti-biotic resistance [7].
- The predator prey dynamics with phenotypic and genetic variation [2, 4].

## 1.2 Main contributions of the thesis

The main contributions of the thesis are as follows:

### **Main contribution of Chapter 4 – A Bifurcation Learning Algorithm.**

In this chapter we continue a line of research which, for over two decades or more, asks “Does a stabilising adaptive feedback controller learn a stabilising gain?” We restrict attention to classes of adaptive feedback controllers inspired by so-called Byrnes-Willems high-gain adaptive controllers [8]. The main results are:

- For non-negative systems arising in population ecology we can prove that the Byrnes-Willems adaptive high-gain stabilising controller does indeed learn a positive enough sta-

bilising gain – Theorem 4.4. Here positive enough means greater than the critical gain;

- We also consider destabilisation, a.k.a persistency. Borrowing from the Byrnes-Willems approach we design an adaptive destabilising controller. Again, for non-negative systems, we can prove that the adaptive high-gain destabilising controller does indeed learn a negative enough destabilising gain – Theorem 4.8. Here negative enough means less than the critical gain;
- The class of “population-ecology” inspired non-negative systems under consideration admits a simple transition: there is a critical saddle-node bifurcation threshold so that gains above this critical threshold are stabilising, gains below are destabilising. Surprisingly we find, if the positive high-gain and negative high-gain algorithms are combined, then the saddle-node bifurcation is learnt – Theorem 4.13.
- We use the main result in Theorem 4.13 to develop a novel set-point controller. For a target set-point  $r$ , the new adaptive controller achieves asymptotic tracking of  $r$  without knowledge of system parameters. Because the underpinning system has a linearly stable equilibrium there is guaranteed robustness. This contrasts with the usual sensitivity and fragility of adaptive controllers to unmodelled disturbances.

### **Main contribution of Chapter 5 – Adaptive Stabilisation and Destabilisation and an Adaptive "Arms Race".**

The main new results are:

- Theorem 5.3: This result is the discrete-time analogue of Theorem 4.4. It gives an adaptive mechanism that drives the population to zero without knowledge of the system parameters;
- Theorem 5.6: This result is the discrete-time analogue of Theorem 4.8. It gives an adaptive

mechanism that drives the population to exponential growth without knowledge of the system parameters;

- A simulation study of an adaptive algorithm that combines the controllers from Theorems 5.3 and 5.6 in an adaptive arms race. This is the discrete-time analogue of Theorem 4.13. The arms race simulations are developed in the cases of  $n = 1, 2$  and 3 state dimensions. Since the gain adaptation adds a further dimension we refer to these as the  $1 + 1$ ,  $2 + 1$  and  $3 + 1$  arms races models, respectively:
  - In Section 5.3 we show that the  $1 + 1$  dimensional arms race model (5.13) results in an unstable spiral – see Proposition (5.11). This is similar to the result in Chapter 4 – see Remark (4.12).
  - In Section 5.3 we show that the  $2 + 1$  dimensional arms race model (5.16) admits both oscillatory behaviour – 5.11 – and divergent behaviour – 5.13. We prove that convergent behaviour is not possible.
  - In Section 5.3 we show that the  $3 + 1$  dimensional arms race model (5.26) admits both convergent behaviour – 5.5 and divergent behaviour – 5.7. We explore parameter ranges which produce these two behaviour types – see Figure 5.15.

### **Main contribution of Chapter 6 – Adaptive Control Inspired Habitat Renewal.**

Borrowing from adaptive control, we develop a simple model of mechanism for self-regulation by habitat renewal. This self-regulation forces co-existence when otherwise competitive exclusion would prevail. The main results are:

- Simulation Result 6.1: We find a simple mechanism for the renewal of otherwise degrading habitats that “stabilises” the interacting population to a co-existence equilibrium.

The habitat renewal provides a stabilising mechanism in a way similar to Watt’s Flyball Governor [9] .

- Simulation Result 6.2: If the habitat renewal dynamics are frozen or switched off, then the system reverts back to competitive exclusion. Crucially, which species persists (or is driven extinct) in the resulting the exclusion, is sensitive to the timing of the switching off. Simulations are depicted in Figures 6.3, 6.4 and 6.5.

### 1.3 Publications

1. In preparation: a paper on “A bifurcation learning algorithm” (see Chapter 4) for *Systems & Control Letters*.
2. I applied for a Poster an idea “Adaptive Arms Race in terms of switching between positive population projection models“ (see Chapter 5) for *Models in Population Dynamics, Ecology, and Evolution (MPDEE’20)*. – Cancelled because of the COVID.
3. I Contributed: a Poster an idea “Adaptive Arms Race in terms of switching the pest and pesticide“ (see Chapter 5) for *BMC-BAMC Glasgow 2021*.
4. In preparation: a paper on “Adaptive control inspired habitat renewal“ (see Chapter 6) for *Mathematical Modelling and Numerical Simulation with Applications*.

## Chapter 2

# Population Dynamics

**Overview.** The purpose of this chapter is to introduce a number of modelling approaches to population dynamics. The intention is one of scene-setting as a pre-cursor to what will follow in subsequent chapters. Specifically:

- We will review continuous-time dynamics of interacting populations, focusing on predator-prey interactions, competitive interactions and mutualism. Here, a key part of the narrative is that natural systems interact with each other and, importantly, also their habitats – leading to some form of evolution or adaptation or to a depletion or renewal of habitats. See Chapter 6;
- Then we will review discrete-time population dynamics, focusing on population projection matrix models. Here, a key part of the narrative is that at all times, the state of the population projection system has strong non-negativity properties that can be used to construct adaptive stabilization and persistence algorithms. These ideas leads to adaptive algorithms that learn a bifurcation – Chapter 4 – and also to a so-called adaptive “Arms Race” – see Chapter 5.

## **2.1 Interacting populations – predator-prey dynamics, competition and mutualism**

In developing the models and theory for cyber-natural systems we will look to population interactions as a source of motivation. Populations interact in various ways and provide a rich source of potential dynamics. Even without evolution, numerous behaviours are possible. But evolution is also a key process which will inspire how we build an understanding of cyber-natural systems. In this section we review three of the main types of interactions between two species:

- Predator-prey interactions leading to a well known cycle relationship between the species. Here, if the growth rate is increasing in one species, the other one is decreasing;
- Competitive interactions. Here each growth rate is reduced by the presence of the other species;
- Mutualism. Here the growth rate of each species increases from the presence of the other species.

For a detailed treatment of this, see the book by Murray – Chapter 3 [10].

### **Predator-prey dynamics and Lotka-Volterra systems**

Interactions amongst populations are important in modelling population dynamics. They affect the species by changing their dynamics (behaviours) through time. The Lotka-Volterra model is a widely-known model for predator-prey interactions and one of the oldest for a two species predator-prey interaction. Solutions of the model are periodic, capturing a cyclical movement of populations [11]. The Lotka-Volterra model describes the predation of one species on another and clearly shows the oscillation levels between both populations. The traditional Lotka-Volterra

model is given by

$$\frac{dX}{dt} = X(a - bY) \quad (2.1a)$$

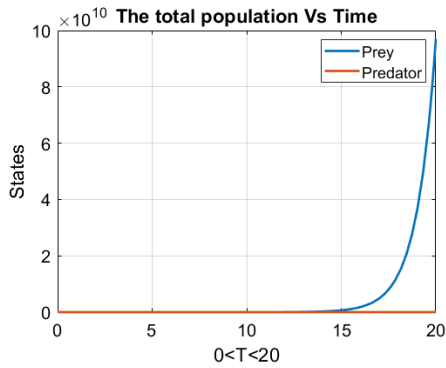
$$\frac{dY}{dt} = Y(cX - d). \quad (2.1b)$$

In (2.1),  $X$  is the population of prey, for example rabbits,  $Y$  is the population of predator, such as foxes. The parameters  $a$ ,  $b$ ,  $c$  and  $d$  are positive.

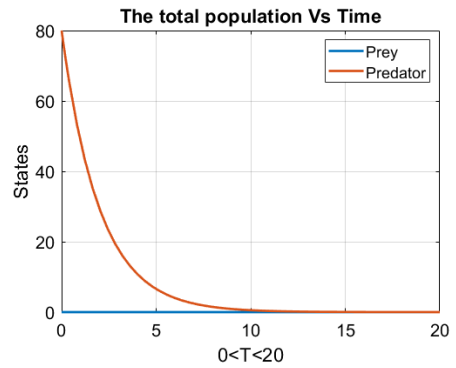
We consider the predator-prey system given by (2.1) in a few scenarios:

- (a) If there is no predator, the prey increases without limit. This is through  $+aX$  in (2.1a).
- (b) The growth of the prey population is reduced due to the effect of predation – this is captured by the  $-bXY$  term in (2.1a).
- (c) In the absence of prey, to feed or increase the population of predators, there is an exponential decay of predators – this is captured by the  $-dY$  term in (2.1b).
- (d) The growth rate of predators is increase by the presence of prey – this is captured by the  $+cXY$  in (2.1b).

In the simulation of (2.1) there are three cases: (i) when there is no prey, (ii) when there is absence of predator, and (iii) when both populations are present.



(a) Simulation of system (2.1) in case (i).



(b) Simulation of system (2.1) in case (ii).

Figure 2.1: The evolution of (2.1) on two different scenarios

In Figure 2.1a the predator is set to zero in the system (2.1). This leads the prey to having unbounded growth as shown.

In Figure 2.1b the prey is set to zero in the system (2.1). We clearly can see that predator tends to zero because the predator has no food source.

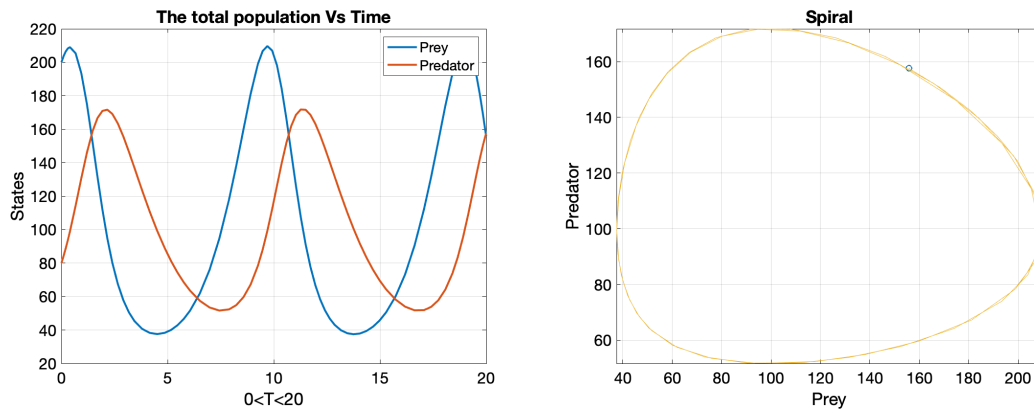


Figure 2.2: Simulation of system (2.1) in case (iv).

Left plot. Density of predator and prey against time; Right plot. Predator-prey cycle in phase space.

In Figure 2.2, left plot, we see that the population densities of the both systems interact with each

other, over a 20 year period. The parameters are fixed as  $a = 1$ ,  $b = 0.01$ ,  $c = 0.005$  and  $d = 0.5$ . Initially the prey has density 200, and the predator 80. This shows the classical predator-prey cycle and explains Figure 2.2, right plot.—See [10], pages 79-82 for a detailed discussion of this classical result.

**Remark 2.1.** In Section 2.2 we consider predator-prey interactions in combination with evolution – this is a first glance at “cyber-natural” systems.

### **Competitive exclusion**

In the previous section we briefly reviewed the well known predator-prey interaction. In this subsection we focus on the well known competitive interaction. In Chapter 6 we will revisit competitive interaction in a context of habitat renewal. For this reason we discuss this population interaction in more detail. The main goal of studying competitive models in mathematical biology is to explore conditions on the species under which one species out-competes the other species which, as a result, goes extinct. The celebrated concept of competitive exclusion argues that when there is intense competition for a particular resource, all but one competitor will eventually become extinct [12], [13]. Competitive exclusion occurs when the inter-specific competition is greater than the intra-specific competition. Competitive exclusion can determine organism distribution and abundance and how a community is structured – see [14]. In Chapter 6 we will consider a competitive system in feedback with its habitat whereby a species’ habitat is depleted by an over-abundance of population.

Interspecific competition signifies competition between numbers of species living together. Two or more species race for the same limited resource and impact on each other in terms of growth [15]. As a result of limited resources, one of these species perhaps decreases until the extinction. The following equation is the simple, classical competitive exclusion model (see [10] for more

details):

$$\frac{dN_1}{dt} = r_1 N_1 \left[ 1 - \frac{N_1}{K_1} - b_{12} \frac{N_2}{K_1} \right] \quad (2.2a)$$

$$\frac{dN_2}{dt} = r_2 N_2 \left[ 1 - \frac{N_2}{K_2} - b_{21} \frac{N_1}{K_2} \right] \quad (2.2b)$$

In Equation (2.2),  $N_1$  and  $N_2$  are prey and predator species competing with each other depending continuously on time  $t$ . The parameters  $r_1, K_1, b_{12}, r_2, K_2$  and  $b_{21} > 0$ , which means they are all positive constant. The interpretation of parameters are; For  $i = 1, 2$ ,  $r_i$  represents the growth rates,  $K_i$  are the carrying capacities,  $b_{12}$  and  $b_{21}$  are the competition coefficients.  $b_{12}$  expresses species  $N_2$ 's inhibitory effect on the population growth of species  $N_1$  and  $b_{21}$  exerts the opposite side of effect on  $N_2$ . It is significant to mention that the growth of each population has an inhibitory effect on the evolution of the population itself whether, in  $N_1$  or  $N_2$ . This status is described as intra-specific competition, which can be described as the competition among the two types of population. However, when the competition is between the individual and the population itself, it is called interspecific competition. [16]. Each separate member in the  $N_1$  population has a  $\frac{1}{K_1}$  inhibitory influence on its evolution, whereas the other inhibition for  $N_1$  in the  $N_2$  population is shown in the equation (2.2b) by  $\frac{b_{21}}{K_2}$ . In terms of the evolution of the individuals' population of  $N_2$ , they are inhibited by  $\frac{b_{12}}{K_1}$  in the  $N_1$  population and by  $\frac{1}{K_2}$  in their population. Precisely, the side effect of the absence of one of the species in the equation (2.2), the system is naturally described as the well-known logistic growth. [4].-More explanation about this is provided the Appendix.

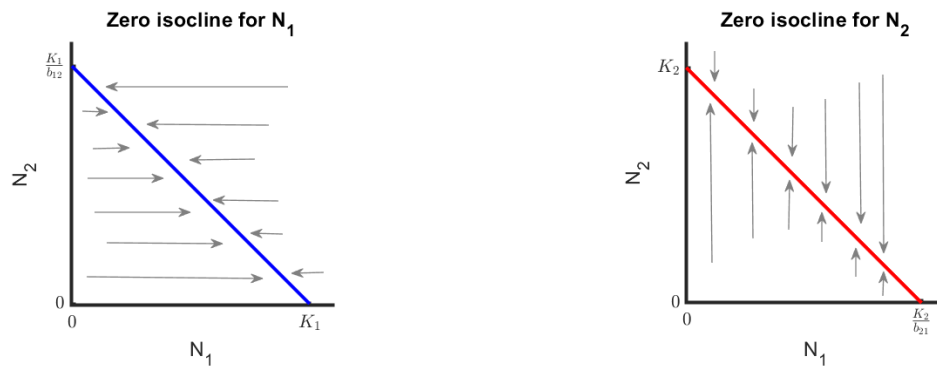
It is essential to look at graphs that demonstrate how the size of each population grows or shrinks when we start with various combinations of species abundances. The subsequent two Figures 2.3a&2.3b show the state-space behaviour for (2.2). The  $x$ -axis represents the abundance of  $N_1$ , and the  $y$ -axis shows the quantity of  $N_2$ . In the state-space figures, each node reflects the com-

bination of the abundances of both species. The bottom left has a low number of both species, while the top right has a high number of both species. On the graphs, a zero isocline exists for each species. Any point along the zero isocline of species  $N_1$  or  $N_2$  reflects a combination of abundances of the two species where the population of species  $N_1$  or  $N_2$  neither increases nor decreases. The zero isocline of species  $N_1$  is obtained by solving  $\frac{dN_1}{dt} = 0$  in (2.2a), that is with zero growth rate. The same is done for species  $N_2$  [17]. So

$$\dot{N}_1 = 0 \implies N_1 = 0 \text{ or } K_1 - N_1 - b_{12}N_2 = 0$$

$$\dot{N}_2 = 0 \implies N_2 = 0 \text{ or } K_2 - N_2 - b_{21}N_1 = 0.$$

The two non-trivial isoclines are depicted in Figure 2.3.



(a) Non-trivial zero isocline for  $N_1$ .

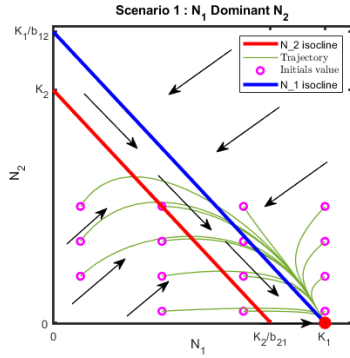
(b) Non-trivial zero isocline for  $N_2$ .

Figure 2.3: The zero isoclines that are produced by the competitive exclusion equation (2.2). The left diagram (2.3a) indicates the zero isocline for  $N_1$ ; the right diagram (2.3b) explains the zero isocline for  $N_2$ .

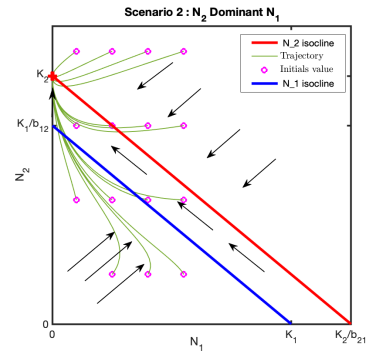
Each graph is divided into two parts by the zero isocline. The left diagram 2.3a reveals that the size of species  $N_1$  diminishes above and right of the isocline of  $N_1$  since the sum of both populations' species exceeds the carrying capacity  $K_1$ . In contrast,  $N_1$  rises from below to its left since the total population of both species is less than the carrying capacity  $K_1$ . In the left

diagram 2.3a, in the absence of individuals of  $N_2$ , the zero isocline reaches the intersection with X-axis which is  $N_1$  axis in Figure 2.3a at  $K_1$ . In this case 2.3a, the isocline crosses the y-axis at the point  $N_2 = \frac{K_1}{b_{12}}$  [18]. In Figure 2.3b, follow the same procedure; identical circumstances will appear just in a reverse process.

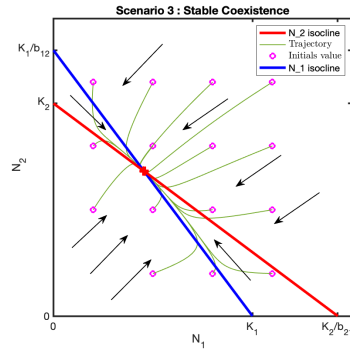
Generating the expected behaviour for the system (2.2); utilizing the zero isoclines for  $N_1$  and  $N_2$ . Hence they are essentially depending on the values of carrying capacity  $K_i$  where  $i = 1, 2$  and the competition coefficient  $b_{ij}$  where  $i = 1, 2$  and  $j = 1, 2$  with  $i \neq j$  by rearranging them relative to each other. As a result, four different scenarios could emerge. In each case, the competition's outcome will be unique compared to the others. The interspecific competition system in the equation (2.2) has four possible outcomes. Figure 2.4 shows the phase-plane diagram trajectories. The outcomes can emerge from the isocline for both species included in each figure and relative to each other. The blue line in each graph represents the isocline of species 1, while the red line in each graph represents the isocline of species 2. Pink dots represent the initial values as the initial location points for green trajectories, explaining the phase-plane moving towards the equilibrium points. The black arrows indicate the change in the population size for the species. The red dots determine a stable equilibrium point, and the grey dot shows an unstable equilibrium point.



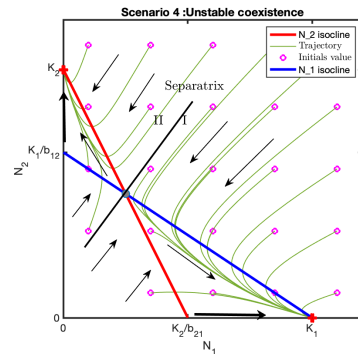
(a) Constraints  $\frac{K_1}{b_{12}} > K_2$  and  $K_1 > \frac{K_2}{b_{21}}$ .



(b) Constraints  $K_2 > \frac{K_1}{b_{12}}$  and  $K_1 < \frac{K_2}{b_{21}}$ .



(c) Constraints  $\frac{K_1}{b_{12}} > K_2$  and  $\frac{K_2}{b_{21}} > K_1$ .



(d) Constraints  $K_2 > \frac{K_1}{b_{12}}$  and  $K_1 > \frac{K_2}{b_{21}}$ .

Figure 2.4: The four potential findings of the Interspecific Competition model (2.2).

The first case in Figure 2.4a shows the inequality:

$$\frac{K_1}{b_{12}} > K_2 \quad \text{and} \quad K_1 > \frac{K_2}{b_{21}} \quad (2.3)$$

As a result, the two isoclines of  $N_1$  and  $N_2$  do not intersect and the isocline of  $N_1$  located above and to the right of the isocline of  $N_2$ , by rearranging the inequality of (2.3)

$$K_1 > K_2 b_{12} \quad \text{and} \quad K_1 b_{21} > K_2 \quad (2.4)$$

The term of the inequality  $K_1 > K_2 b_{12}$  denotes that the intra-specific inhibitory effects population  $N_1$  can impose on itself are more significant than the interspecific effects that population  $N_2$  could impose on population  $N_1$ . The other component of the inequality,  $K_1 b_{21} > K_2$ , implies that  $N_1$  has a greater impact on the population ( $N_2$ ) than the population has on itself of ( $N_2$ ). Consequently, the population of  $N_1$  appears as a more robust interspecific competitor than the population of  $N_2$ . Resulting in  $N_1$  forcing  $N_2$  to go extinct.

In the second scenario, the inequality of Figure 2.4b is a reverse of behaviour of the first scenario in Figure 2.4a. So one population will always have the ability to survive over the other in both scenarios.

**Remark 2.2.** The first two cases have an opposite behaviour:

- In 2.4a  $N_1$  excludes  $N_2$ .
- In 2.4b  $N_2$  excludes  $N_1$ .

In the third case 2.4c, the constrains of the inequality are:

$$\frac{K_1}{b_{12}} > K_2 \quad \text{and} \quad \frac{K_2}{b_{21}} > K_1 \quad (2.5)$$

As a result, the two isoclines of  $N_1$  and  $N_2$  intersect. Rearranging the inequality of (2.5) gives

$$K_1 > K_2 b_{12} \quad \text{and} \quad K_2 > K_1 b_{21} \quad (2.6)$$

Thus the inequalities in (2.6) show interspecific competition has a weaker impact on populations, whether on  $N_1$  or  $N_2$ , than intraspecific competition. Therefore, the two isoclines to accomplish a stable coexistence equilibrium (red circle). In the last scenario, we have the following inequalities:

$$K_2 > \frac{K_1}{b_{12}} \quad \text{and} \quad K_1 > \frac{K_2}{b_{21}} \quad (2.7)$$

Rearranging (2.7) gives

$$K_2 b_{12} > K_1 \quad \text{and} \quad K_1 b_{21} > K_2 \quad (2.8)$$

The two isoclines for  $N_1$  and  $N_2$  cross each other as a result of the inequalities (2.7) and (2.8). The individuals that are emerging in both populations,  $N_1$  and  $N_2$ , are contending aggressively with the other individuals from the different population. At the same time, the level of competition between the individuals of each species amongst themselves is low. As in figure 2.4d, the consequence is that the evolution of interaction between the individuals of both populations  $N_1$  and  $N_2$  causes an unstable co-existence equilibrium. When the population  $N_1$  reaches its carrying capacity  $K_1$  leading  $N_2$  to go extinct. Also, if  $N_2$  reaches carrying capacity  $K_2$ , then  $N_1$  goes extinct.

**Remark 2.3.** Under the Constraints of  $K_2 > \frac{K_1}{b_{12}}$  and  $K_1 > \frac{K_2}{b_{21}}$  the system exhibits competitive exclusion. In Chapter 6 we show that introducing a habitat renewal feedback forces a system that would otherwise exhibit competitive exclusion into one that exhibits competitive coexistence. The feedback mechanism is adaptive. If the mechanism is switched off, then the system reverts back to competitive exclusion.

### Mutualism

In contrast to competitive interaction, mutualism (or symbiosis) is where species interact to the benefit of each other. One example is plant and seed dispersal, [10]. For two species, a mutualistic interaction is captured by

$$\frac{dN_1}{dt} = r_1 N_1 \left( 1 - \frac{N_1}{k_1} + b_{12} \frac{N_2}{k_1} \right), \quad (2.9a)$$

$$\frac{dN_2}{dt} = r_2 N_2 \left( 1 - \frac{N_2}{k_2} + b_{21} \frac{N_1}{k_2} \right), \quad (2.9b)$$

see Murray [10]. In (2.9), the parameters  $r_1, r_2, b_{12}, b_{21}, k_1$  and  $k_2$  are all positive.

System (2.9) has four equilibria:  $(0,0)$ ,  $(k_1,0)$ ,  $(0,k_2)$  and

$$\left( \frac{k_1 + b_{12}k_2}{1 - b_{12}b_{21}}, \frac{k_2 + b_{21}k_1}{1 - b_{12}b_{21}} \right).$$

Using the Jacobian matrices method (A.3), we find that  $(0,0)$  is unstable, whilst  $(K_1,0)$  and  $(0,K_2)$  are unstable saddles. The last point  $\left( \frac{k_1 + b_{12}k_2}{1 - b_{12}b_{21}}, \frac{k_2 + b_{21}k_1}{1 - b_{12}b_{21}} \right)$  we get two different scenarios depending on whether  $b_{12}b_{21} > 1$  or  $b_{12}b_{21} < 1$ . See [10] pages The following figure shows the phase-plane diagram trajectories for the last steady state. Pink dots represent the initial values as the initial location points for green trajectories, explaining the phase-plane plane. The black arrows indicate the change in the population size for the species. The grey circle depicts the equilibrium point.

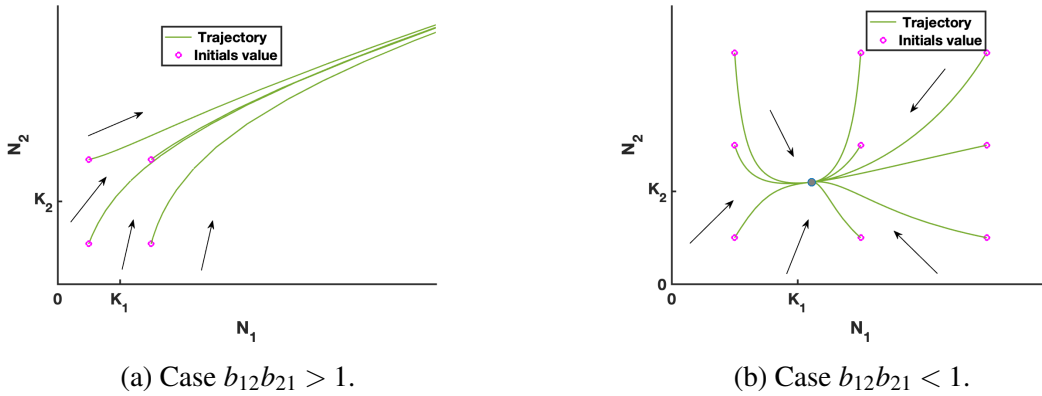


Figure 2.5: Phase plane for the Mutual system (2.9).

In Figure 2.5a, where  $b_{12}b_{21} > 1$ , we see unbounded growth with  $N_1 \rightarrow \infty$  and  $N_2 \rightarrow \infty$ . In Figure 2.5b, where  $b_{12}b_{21} < 1$ , all the trajectories are moving towards a stable coexistence point with  $N_1 > K_1$  and  $N_2 > K_2$ . This is because the carrying capacity for each species is more significant when there is mutual interaction and the benefit accrues.

## 2.2 Predator prey systems and evolution

Natural populations are subject to evolution. In a context of predator prey systems, predation induces a selection pressure on either/both the prey and predator populations. This might lead to the predator seeking alternative prey or the prey developing novel evasion strategies. Since the pioneering work of Lotka and Volterra [4], predator-prey dynamics have been the subject of much research. Recently, authors have considered how predation may affect phenotypic and genetic variation and in turn the evolution/adaptation of the predator–prey system.

The idea behind this thesis finds inspiration in the paper “The community effects of phenotypic and genetic variation within a predator population” by Schreiber et al. [2]. Here, specific parameters in model are not fixed but adapt through evolutionary processes. A predator-prey model is combined with evolution of traits and described by

$$\begin{aligned}\frac{dN_i}{dt} &= r_i N_i \left(1 - \frac{N_i}{K_i}\right) - p \bar{a}_i N_i \\ \frac{dP}{dt} &= P \bar{W} \\ \frac{d\bar{x}}{dt} &= \sigma_G^2 \frac{d\bar{W}}{d\bar{x}},\end{aligned}\tag{2.10}$$

where

$$\begin{aligned}\bar{W}(\bar{x}, N_1, N_2) &= \sum_{i=1}^2 e_i \bar{a}_i(\bar{x}) N_i - d, && \text{Fitness landscape} \\ a_i(x) &= \alpha_i \exp\left[-\frac{(x - \theta_i)^2}{2(2\tau_i^2)}\right] && \text{Species fitness function,} \\ \frac{d\bar{W}}{d\bar{x}} &= \sum_{i=1}^2 \frac{e_i N_i \tau_i \alpha_i}{(\tau_i^2 - \sigma^2)^{1.5}} \exp\left[-\frac{(\bar{x} - \theta_i)^2}{2(\tau_i^2 + \sigma^2)}\right].\end{aligned}\tag{2.11}$$

The parameters of the system (2.10) with (2.11) are described in Table 2.1 where  $i = 1, 2$ .

Parameter	Definition	Parameter	Definition
$N_i$	Prey	$P_i$	Predator
$t$	Time	$x$	Dependence variable
$d$	Mortality rate	$e_i$	Efficiencies
$W$	Fitness of predator	$a_i$	Attack rate
$\alpha_i$	Maximum attack rate	$\tau_i$	Attack rate decline
$\theta_i$	Optimal trait	$\sigma$	phenotypic variance
$K_i$	Carrying Capacity	$r_i$	Growth rate

Table 2.1: Definitions of variables and parameters for the Schreiber et al. model (2.10) with (2.11).

We are interested in these equations to study their dynamic behaviours. We have used MATLAB and ODE45 to simulate this model. Note, we have not achieved identical results to those in the paper because it is unclear what initial conditions they have used<sup>1</sup>. It turns out that the dynamics are very sensitive to initial conditions. In the simulation, parameters are fixed as described in the paper excluding the initial conditions. Where phenotypic variance  $\sigma$  has a genetic component  $\sigma_G$ . Heritability is  $h^2 = \frac{\sigma_G^2}{\sigma^2}$  and the constant variance is  $\sigma^2 = 0.04$  or  $\sigma^2 = 0.01$ . Others parameters have been fixed as  $r_1 = 0.2$ ,  $r_2 = 0.1$ ,  $K_1 = K_2 = 500$ ;  $\tau_1 = \tau_2 = 0.1$ ,  $-\theta_1 = \theta_2 = 0.2$ ;  $e_1 = e_2 = d = 0.5$  and  $\alpha_2 = \alpha_1 = 0.02$ . In next Figures 2.6, 2.8, 2.8 and 2.9, in each plot the top figure describes the densities over a long time, whereas the bottom figure is the mean trait. In each simulation we I picked different initial values which informed in each caption to duplicate the result that provides in [2].

---

<sup>1</sup>I contacted Sebastian Schreiber personally but the parameters he gave me still did not match up the simulation.

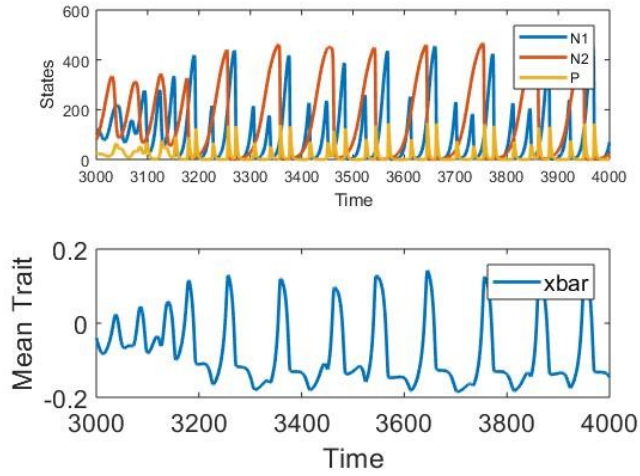


Figure 2.6: Experiment 1 : Simulating Schreiber et al's Model (2.10); The initial conditions are  $N_1 = 120$ ,  $N_2 = 80$ ,  $P = 30$  and  $X = -0.04$  and the parameters are  $\sigma = 0.01$  and  $h = 0.25$ .

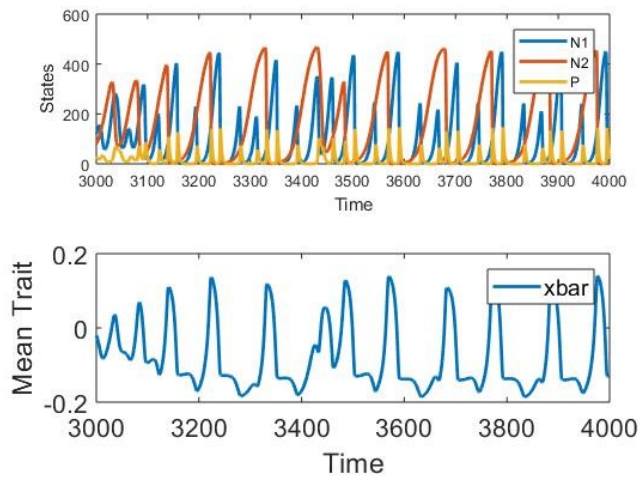


Figure 2.7: Experiment 2 : Simulating Schreiber et al's model (2.10) with (2.11); The initial conditions are  $N_1 = 120$ ,  $N_2 = 80$ ,  $P = 30$  and  $X = -0.02$ , and the parameters are  $\sigma = 0.01$  and  $h = 0.25$ .

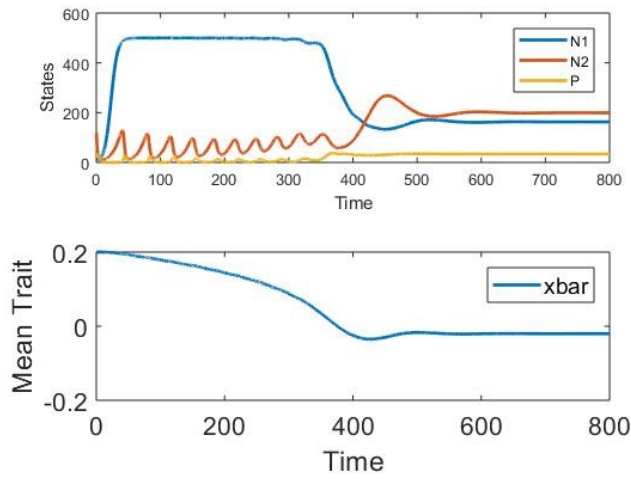


Figure 2.8: Experiment 3 : Simulating Schreiber et al's model (2.10) with (2.11); The initial conditions are  $N_1 = 5$  ,  $N_2 = 120$  ,  $P = 20$  and  $X = 0.2$ , and the parameters are  $\sigma = 0.01$  and  $h = 0.02$ .

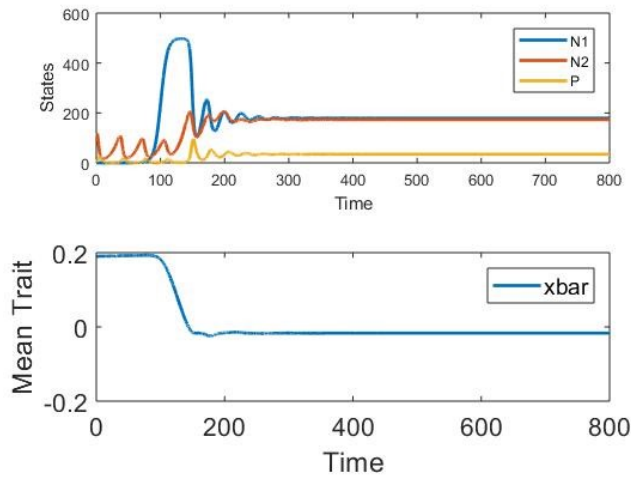


Figure 2.9: Experiment 4 : Simulating Schreiber et al's model (2.10) with (2.11).; The initial conditions are  $N_1 = 0.00009$  ,  $N_2 = 120.1$  ,  $P = 2.9$  and  $X = 0.1900009$ , and the parameters are  $\sigma = 0.04$  and  $h = 0.025$

As we can see from the Figures 2.6 , 2.8 , 2.8 and 2.9, the system (2.10) exhibits a range of

dynamics – quite simple in Figures 2.8 and 2.9, quite complex in Figures 2.6 and 2.7.

**Remark 2.4.** In the approach of Schrieber et al., parameters adapt through evolution. In our approach, parameter adaptation is engineered. However, in both approaches, the populations themselves feedback on the mechanisms of interaction. It is this feedback that we explore throughout the thesis.

## 2.3 Structured population models

In Chapter 5 we will explore an adaptive arms race motivated by adaptive stabilisation and destabilisation (persistence) for classes of structured, discrete-time population models. So in this section we review some basic properties of such models.

In general, structured population models are classified by whether they consider a population in discrete or continuous time and whether the states of the system are discrete or continuous. The different types are summarised in Table 2.2, see [19].

	Discrete-state	Continuous-states
Discrete-time	Matrix population models	Integrodifference equations
Continuous-time	Delay-differential equations	Partial differential equations

Table 2.2: Types of structured population models

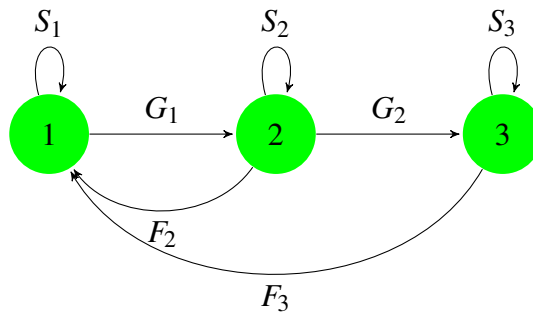


Figure 2.10: The cycle of life of 3 stages population.

### *Population Projection model*

A population projection matrix takes the form

$$x(t+1) = Ax(t). \quad (2.12)$$

In (2.12):

- $x(t)$  is the stage-structured population vector at time  $t$ ;
- $t$  is time in discrete steps  $t = 0, 1, 2, \dots$ ;
- $A$  is the matrix population model.

To find  $A$ , we use the figure 2.10 above as shown for a three stage population (more or less stages are handled similarly). In this 3-stage case,  $A$  is represented by

$$A = \begin{pmatrix} S_1 & F_2 & F_3 \\ G_1 & S_2 & 0 \\ 0 & G_2 & S_3 \end{pmatrix} \quad (2.13)$$

The first row of  $A$  contains the fecundities or reproductive values  $F_2$  and  $F_3$ , the diagonal entries  $S_1, S_2$  and  $S_3$  are the survival rates and the sub-diagonal entries  $G_1$  and  $G_2$  are the growth rates. A Leslie Matrix is a special Population Projection Model (PPM) where the survival rates in (2.13) are zero. More generally, for populations structured in  $n$  stages,  $A$  will simply be a non-negative matrix, that is a matrix whose elements are non-negative numbers.

Matrix population models are extremely useful to ecologists, helping them to determine the evolution of a population: Does the population grow or decline? For population projection matrix models, this can be determined by using the celebrated Perron-Frobenius theorem in [19] for irreducible non-negative matrices. The Perron-Frobenius theorem asserts that:

- There is at least one real and positive eigenvalue, greater than or equal in magnitude to any other eigenvalues. This eigenvalue is the dominant or Perron eigenvalue ( $\lambda_{max}(A)$ );
- $\lambda_{max}(A)$  is simple;
- The corresponding left and right Perron eigenvectors  $v^T$  and  $w$  are positive.

Using the Perron eigenvalue we have:

- if  $\lambda_{max}(A) < 1$ , then the total population decreases to zero;
- if  $\lambda_{max}(A) > 1$ , then the population increases asymptotically;
- if  $\lambda_{max}(A) = 1$ , then the population is asymptotically unchanged.

***Illustrative example***

Consider a population with three age classes. Suppose that at each time step, stage 2, respectively stage 3, produces 9 and 12 off-spring. Assume growth rates  $G_1 = 0.25$  and  $G_2 = 0.5$  and zero survival rates. This gives a PPM

$$A = \begin{pmatrix} 0 & 9 & 12 \\ 0.25 & 0 & 0 \\ 0 & 0.5 & 0 \end{pmatrix} \tag{2.14}$$

Assume an initial population

$$x_0 = \begin{pmatrix} 12 \\ 12 \\ 12 \end{pmatrix} .$$

Simulation of this system using (2.12) is depicted in Figure 2.11. As we can see the population grows exponentially.

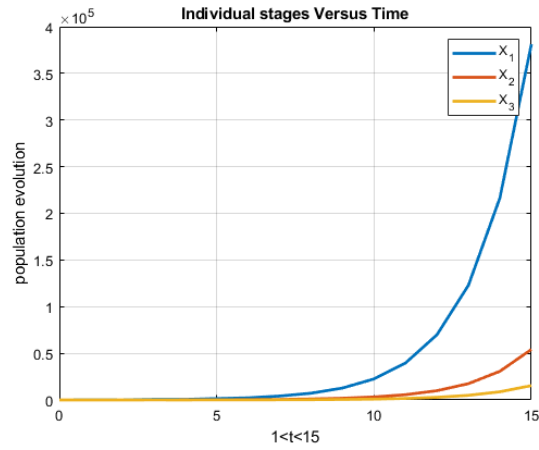


Figure 2.11: The evolution of the population (2.14).

This exponential growth is confirmed by the Perron eigenvalue. Indeed, in this case  $\lambda_{max} = 1.7612 > 1$ . So the system state increases exponentially.

Now consider a declining population with PPM

$$A = \begin{pmatrix} 0 & 2 & 3 \\ 0.25 & 0 & 0 \\ 0 & 0.5 & 0 \end{pmatrix} \quad (2.15)$$

We use the same initial condition as in (2.3). Simulation of this system using (2.12) is depicted in Figure 2.12. As we can see the population decreases exponentially.

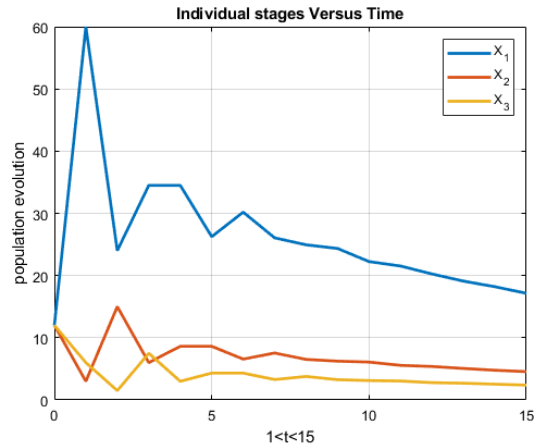


Figure 2.12: The evolution of the population (2.15).

This exponential decrease is confirmed by the Perron eigenvalue. Indeed, in this case  $\lambda_{max} = 0.9466 < 1$ . So the system statedecreases exponentially.

**Remark 2.5.** In Chapter 5, we will consider population projection matrix models and exploit these non-negative properties, specifically making repeated use of the positive Perron eigenvectors. In particular, these non-negativity properties play a pivotal role in the proof of Theorem 4.13.

## 2.4 Conclusion

In this chapter we have discussed a variety of population dynamic models. The purpose was not to offer a comprehensive treatment of a vast topic. Instead, we used this chapter to highlight some simple examples of population dynamic models that play key roles in later chapters. Specifically we considered:

- Simple examples of predator-prey, competitive and mutualistic population interactions. These are especially relevant to setting the context for Chapter 6.

- Predator-prey systems with evolution. This topic offered much inspiration to the overall development of the thesis and is a topic I would return to in the future.
- Population projection matrix models. These feature quite significantly in Chapter 5. They are a really good model class to develop ideas with.

# Chapter 3

## Adaptive Control

**Overview.** A key theme of the thesis is the interplay between adaptive systems – on the one hand natural systems that adapt through evolution or acquired resistance; and technological systems that have engineered adaptation. The purpose of this chapter is to provide some basic ideas and tools from adaptive control theory – or the theory of engineered adaptation.

### 3.1 Adaptive control

In language, “adapt” means a change of the behaviour to accept new circumstances [20]. In control theory, adaptive control arises when the control action or feedback is modified in response to observations. Adaptation of the controller tries to cope with uncertainty in the system dynamics, see [21]. Uncertainty might arise due to unexpected changes in the dynamics or other disorder [22]. Broadly speaking there are two types of adaptive control: Indirect adaptive control and direct adaptive control. In the former, the adaptive controller is based on a model, the control is designed on the basis of this model and then adapted in real time as the model is adapted via parameter estimation algorithms. In direct adaptive control, there is no model proposed and no parameter estimation. Instead, the adaptive control algorithm works directly with system

assumptions. The similarities and differences are best seen via example.

## 3.2 Indirect vs. Direct Adaptive Control – An example

Consider a system

$$\dot{y}(t) = ay(t) + u(t)$$

with scalar state  $y(t)$  and in which the scalar parameter  $a$  is unknown. If we did know  $a$ , then

$$u = -ay - y$$

would give

$$\dot{y} = -y$$

and so  $u$  would be a stabilizing feedback controller based on knowledge of the system. However we do not know  $a$ . So instead we estimate  $a$  by  $\hat{a}$  and use  $\hat{a}$  in the controller in place of  $a$ . So now

$$u = -\hat{a}y - y,$$

giving a closed loop system

$$\dot{y} = -y + (a - \hat{a})y.$$

We need to design a parameter estimate for determining  $\hat{a}$ : To do this, introduce a Lyapunov-like function

$$V = y^2 + (\hat{a} - a)^2$$

Then

$$\begin{aligned}\dot{V} &= 2y\dot{y} + 2(\hat{a} - a)\dot{\hat{a}} \\ &= 2y(-y + (a - \hat{a})y)\dot{y} + 2(\hat{a} - a)\dot{\hat{a}} \\ &= -2y^2 + 2(\hat{a} - a)(-y^2 + \dot{\hat{a}}).\end{aligned}$$

It follows that if we use a parameter estimation

$$\dot{\hat{a}} = y^2$$

then

$$\dot{V} = -2y^2 \leq 0.$$

It then follows that

$$\lim_{t \rightarrow \infty} y(t) = 0 \quad \lim_{t \rightarrow \infty} \hat{a}(t) = \hat{a}(\infty).$$

This procedure yields the **indirect adaptive controller**

$$\begin{aligned}u &= -\hat{a}y - y, \\ \dot{\hat{a}} &= y^2.\end{aligned}\tag{3.1}$$

However, in this simple set-up we do not need to introduce the parameter estimate  $\hat{a}$ . With the same system

$$\dot{y}(t) = ay(t) + u(t)$$

we simply try

$$u = -ky$$

directly, the idea being to make  $k$  large enough to “beat”  $a$ , whatever its value. We consider a candidate Lyapunov function

$$V = y^2 + (k - a)^2.$$

Then

$$\begin{aligned}\dot{V} &= 2y\dot{y} + 2(k - a)\dot{k} \\ &= 2(a - k)y^2 + 2(k - a)\dot{k}\end{aligned}$$

Inspired by the indirect control design we try

$$\dot{k} = y^2.$$

Then

$$\dot{V} = 0.$$

Integrating we have that

$$V + (ak - a)^2 = \text{constant}.$$

It then follows that

$$\lim_{t \rightarrow \infty} y(t) = 0 \quad \lim_{t \rightarrow \infty} k(t) = k(\infty).$$

This procedure yields the the **direct adaptive controller**

$$\begin{aligned}u &= -ky, \\ \dot{k} &= y^2.\end{aligned}\tag{3.2}$$

**Remark 3.1.** Even though the motivation for designing the controller is different, one with the parameter estimation the other without, the underlying dynamics are essentially the same.

**Remark 3.2.** For the rest of the thesis we will focus only on direct adaptive control

### 3.3 Byrnes-Willems direct adaptive control

Byrnes and Willems [8] developed a so-called high-gain adaptive controller

$$\dot{x}(t) = Ax(t) + bu(t), \quad x(0) = x_0, \quad y(t) = c^T x(t) \quad (3.3)$$

for relative degree one, minimum-phase systems. Here  $x(t) \in \mathbb{R}^n$ ,  $u(t), y(t) \in \mathbb{R}$ ,  $A \in \mathbb{R}^{n \times n}$ ,  $b, c \in \mathbb{R}^n$ . The relative degree one, minimum-phase assumption means that the system (3.3) satisfies:

- $c^T b > 0$  (relative degree one condition with known sign of the high frequency gain);
- the zeros of  $c^T (sI - A)^{-1} b$  have negative real parts, (minimum phase condition).

The relative degree one and minimum-phase assumptions permit the use of the coordinate transformation

$$x = Tw, \quad T = \begin{bmatrix} b \\ c^T b \end{bmatrix} V, \quad w = \begin{pmatrix} y \\ z \end{pmatrix},$$

where the columns of  $V \in \mathbb{R}^{n \times (n-1)}$  span the kernel of  $c^T$ , to rewrite the dynamics (3.3) in the form

$$\begin{aligned} \dot{y}(t) &= ay(t) + \alpha^T z(t) + c^T bu(t) \\ \dot{z}(t) &= \beta y(t) + A_2 z(t), \end{aligned} \quad (3.4)$$

for some  $a \in \mathbb{R}$ ,  $\alpha, \beta \in \mathbb{R}^{n-1}$  and  $A_2 \in \mathbb{R}^{(n-1) \times (n-1)}$ . The zeros of  $c^T (sI - A)^{-1} b$  are the eigenvalues of  $A_2$ . So the minimum-phase assumption means that every eigenvalue of  $A_2$  has negative real part, i.e.  $A_2$  is Hurwitz.

**Remark 3.3.** The transformed system (3.4) can be interpreted as the feedback connection between a scalar system and a stable system:

$$v = u + \frac{1}{c^T b} w, \quad \begin{cases} \dot{y}(t) = ay(t) + c^T bv(t), \\ \dot{z}(t) = A_2 z(t) + \beta y(t), \quad w(t) = \alpha^T z(t). \end{cases} \quad (3.5)$$

**Proposition 3.4. *Byrnes-Willems High Gain Adaptive Controller:***

Let

$$\begin{aligned} u(t) &= -k(t)y(t). \\ \dot{k}(t) &= y^2(t). \end{aligned} \quad (3.6)$$

Then for all  $x(0) = x_0 \in \mathbb{R}^n$ , i.e.  $y(0) \in \mathbb{R}$  and  $z(0) \in \mathbb{R}^{n-1}$  we have that

$$\lim_{t \rightarrow \infty} \begin{pmatrix} y(t) \\ z(t) \end{pmatrix} = 0 \quad \text{and} \quad \lim_{t \rightarrow \infty} k(t) = k_\infty(x_0) < \infty.$$

**Remark 3.5.** We can modify the controller of the system (3.6), without changing the outcome, by adding a parameter  $\varepsilon_1 > 0$  to the adaptation:

$$\dot{k}(t) = \varepsilon_1 y^2(t).$$

This will be useful later to speed up or slow down the adaption when are comparing different algorithms.

**Remark 3.6.** Proposition 3.4 guarantees that the state  $x(t)$  converges to zero without knowledge of the system parameters  $A, b$  and  $c$  and initial condition  $x(0) = x_0$ . Moreover, the gain parameter  $k(t)$  always converges. This begs the question: Is the limiting gain  $k_\infty(x_0)$  itself stabilising, that is to say is the matrix

$$A - k_\infty(x_0)bc^T \quad (3.7)$$

stable? See Section 3.6 for a discussion of this fundamental question.

### 3.4 Adaptive control and pest management

We now discuss discrete-time analogues of the results in the previous two sections. In the 21st century, the world's population has climbed significantly, leading to high pressure on food production and a resulting a huge competition for arable farming [23]. Food production is at risk from pests and so pest management research continues to develop. Recently, Guiver et al. [1], developed an approach to pest management inspired by adaptive control. Specifically, [1] proposed the following simple adaptive stabilizing control system.

$$\left. \begin{aligned} x(t+1) &= (A - B\phi(u(t))F)x(t), & x(0) &= x_0 \\ y(t) &= Cx(t), \\ u(t+1) &= u(t) + \|y(t)\|^p, & u(0) &= u_0 \end{aligned} \right\} t \in \mathbb{N}_0. \quad (3.8)$$

In (3.8),  $n, m \in \mathbb{N}$ ,  $x(t) \in \mathbb{R}_+^n$  is the population structure,  $A \in \mathbb{R}_+^{n \times n}$  is the projection matrix for the population,  $(B, F) \in \mathbb{R}_+^{n \times m} \times \mathbb{R}_+^{m \times n}$  are control design parameters related to which states are targeted by the pesticide. The parameter  $u(t)$  represents the volume of pesticide applied and  $y = Cx$  with  $C \in \mathbb{R}_+^{p \times n}$  is the measurement or information about  $x(t)$ .

The initial pesticide effort in the scheme (3.8) is represented by  $u_0$ .

The term  $\|y(t)\|^p$ ,  $p > 1$ , is used to convert measured pest abundance  $\|y(t)\|$  into a change of control effort at the following time step and so determines how quickly the control effort  $u$  rises <sup>1</sup>. The function  $\phi$  is a design parameter, capturing the efficacy of the pesticide action in response to applied pesticide  $u$ .  $\phi : \mathbb{R}_+ \rightarrow \mathbb{R}_+^{m \times m}$  with continuous, strictly increasing components  $\phi_i$  vanishing at zero and satisfying image  $\phi_i \subset [0, 1]$ . Examples of  $\phi_i$  functions are

$$\phi_i(u) = 1 - e^{-au}, \quad \phi_i(u) = \tanh(au) \quad \text{or} \quad \phi_i(u) = \frac{u}{a+u},$$

---

<sup>1</sup>Note, we have adopted a slightly simpler set up than [1]

where  $a > 0$ .

The following result is proved in [1].

**Proposition 3.7.** *Suppose for all  $\omega \in [0, \infty)$ , that the resulting matrix as  $A - B\phi(\omega)F$  is non-negative and irreducible and that  $\lambda(A - B\phi(\omega)F) < 1$  for some  $\omega$ . Then for all  $x_0 \in \mathbb{R}_+^n$  and  $u_0 \in \mathbb{R}_+^m$ , the solution of the scheme (3.8) satisfies*

$$\|x(t)\| \leq M\gamma^t \|x_0\|, t \in \mathbb{N}_0 \quad \text{for some } M > 0 \text{ and } \gamma \in (0, 1), \quad (3.9)$$

there exists  $u_\infty \geq 0$  so that

$$\lim_{t \rightarrow \infty} u(t) = u_\infty$$

and

$$\lambda(A - B\phi(u_\infty)F) < 1. \quad (3.10)$$

**Remark 3.8.**

(i) For each fixed  $x_0$ , the inequality (3.9) ensures that the  $x(t)$  component of the solution  $(x, u)$  of (3.8) converges to zero exponentially. However, the positive constants  $M$  and  $\gamma$  that appear in (3.9) both depend on the initial conditions  $x^0$  and  $u^0$ . Therefore, (3.9) does not yet imply that (3.8) is globally exponentially stable.

(ii) The conclusions of Proposition 3.7 need not hold if the assumption that  $A - B\phi(\omega)F$  is irreducible for every  $\omega \in [0, \infty)$  in 3.7 is relaxed. For example, consider

$$A = \begin{bmatrix} f_1 & 0 \\ 0 & f_2 \end{bmatrix}, \quad B = \begin{pmatrix} 1 \\ 0 \end{pmatrix}, \quad F = \begin{bmatrix} f_1 & 0 \end{bmatrix}, \quad C = \begin{bmatrix} 0 & 1 \end{bmatrix}, \quad q = 1,$$

where  $f_1 > 1$  and  $f_2 \in (0, 1)$ . Here  $A - \gamma BF$  is reducible for any  $\gamma \in [0, 1)$ . Furthermore,

$y(t) = f_2^t x_2(0) \rightarrow 0$  exponentially as  $t \rightarrow \infty$ , and thus

$$u(t) = u^0 + \sum_{j=0}^{t-1} \|y(t)\| \rightarrow u^0 + \frac{x_2^0}{1 - f_2} =: u_\infty < \infty \quad \text{as } t \rightarrow \infty.$$

Now

$$x_1(t+1) = f_1(1 - \phi(u(t)))x(t) \geq f_1(1 - \phi(u_\infty))x(t) \implies x_1(t) \rightarrow \infty \text{ as } t \rightarrow \infty,$$

when  $f_1(1 - \phi(u_\infty)) > 1$ .

(iii) If  $x_0 = 0$ , then  $x(t) = 0$  for all  $t \in \mathbb{N}_+$ , and hence (3.9) trivially holds. In this case,  $u(t) = u^0$  for  $t \in \mathbb{N}_+$  and so  $(0, u^0)$  is an equilibrium of (3.8) for all  $u^0 \in \mathbb{R}_+$ . However, one striking property is that for all nonzero  $x^0$ , and any  $u^0 \geq 0$  the limiting control effort  $u_\infty$  is stabilising. This is analogous to Theorem 4.4 in Chapter 4. See also Section 3.6 for further context.

**Remark 3.9.** The relative degree one and minimum phase assumptions used in the continuous-time set up are replaced with an assumption about the existence of a stabilising feedback  $F$ . In fact, the continuous-time minimum phase assumption does not have a meaningful analogue for discrete-time systems.

### 3.5 Adaptive destabilization and persistence

In Proposition 3.7 the emphasis is on stabilisation, that is, driving the population to zero. This is relevant in a context of eliminating a pest. Alternatively, we might want population persistence. This is explored in [24]. The idea used there is to switch between possible population dynamics in search of a growing population and then find a way for the switching to converge. This is summarised as follows in the simplified case from [24] where the dynamics are given by the density independent population projection.

Consider a switching system

$$\begin{aligned} x(t+1) &= A_{s(t)}x(t), \\ u(t+1) &= u(t) + \begin{cases} 0, & M \leq \|u(t)\| \quad \text{or} \quad \|u(t)\|=0, \\ \frac{1}{\|u(t)\|^q}, & \|u(t)\| < M. \end{cases} \end{aligned} \quad (3.11)$$

Here  $A_{s(t)} \in \{A_1, \dots, A_l\} \subset \mathbb{R}_+^{n \times n}$ ,  $n \in \mathbb{N}$ ,  $u(0) = u_0$ ,  $t \in \mathbb{Z}_+$ . In (3.11)  $M$  is positive and represents a design parameter, and  $q > 1$ . The key point is that  $A_{s(t)}$  switches through a set of possible matrices.

**The procedure of picking the switching condition**

(a) Let  $\{\tau(j)\}_{j=0}^\infty$  be a sequence of positive numbers satisfying a growth condition

$$\frac{\tau(j+1)}{\tau(j)} \rightarrow \infty \quad \text{as} \quad j \rightarrow \infty.$$

So  $\tau$  grows faster than exponentially

(b) Now define a function  $\kappa : \mathbb{R}_+ \rightarrow \{1, \dots, l\}$  by

$$\kappa(z) = \begin{cases} 1, & z = 0, \\ (j \bmod l) + 1, & z \in (\tau(j-1), \tau(j)], \quad j \in \mathbb{N} \quad \text{and} \quad l \in \mathbb{N}. \end{cases} \quad (3.12)$$

(c) The matrices  $A_{s(t)}$  switch between the  $q$  matrices  $A_1, \dots, A_l$  according to

$$s(t) = \kappa(u(t)). \quad (3.13)$$

**Proposition 3.10.** *Assume that*

- *each  $A_i, i = 1, \dots, l$ , are irreducible and*
- *at least one  $A_i$  satisfies  $\lambda(A_i) > 1$ .*

*Then for all initial conditions  $x(0) = x_0$  and  $u(0) = u_0$ , with  $x_0 \in \mathbb{R}_+^n$ ,  $u(t)$  and  $x(t)$  given by*

(3.11), with switching given by (3.5), (3.12) and (3.13), satisfy  $u(t)$  converges to  $u(\infty)$ , so that  $\lambda(A_{s(\infty)}) > 1$  and  $x(t)$  diverges exponentially.

**Remark 3.11.** Here we see that the limiting system matrix  $A_{s(\infty)}$  is unstable unless  $x_0 = 0$ . See Section 3.6 for further context.

### 3.6 Do adaptive controllers learn to stabilise?

The adaptive controllers considered in Sections 3.3 and 3.4 fall under a general set up of an adaptive or nonlinear feedback

$$u(t) = F(x(t), p(t)), \quad (3.14)$$

where the parameter  $p(t)$  is subject to its own dynamics that are updated with information about the state  $x(t)$ . For example, in the Byrnes-Willems controller, (3.14) has  $p = k$ ,

$$F(x, p) = -kCx, \quad \text{with update dynamics} \quad \dot{k} = \|Cx\|^2.$$

In the adaptive pest control algorithm, the updates involve a switching through potential systems (in general this would be switching through potential feedbacks). These general adaptive controllers are powerful in that they can stabilise whole families of unknown systems. They do so, so long as the adaptation is kept active. They also guarantee convergence of the parameter  $p(t)$  to some limiting value  $p(\infty)$  which, in general, will depend on the initial conditions imposed and, of course, the system data. This leads to a fundamental question: Do the parameter updates converge to stabilising values – values which would guarantee stabilisation if used in a nonadaptive controller. That is, does the feedback

$$u(t) = F(x(t), p(\infty)) \quad (3.15)$$

stabilise? If true, then the adaptive controller would learn a non-adaptive stabilising controller. In an award-winning paper by Krstic [25], it is claimed that this is indeed the case. Specifically, Krstic showed that, except for a set of initial conditions in a “bad set” with Lebesgue measure zero, the parameter estimates  $p(t)$  do converge to stabilising values  $p(\infty)$  and a non-adaptive feedback is learnt – at least generically. Unfortunately, the result by Krstic turned out to be flawed. Indeed, Townley [26] gave a simple, two-dimensional example with quadratic nonlinearity in which the “bad set” is actually one quarter of the  $(x, p)$  state space. This is something of a pity because it would be quite remarkable if these classes of adaptive controllers did possess such learning properties. However, some positive statements can be made with regards to the “bad set”:

- Lamooki et al. [27] use advanced bifurcation methods to show, in the case of the Byrnes-Willems adaptive controller, that the “bad set” does indeed have Lebesgue measure zero. The key idea is to draw on the theory of normal forms for dynamical systems;
- Using a topological approach, it is shown in Townley [28], for a class of switching adaptive systems, that again the “bad set” has measure zero – in fact in this case the “bad set” is at most a countable union of sets with dimension less than  $n$ , the dimension of the state space. Here the key is to decompose the closed loop system dynamics into a sequence of diffeomorphisms derived from the switching structure.

In Chapter 4 we will return to the “learning” question. Specifically, we show for a subset of systems that the Byrnes-Willems adaptive controller is guaranteed to learn a stabilising feedback unless the initial condition is zero - that is the “bad set” is a point. We go further and develop an algorithm that actually learns a threshold parameter.

## 3.7 Conclusion

The purpose of this chapter was to review some essential elements of the vast topic of adaptive control. We first looked briefly at the ideas of direct versus indirect adaptive control via an example. We then focused on specific examples of direct adaptive control relevant to the remainder of the the thesis. Specifically we considered:

- The Byrnes-Willems high-gain adaptive controller;
- Recent developments in adaptive control and pest management;
- Adaptive destabilisation or persistence through adaptive switching idea.

The final section of this chapter posed and discussed the question: “Do adaptive controllers learn to stabilise”. This fundamental question became a central part of the thesis and is developed substantially in Chapter 4, as well as in Chapter 5.

# Chapter 4

## A Bifurcation Learning Algorithm

**Overview:** in this chapter we continue a line of research which, for over two decades or more, asks: “Does a stabilising adaptive feedback controller learn a stabilising gain?” We restrict attention to classes of adaptive feedback controllers inspired by so-called Byrnes-Willems high-gain adaptive controllers. The main results are:

- For non-negative systems arising in population ecology, we can prove that the Byrnes-Willems adaptive high-gain stabilising controller does indeed learn a (positive enough) stabilising gain – Theorem 4.4;
- We also consider destabilisation, a.k.a persistency. Borrowing from the Byrnes-Willems approach we design an adaptive destabilising controller. Again, for non-negative systems, we can prove that the adaptive high-gain destabilising controller does indeed learn a (negative enough) destabilising gain – Theorem 4.8;
- The class of “population-ecology” inspired non-negative systems under consideration admits a simple transition: there is a critical saddle-node bifurcation threshold so that gains above this critical threshold are stabilising, gains below are destabilising. Surprisingly we

find that if the positive high-gain and negative high-gain algorithms are combined, then the saddle-node bifurcation is learnt – Theorem 4.13.

- We use the main result in Theorem 4.13 to develop a novel set-point controller. For a target set-point  $r$ , the new adaptive controller achieves asymptotic tracking of  $r$  without knowledge of system parameters. Because the underpinning nonlinear system has a locally stable equilibrium there is guaranteed robustness. This contrasts with the usual sensitivity and fragility of adaptive controllers to unmodelled disturbances.

**Simulation Result 4.1.** In Subsection 4.4, Figures 4.1, 4.2, 4.4, 4.3, A.4, A.5 and A.6 we compare the results from Theorems 4.4, 4.8 and 4.13 for various systems of dimensions 3, 4, 5, 8, 9, 10 and 13. These results suggest quite strongly that the already proved local stability is in fact global.

## 4.1 Byrnes-Willems adaptive control with a stabilising limit gain

Recall from Chapter 3 the development of a Byrnes and Willems adaptive controller [8] for relative degree one, minimum-phase systems

$$\dot{x}(t) = Ax(t) + bu(t), \quad x(0) = x_0, \quad y(t) = c^T x(t). \quad (4.1)$$

Here  $x(t) \in \mathbb{R}^n$ ,  $u(t), y(t) \in \mathbb{R}$ ,  $A \in \mathbb{R}^{n \times n}$ ,  $b, c \in \mathbb{R}^n$ . The relative degree one and minimum-phase assumptions permit the use of the coordinate transformation

$$x = Tw, \quad T = \begin{bmatrix} b \\ c^T b \end{bmatrix} V \quad w = \begin{pmatrix} y \\ z \end{pmatrix},$$

where the columns of  $V \in \mathbb{R}^{n \times (n-1)}$  span the kernel of  $c^T$ , and so to rewrite the dynamics (3.3) in the form

$$\begin{aligned}\dot{y}(t) &= ay(t) + \alpha^T z(t) + c^T bu(t) \\ \dot{z}(t) &= \beta y(t) + A_2 z(t).\end{aligned}\tag{4.2}$$

The Byrnes-Willems High Gain adaptive controller is given by

$$\begin{aligned}u(t) &= -k(t)y(t) \\ \dot{k}(t) &= y^2(t).\end{aligned}\tag{4.3}$$

Then for all  $x(0) = x_0 \in \mathbb{R}^n$ , i.e.  $y(0) \in \mathbb{R}$  and  $z(0) \in \mathbb{R}^{n-1}$  we have that

$$\lim_{t \rightarrow \infty} \begin{pmatrix} y(t) \\ z(t) \end{pmatrix} = 0 \quad \text{and} \quad \lim_{t \rightarrow \infty} k(t) = k_\infty(x_0) < \infty.$$

In Section 3.6 of Chapter 3 we introduced the question of whether adaptive controllers learn to stabilize. In general the answer is negative as discussed in Section 3.6. However, for a subset of relative degree one systems we can prove that the Byrnes-Willems adaptive controller does indeed learn to stabilise. We first recall some facts about Metzler matrices.

**Definition 4.2.** 1. A matrix  $M$  is Metzler if  $(pI + M)$  has only positive entries for some  $p \in \mathbb{R}$ .

2. A matrix  $M$  is irreducible if, in its corresponding di-graph, every node  $i$  is connected to a node  $j$  by a path of some length dependent on  $i$  and  $j$ .

3. A non-zero vector  $v$  is positive (non-negative) if all its entries are positive. (non-negative).

**Lemma 4.3.** *If  $M$  is Metzler and irreducible, then the eigenvalue of  $M$  with largest real part is a real eigenvalue of  $M$  and its corresponding left and right eigenvectors are strictly positive – we call this real eigenvalue with largest real part the Perron eigenvalue of  $M$ .*

See Theroem 3.4 in [29].

**Theorem 4.4.** *The limit gain is stabilising. In addition to the relative degree one and minimum-phase assumptions, suppose also that*

$A_2$  is Metzler, and  $\alpha$  and  $\beta$  are non-negative

and

$$\begin{pmatrix} a & \alpha^T \\ \beta & A_2 \end{pmatrix}$$

is irreducible. Then for all non-negative initial  $y(0)$  and  $z(0)$ , the limit gain  $k_\infty(x_0)$  is stabilizing in the sense that every eigenvalue of the limiting system matrix

$$A - k_\infty(x_0)bc^T = \begin{pmatrix} a - k_\infty(x_0)c^Tb & \alpha^T \\ \beta & A_2 \end{pmatrix} \quad (\text{in transformed coordinates})$$

has negative real part.

**Remark 4.5.** This subset of minimum phase, relative degree one systems used in Theorem 4.4 can be interpreted as the feedback connection between a scalar system and a stable and monotone Metzler system:

$$v = u + \frac{1}{c^Tb}w \quad \begin{cases} \dot{y}(t) = ay(t) + c^Tbv(t) \\ \dot{z}(t) = A_2z(t) + \beta y(t), \quad w(t) = \alpha^Tz(t). \end{cases} \quad (4.4)$$

**Proof of Theorem 4.4** We work in the new coordinate system so that

$$A - kbc^T = \begin{pmatrix} a - kc^Tb & \alpha^T \\ \beta & A_2 \end{pmatrix}$$

and in which  $A - kbc^T$  is both Metzler and irreducible.

We already know from Proposition 3.4 that the gain  $k(t)$  converges to a limit  $k_\infty(x_0)$ .

Suppose that  $k_\infty(x_0)$  is not stabilizing, that is at least one eigenvalue of  $A - k_\infty(x_0)bc^T$  has non-negative real part. It follows, from the Metzler property and irreducibility, that the Perron eigenvalue of  $A - k_\infty(x_0)bc^T$  is non-negative. Then for all  $t$  we have that

$$(A - k(t)bc^T) \geq (A - k_\infty(x_0)bc^T) \implies \dot{x}(t) \geq (A - k_\infty(x_0)bc^T)x(t).$$

It follows that

$$x(t) \geq e^{(A - k_\infty(x_0)bc^T)t} x(0)$$

and every component of  $x(t)$  is bounded from below by a positive number. It follows that  $k(t)$  cannot converge. But we already know that  $k(t)$  converges. This is a contradiction. So no eigenvalue of  $A - k_\infty(x(0))bc^T$  has non-negative real part and so all eigenvalues of  $A - k_\infty(x(0))bc^T$  have negative real parts. It follows that  $A - k(t^*)bc^T$  has only eigenvalues with negative real part if  $t^*$  is large enough. But then for all  $t \geq t^*$ ,

$$\dot{x}(t) = (A - k(t)bc^T)x(t) \leq (A - k(t^*)bc^T)x(t)$$

and so

$$x(t) \leq e^{(A - k(t^*)bc^T)(t - t^*)} x(t^*) \rightarrow 0 \text{ exponentially.}$$

□

**Remark 4.6.** (a) Theorem 4.4 is a continuous-time parallel of the discrete-time Proposition 5.3 in Chapter 5.

(b) In the 1990s, there was much interest in the question of whether these simple adaptive controllers can “find” stabilizing gains. For general systems the best we can hope for is that the limit system (3.7) is stable for almost all initial conditions. For Metzler systems however, the stabilizing property does hold and the limit system (3.7) is always stable.

(c) For the system (4.4) with  $A_2$  Metzler, we have that there exists  $k_c$  so that if  $k > k_c$  then  $A - kbc^T$  is stable whilst if  $k < k_c$  then  $A - kbc^T$  is unstable. Moreover, for  $k < k_c$  but close to  $k_c$ ,  $A - kbc^T$  has one, and only one, and hence real, eigenvalue with positive real part. It follows, that  $k_c$  is a saddle-node bifurcation.

(d) In fact, in the set up of (3.4),

$$k_c = a + \alpha^T (A_2)^{-1} \beta. \quad (4.5)$$

We know that

$$k_\infty(x(0)) > k_c,$$

but this can be very conservative. Indeed, in the case of a scalar system

$$\begin{aligned} \dot{y}(t) &= (a - k(t))y(t) \\ \dot{k}(t) &= y(t)^2, \end{aligned}$$

we have that  $k_c = a$  and

$$y^2 + (k - a)^2 = y(0)^2 + (k(0) - a)^2 \implies k(\infty) = a + \sqrt{y(0)^2 + (k(0) - a)^2}.$$

so that for all  $k > k_c$ , there will exist  $y(0)$  and  $k(0)$  so that  $k_\infty(x(0)) > k$ .

## 4.2 Byrnes-Willems style adaptive destabilisation with a destabilising limit gain

In Section 4.1, the focus is on stabilisation – the usual setting in control theory/dynamical systems contexts. In population ecology this translates to population abundance being driven to zero – i.e. population eradication. This is relevant when the population under consideration is an unwanted pest. But in ecology there is at least equal interest in populations that are not eradicated, with conservation actions looking for persistent populations. With this motivation,

here we develop adaptive destabilizing (i.e. persistency) controllers in the spirit of Byrnes and Willems.

**Lemma 4.7.** *As above in the transformed coordinates, let  $A$  be Metzler and  $b$  and  $c$  be non-negative with  $c^T b > 0$ . There exist positive  $g^*, s$  and  $p$  so that*

$$c^T (sI + A + g^* bc^T) \geq pc^T.$$

The following theorem is a parallel to the discrete-time Proposition 5.6 in Chapter 5..

**Theorem 4.8.** *A Byrnes – Willems style adaptive destabilizing controller*

*Let  $x(t)$  and  $g(t)$  be the solution of<sup>1</sup>*

$$\begin{aligned} \dot{x}(t) &= (A + g(t)bc^T)x(t), & x(0) &= x_0 \geq 0 \\ \dot{g}(t) &= \frac{1}{c^T x(t)}, & g(0) &= g_0 > 0. \end{aligned} \tag{4.6}$$

*Then  $x(t)$  is non-negative,  $g(t)$  is positive for all  $t \geq 0$ , and*

$$\lim_{t \rightarrow \infty} g(t) = g_\infty(x_0) < \infty.$$

*Moreover, the limit matrix  $A + g_\infty(x_0)bc^T$  is exponentially unstable, so that  $g_\infty(x_0) > -k_c$ , and  $x(t) \rightarrow \infty$  component-wise-exponentially.*

**Remark 4.9.** We can modify the controller of the system (4.6), without changing the outcome, by adding a parameter  $\varepsilon_2 > 0$

$$\dot{g}(t) = \frac{\varepsilon_2}{c^T x(t)}$$

---

<sup>1</sup>Here the gain is labelled  $g$  and since we expect it to be destabilising it appears as  $+g$  (so plus  $g$ ), in contrast to the gain  $k$  in Section 4.2 which is stabilising and appears as  $-k$  (so minus  $k$ ). In comparing the two, it is  $g$  compared to  $-k$ , relative to a critical  $-k_c$ .

This will be useful to speed up or slow down the adaption when are comparing different algorithms.

**Proof**

Let

$$W(t) = \frac{1}{c^T x(t)} + \frac{1}{2} c^T b \left( g(t) - \frac{s + g^* c^T b}{c^T b} \right)^2.$$

Set  $c^T x = y$ . Then, in view of Lemma 4.7

$$\begin{aligned} \frac{d}{dt} W &= -\frac{1}{y^2} c^T \dot{x} + c^T b \left( g(t) - \frac{s + g^* c^T b}{c^T b} \right) \dot{g} \\ &= -\frac{1}{y^2} \underbrace{c^T (sI + A + g^* b c^T)}_{\geq p c^T x} x + \underbrace{\frac{1}{y^2} (sI + (g^* - g) c^T b) \underbrace{c^T x}_{=y} + c^T b \left( g(t) - \frac{s + g^* c^T b}{c^T b} \right)}_{=0} \frac{1}{y} \\ &\leq -\frac{p}{y}. \end{aligned}$$

It follows that

$$\int_0^t \frac{1}{y(s)} ds \leq \frac{1}{p} (W(0) - W(t)) \leq \frac{1}{p} W(0) < \infty.$$

Now  $y(t)$  is always non-negative and so  $\int_0^t \frac{1}{y(s)} ds$  is a non-decreasing and bounded function.

Therefore

$$g(t) = g(0) + \int_0^t \frac{1}{y(s)} ds \quad \text{converges to a limit } g_\infty(x_0).$$

Suppose that  $A + g_\infty(x_0) b c^T$  is not exponentially unstable. Then the Perron eigenvalue  $r$  of  $A + g_\infty(x_0) b c^T$  is non-positive.

Let  $v^T$  be the positive left eigenvector of the Metzler matrix  $A + g_\infty(x_0) b c^T$  corresponding to the non-positive Perron eigenvalue  $r$ . So

$$v^T (A + g_\infty b c^T) = r v^T.$$

Since  $v^T$  is positive it follows that

$$c^T x(t) \leq \alpha v^T x(t), \quad \text{for some positive } \alpha \quad \implies \frac{1}{c^T x(t)} \geq \frac{1}{\alpha} \frac{1}{v^T x(t)}, \text{ for all } t \geq 0.$$

Now

$$\begin{aligned} \frac{d}{dt} v^T x(t) &= v^T (A + g(t)bc^T)x(t) \\ &= v^T (A + g_\infty(x_0)bc^T)x(t) - (g_\infty(x_0) - g(t))v^T bc^T x(t) \\ &= rv^T x(t) - (g_\infty(x_0) - g(t))v^T bc^T x(t) \leq rv^T x(t) \implies v^T x(t) \leq v^T x(0). \end{aligned}$$

But then

$$\frac{1}{v^T x(t)} \geq \frac{1}{v^T x(0)} \implies \frac{1}{c^T x(t)} \geq \frac{1}{\alpha} \frac{1}{v^T x(0)} > 0, \text{ for all } t \geq 0.$$

This contradicts that  $\int_0^\infty 1/y(t)dt < \infty$ . So  $A + g_\infty(x_0)bc^T$  has to be exponentially unstable.

Then  $A + g(t^*)bc^T$  is unstable for some  $t^* \geq 0$  and

$$\dot{x}(t) = (A + g(t)bc^T)x(t) \geq (A + g(t^*)bc^T)x(t) \quad \text{for all } t \geq t^*$$

guarantees that  $x(t)$  diverges component-wise exponentially. □

**Remark 4.10.** We see from the Theorem above that the adaptive controller learns a destabilizing gain  $g_\infty(x_0) > -k_c$ . However, as with Byrnes-Willems adaptive stabilization, for all  $g > -k_c$  there will exist initial conditions so that  $g_\infty(x_0) > g$ .

**Corollary 4.11.** *The following inequality holds*

$$\frac{1}{c^T x(t)} + \frac{1}{2}c^T b \left( g(t) - \frac{s + g^*c^T b}{c^T b} \right)^2 \leq \frac{1}{c^T x(0)} + \frac{1}{2}c^T b \left( g(0) - \frac{s + g^*c^T b}{c^T b} \right)^2 \quad \text{for all } t \geq 0. \quad (4.7)$$

The bound (4.7) is a consequence of the Lyapunov-based proof of Theorem 4.8. It constrains

the dynamics quite strongly. In particular we have that

$$\frac{1}{y(t)} = \frac{1}{c^T x(t)} \leq \frac{1}{c^T x(0)} + \frac{1}{2} c^T b \left( g(0) - \frac{s + g^* c^T b}{c^T b} \right)^2 \quad \text{for all } t \geq 0.$$

### 4.3 Byrnes-Willems style bifurcation–learning adaptive algorithm

As a starting point, consider a one-plus-one system

$$\begin{aligned} \dot{y}(t) &= (g(t) - k(t))y(t) \\ \dot{k}(t) &= y^2(t) \\ \dot{g}(t) &= \frac{1}{y(t)} \end{aligned} \tag{4.8}$$

which combines the adaptive stabilization and destabilization algorithms from Sections 4.1 and 4.2, respectively. Then

$$\begin{aligned} y(t)\dot{y}(t) &= (g(t) - k(t))y^2(t) = (g(t) - k(t))\dot{k}(t) \\ -\frac{1}{y^2(t)}\dot{y}(t) &= -(g(t) - k(t))\frac{1}{y(t)} = -(g(t) - k(t))\dot{g}(t) \end{aligned}$$

With

$$W = \frac{1}{2}(g(t) - k(t))^2 + \frac{1}{2}y^2(t) + \frac{1}{y(t)}$$

we have

$$\frac{d}{dt}W = (g - k)(\dot{g} - \dot{k}) + y\dot{y} - \frac{1}{y^2}\dot{y} = (g - k)(\dot{g} - \dot{k}) + (g - k)\dot{k} - (g - k)\dot{g} = 0.$$

Therefore

$$\frac{1}{2}(g(t) - k(t))^2 + \frac{1}{2}y^2(t) + \frac{1}{y(t)} = \frac{1}{2}(g(0) - k(0))^2 + \frac{1}{2}y^2(0) + \frac{1}{y(0)} \quad \text{for all } t \geq 0. \tag{4.9}$$

**Remark 4.12.** Let  $q = k - g$ . Then we can rewrite the (4.8) in the form

$$\dot{y} = -qy \quad \dot{q} = y^2 - \frac{1}{y}. \quad (4.10)$$

$y = 1, q = 0$  is an equilibrium with linearisation

$$\dot{w} = \begin{pmatrix} 0 & -1 \\ 3 & 0 \end{pmatrix} w.$$

So  $y = 1, g = k$  is a centre. The inequality (4.9) constrains the difference of  $k$  and  $g$  but allows the stabilizing and destabilizing gains to interweave. Such interweaving of stabilizing and destabilizing gains is explored further in Chapter (5).

We have seen in the above that for relative degree one, minimum phase, Metzler systems,

- the adaptive stabilizing controller learns a stabilizing gain, whilst
- the adaptive destabilizing controller learns a destabilizing gain.

However, both approaches can be highly conservative with neither approach getting close to learning the threshold gain  $k_c$ . Somewhat remarkably, combining the stabilizing and destabilizing adaptation mechanisms yields a convergent adaptation with limit gain actually equal to the threshold  $k_c$ .

**Theorem 4.13.** *Assume that*

$$\begin{aligned} \dot{y}(t) &= ay(t) + \alpha^T z(t) + c^T bu(t) \\ \dot{z}(t) &= \beta y(t) + A_2 z(t) \end{aligned} \quad (4.11)$$

where  $c^T b > 0$ ,  $\alpha, \beta \in \mathbb{R}_+^{n-1}$  are positive vectors<sup>2</sup> and  $A_2$  is an  $(n-1) \times (n-1)$  stable Metzler

---

<sup>2</sup>Positive vectors are non-zero vectors with non-negative entries

matrix. In addition, as above, assume that

$$\begin{pmatrix} a & \alpha^T \\ \beta & A_2 \end{pmatrix}$$

is irreducible.

Define an adaptive “arms-race” controller by

$$\begin{aligned} u(t) &= -q(t)y(t) \\ \dot{q}(t) &= y^2(t) - \frac{1}{y(t)}. \end{aligned} \quad (4.12)$$

(a) Then for all initial  $y(0) > 0$  and  $z(0) \geq 0$  we have that  $y(t) > 0$  and  $z(t) > 0$  for all  $t > 0$ ;

(b) The nonlinear closed loop system (4.11) and (4.12) has a unique equilibrium

$$\left(1, -A_2^{-1}\beta, \frac{a - \alpha^T(A_2)^{-1}\beta}{c^T b}\right) \quad (4.13)$$

(c) The linearisation of (4.11) and (4.12) around the equilibrium (4.13) is exponentially stable.

(d) For all initial conditions  $y(0), z(0)$  and  $q(0)$  close enough to the equilibrium (4.13),

$$\lim_{t \rightarrow \infty} q(t) = q_\infty(x_0) = k_c = \frac{a - \alpha^T(A_2)^{-1}\beta}{c^T b}.$$

**Remark 4.14.** We refer to the adaption of  $q$  in (4.12) as an “arms race” because the term  $y^2$  drives  $q$  up especially when  $y$  is large, whilst the term  $-1/y$  drives  $q$  down, especially when  $y$  is small. This “arms race” idea is further explored in Chapter 5.

**Remark 4.15.** We can modify the controller of the system (4.12), without changing the outcome, by adding a parameter  $\varepsilon_3 > 0$ :

$$\dot{q}(t) = \varepsilon_3 \left( y^2(t) - \frac{1}{y(t)} \right)$$

This will be useful to speed up or slow down the adaption when are comparing different algorithms.

**Remark 4.16.** (a) In all simulation (see Subsection 4.4) we have always seen that

$$\lim_{t \rightarrow \infty} \begin{pmatrix} y(t) \\ z(t) \end{pmatrix} = \begin{pmatrix} 1 \\ -A_2^{-1}\beta \end{pmatrix} \geq 0;$$

(b) Similarly, in all simulations, we have always seen that

$$\lim_{t \rightarrow \infty} q(t) = k_c = \frac{a - \alpha^T (A_2)^{-1} \beta}{c^T b};$$

(c) Both (a) and (b) are true if we start close enough to the unique equilibrium (4.13);

(d) In a weird sort of relationship, the linearization of (4.11) and (4.12) around the equilibrium (4.13) is given by

$$\dot{w}(t) = \begin{pmatrix} \alpha^T (A_2)^{-1} \beta & \alpha^T & -c^T b \\ \beta & A_2 & 0 \\ 3 & 0 & 0 \end{pmatrix} w(t)$$

which is the closed-loop matrix for the system

$$\dot{x}(t) = Ax(t) + bu(t), \quad y(t) = c^T x(t),$$

under integral control action

$$\dot{u}(t) = 3y(t).$$

**Proof of Theorem 4.13.** Part (a). We have that

$$\dot{y} = (a - qc^T b)y + \alpha^T z$$

$$\dot{z} = \beta y + A_2 z.$$

$y(\cdot)$  and  $z(\cdot)$  are continuous. We have that  $y(0) > 0$  and  $z(t) \geq 0$  and non-zero. Suppose that the scalar function  $y(\cdot)$  is not always positive and let  $T$  be the first time that  $y(T) = 0$ . From the  $\dot{z}$  equation we have, using the Metzler and irreducibility properties of  $A_2$ , that

$$z(t) = e^{A_2 t} z(0) + \int_0^t e^{A_2(t-s)} \beta y(s) \geq e^{A_2 t} z(0) > 0. \quad (4.14)$$

But then from the  $\dot{y}$  equation we have that

$$\dot{y}(T) = \alpha^T z(T) > 0.$$

But it is impossible for a non-negative function to hit zero with positive derivative. It follows that  $y(\cdot)$  is positive for all  $t \geq 0$ .

Now using (4.14) and again that  $A_2$  is Metzler and irreducible we have that  $z(t) > 0$  for all  $t$ .

Part (b). For the equilibrium we solve

$$(a - qc^T b)y + \alpha^T z = 0, \quad \beta y + A_2 z = 0 \quad \text{and} \quad y^2 - \frac{1}{y} = 0.$$

It follows that  $y = 1$ . Then

$$\beta y + A_2 z = 0 \implies z = -A_2^{-1} \beta.$$

Finally

$$(a - qc^T b)y + \alpha^T z = 0 \implies (a - qc^T b) - \alpha^T A_2^{-1} \beta = 0.$$

It follows that

$$q = \frac{a - \alpha^T (A_2)^{-1} \beta}{c^T b}$$

as required.

Part (c). The linearisation matrix has the form

$$L = \begin{pmatrix} m & \alpha^T & -c^T b \\ \beta & A_2 & 0 \\ k & 0 & 0 \end{pmatrix}$$

where  $k > 0$  (actually  $k = 3$ ),  $m = \alpha^T (A_2)^{-1} \beta < 0$ ,  $\alpha, \beta$  are positive (or maybe non-negative) vectors and  $A_2$  is Metzler stable and

$$M = \begin{pmatrix} m & \alpha^T \\ \beta & A_2 \end{pmatrix}$$

is Metzler and marginally stable with unique eigenvalue of maximum real part, which is zero.

We first show that all eigenvalues of  $L$  have non-positive real parts as follows. Let

$$M_\varepsilon = M - \varepsilon I$$

where  $\varepsilon > 0$ . Then  $M_\varepsilon$  is Metzler stable. It follows that  $M_\varepsilon$  is diagonally stable which means we can find a positive definite diagonal matrix [30]

$$D_\varepsilon = \text{diag}[d_1^\varepsilon, \dots, d_n^\varepsilon]$$

so that

$$D_\varepsilon M_\varepsilon + M_\varepsilon^T D_\varepsilon = -Q_\varepsilon, \quad \text{with} \quad Q_\varepsilon > 0$$

Now set

$$V = x^T D_\varepsilon x + \gamma u^2$$

Then computing  $\dot{V}$  along solutions of the system

$$\begin{pmatrix} \dot{x}(t) \\ \dot{u}(t) \end{pmatrix} = \begin{pmatrix} M_\varepsilon & -c^T b \begin{pmatrix} 1 \\ 0 \\ \vdots \\ 0 \end{pmatrix} \\ k[1 \ 0 \ \dots \ 0] & 0 \end{pmatrix} \begin{pmatrix} x(t) \\ u(t) \end{pmatrix}$$

gives

$$\dot{V} = x^T (D_\varepsilon M_\varepsilon + M_\varepsilon^T D_\varepsilon) x - 2x^T D_\varepsilon c^T b \begin{pmatrix} 1 \\ 0 \\ \vdots \\ 0 \end{pmatrix} u + 2\gamma k x_1 u = -x^T Q_\varepsilon x \quad \text{if} \quad \gamma = \frac{c^T b d_1^\varepsilon}{k}$$

It follows from La Salle's Invariance Principle that  $(x, u)$  converge to the largest invariant set contained in

$$\{(x, u) \text{ so that } x^T Q_\varepsilon x = 0\} \implies x \equiv 0 \text{ and } \dot{x} \equiv 0$$

from which it follows, from invariance, that  $u \equiv 0$ . So the matrix  $L_\varepsilon$ , obtained by replacing  $M$  with  $M_\varepsilon$ , is exponentially stable — i.e. all eigenvalues have negative real parts. From continuity of eigenvalues with respect to the parameter  $\varepsilon$  it follows that all the eigenvalues of  $L$  have non-positive real part.

We can show that zero is not an eigenvalue of  $L$  as follows. Suppose, to the contrary, that zero is an eigenvalue of  $L$  with non-zero eigenvector  $w$ . We can write

$$w = \begin{pmatrix} y \\ z \\ u \end{pmatrix} \quad \text{and then} \quad \begin{pmatrix} m & \alpha^T & -c^T b \\ \beta & A_2 & 0 \\ k & 0 & 0 \end{pmatrix} \begin{pmatrix} y \\ z \\ u \end{pmatrix} = \begin{pmatrix} 0 \\ 0 \\ 0 \end{pmatrix}$$

Reading from the equations:  $ky = 0 \implies y = 0$ ; Then  $A_2z = 0 \implies z = 0$ ; Finally  $c^Tbu = 0 \implies u = 0$ . But then  $w = 0$ , giving a contradiction.

Now suppose that  $L$  has an imaginary axis eigenvalue  $i\omega$ ,  $\omega \neq 0$ , with eigenvalue-eigenvector equation

$$\begin{pmatrix} m & \alpha^T & -c^Tb \\ \beta & A_2 & 0 \\ k & 0 & 0 \end{pmatrix} \begin{pmatrix} y \\ z \\ u \end{pmatrix} = i\omega \begin{pmatrix} y \\ z \\ u \end{pmatrix}$$

Without loss of generality we can assume  $y = 1$ . Since otherwise,  $y = 0$  and then trivially,  $z = u = 0$ . So, reading off the equations:

$$i\omega u = k \implies u = \frac{k}{i\omega}; z = (i\omega I - A_2)^{-1}\beta$$

and

$$\alpha^T A_2^{-1}\beta + \alpha^T (i\omega I - A_2)^{-1}\beta - c^T b \frac{k}{i\omega} = i\omega. \quad (4.15)$$

Taking real parts in (4.15) we then have

$$\alpha^T A_2^{-1}\beta + \text{real } \alpha^T (i\omega I - A_2)^{-1}\beta = 0$$

But when  $A_2$  is Metzler stable and  $\alpha$  and  $\beta$  are positive we know that <sup>3</sup>.

$$|\alpha^T (i\omega I - A_2)^{-1} \beta| < |\alpha^T A_2^{-1} \beta| = -\alpha^T A_2^{-1} \beta, \text{ for all } \omega \neq 0.$$

This gives a contradiction. So no such  $\omega$  exists and therefore  $L$  is exponentially stable as claimed.  $\square$

## 4.4 Bifurcation learning – simulation examples

Theorem 4.13 is a local result and so we can only claim convergence of  $q$  to the bifurcation point  $k_c$  for  $q$  starting close to  $k_c$  with  $y$  and  $z$  starting close to their respective equilibrium values. However, in exhaustive simulation studies the claimed convergence is the only global outcome. To demonstrate this we run simulations for a number of randomly generated systems of various randomly generated dimensions. We also use the same systems to illustrate Theorems

<sup>3</sup> Observe that  $\alpha^T (i\omega I - A_2)^{-1} \beta = \int_0^\infty e^{-i\omega t} \alpha^T e^{A_2 t} \beta dt$ . But  $A_2$  is Metzler, so that  $\alpha^T e^{A_2 t} \beta$  is positive. Then for non-zero  $\omega$ ,

$$\begin{aligned} \text{real } \alpha^T (i\omega I - A_2)^{-1} \beta &= \int_0^\infty \cos \omega t \alpha^T e^{A_2 t} \beta dt \\ &< \int_{\{\cos \omega t \geq 0\}} \cos \omega t \alpha^T e^{A_2 t} \beta dt \leq \int_{\{\cos \omega t \geq 0\}} \alpha^T e^{A_2 t} \beta dt < \int_0^\infty \alpha^T e^{A_2 t} \beta dt = -\alpha^T A_2^{-1} \beta. \end{aligned}$$

This can only fail if  $\alpha^T e^{A_2 t} \beta$  is identically zero on some non-zero interval. But this cannot be possible because of the assumed non-negativity. Indeed, we need only assume that the di-graph of  $A_2 + sI$  is irreducible for some  $s$ . Then  $sI + A_2$  is a non-negative irreducible matrix for some  $s$  meaning  $(sI + A_2)^l$  is strictly positive for some  $l$ . Now suppose that  $\alpha^T e^{A_2 t} \beta$  is identically zero for  $t$  in some non-zero interval  $[t_0 - \tau, t_0 + \tau]$ ,  $\tau > 0$ . Then  $e^{st} \alpha^T e^{A_2 t} \beta$  is also non-zero on that interval. It follows that

$$\alpha^T e^{(sI+A_2)t_0} \beta = 0, \alpha^T e^{(sI+A_2)t_0} (sI + A_2) \beta = 0, \dots, \underbrace{\alpha^T e^{(sI+A_2)t_0}}_{\geq 0} \underbrace{(sI + A_2)^l}_{> 0} \underbrace{\beta}_{\geq 0} = 0$$

$\therefore > 0$

But even without irreducibility of  $A_2$ , note also that for  $\omega^2 \neq c^T b/k$ , by taking magnitudes in (4.15), we have

$$|\alpha^T (i\omega I - A_2)^{-1} \beta| = \sqrt{(\alpha^T A_2^{-1} \beta)^2 + \frac{1}{\omega^2} \left( \omega^2 - \frac{c^T b}{k} \right)^2} > |\alpha^T A_2^{-1} \beta|,$$

again a contradiction.

4.4 and 4.8, in particular comparing the limit gains  $k_\infty(x_0) > k_c$ ,  $-g_\infty(x_0) < k_c$  and  $q_\infty(x_0) = k_c$ .

The system matrices for the simulations are given by

$$\begin{aligned}
 M_3 &= \begin{pmatrix} 1 & 4 & 3 \\ 3 & -8 & 2 \\ 3 & 4 & -6 \end{pmatrix}; & M_4 &= \begin{pmatrix} 9 & 3 & 2 & 4 \\ 1 & -7 & 1 & 2 \\ 3 & 1 & -6 & 4 \\ 3 & 1 & 4 & -8 \end{pmatrix}; \\
 M_6 &= \begin{pmatrix} 2 & 1 & 1 & 3 & 2 & 1 \\ 3 & -18 & 3 & 3 & 4 & 4 \\ 1 & 4 & -18 & 2 & 4 & 1 \\ 4 & 3 & 3 & -16 & 2 & 1 \\ 3 & 3 & 4 & 2 & -17 & 4 \\ 3 & 2 & 2 & 4 & 3 & -15 \end{pmatrix}; \\
 M_8 &= \begin{pmatrix} 9 & 1 & 3 & 2 & 3 & 4 & 2 & 4 \\ 1 & -17 & 1 & 2 & 2 & 4 & 4 & 4 \\ 3 & 1 & -16 & 4 & 4 & 1 & 4 & 2 \\ 3 & 3 & 2 & -18 & 1 & 1 & 1 & 2 \\ 3 & 1 & 2 & 2 & -18 & 1 & 3 & 3 \\ 2 & 4 & 1 & 1 & 3 & -17 & 1 & 3 \\ 2 & 4 & 1 & 1 & 1 & 1 & -17 & 2 \\ 4 & 2 & 3 & 3 & 3 & 2 & 4 & -18 \end{pmatrix}.
 \end{aligned} \tag{4.16}$$

**Simulation Result 4.17.** In the following simulations, 4.1, 4.2, 4.3 and 4.4. The left figures show the evolution of the population – Figure A to illustrate 4.4, Figure C to illustrate 4.8 and figure E to illustrate 4.13. The right figures show the limit gain – Figure B to illustrate 4.4, Figure D to illustrate 4.8 and Figure F to illustrate 4.13.

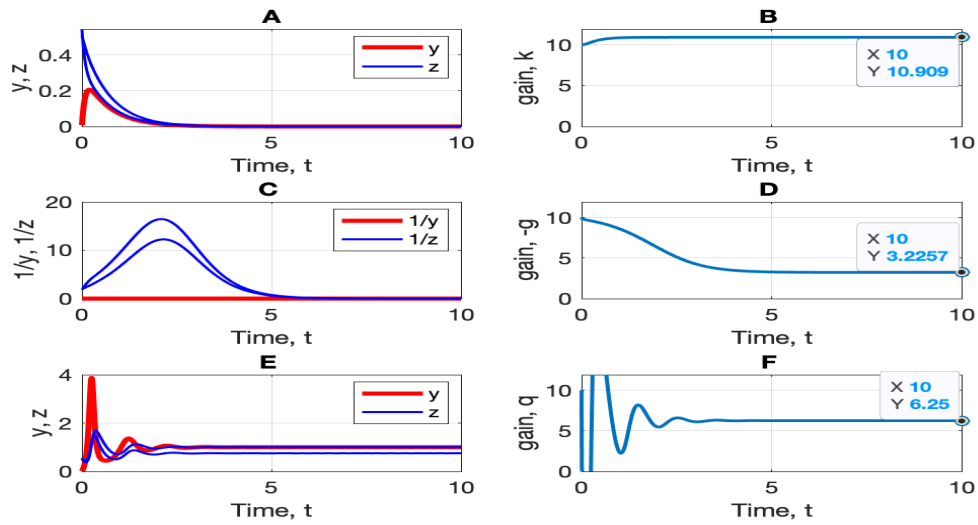


Figure 4.1: 3-dimensional simulation with  $A$  matrix given by  $M_3$  in (4.16) for the three adaptive controllers: A and B for controller (4.3); C and D for controller 4.6; E and F for controller (4.12).

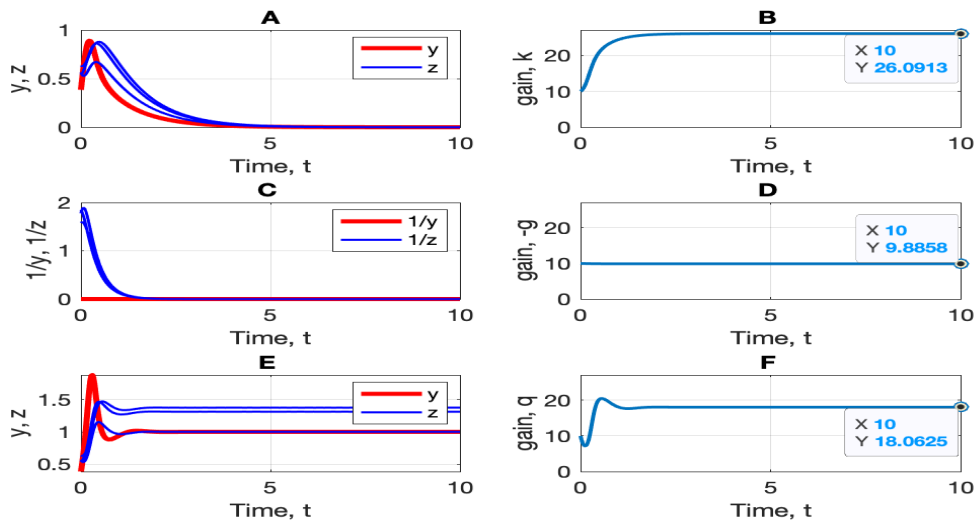


Figure 4.2: 4-dimensional simulation with  $A$  matrix given by  $M_4$  in (4.16) for the three adaptive controllers: A and B for controller (4.3); C and D for controller 4.6; E and F for controller (4.12).

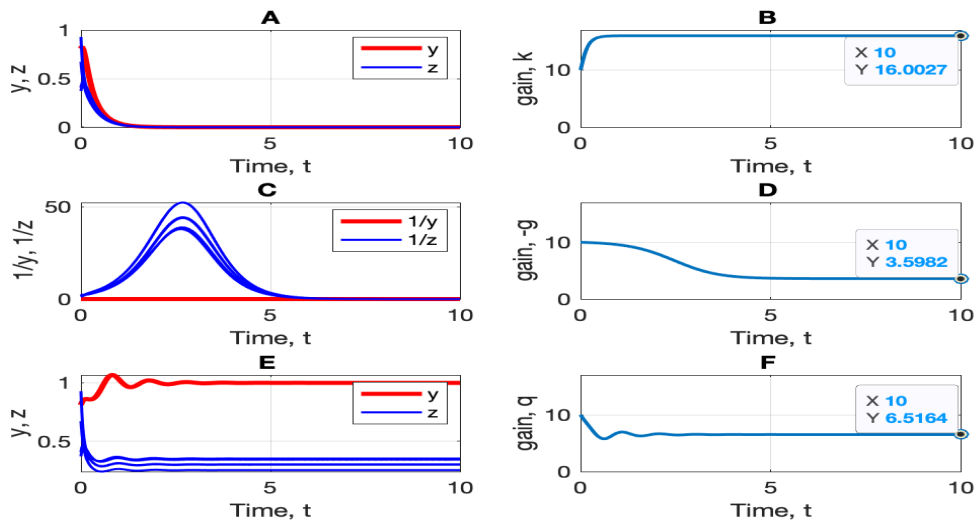


Figure 4.3: 6-dimensional simulation with  $A$  matrix given by  $M_6$  in (4.16) for the three adaptive controllers: A and B for controller (4.3); C and D for controller 4.6; E and F for controller (4.12).

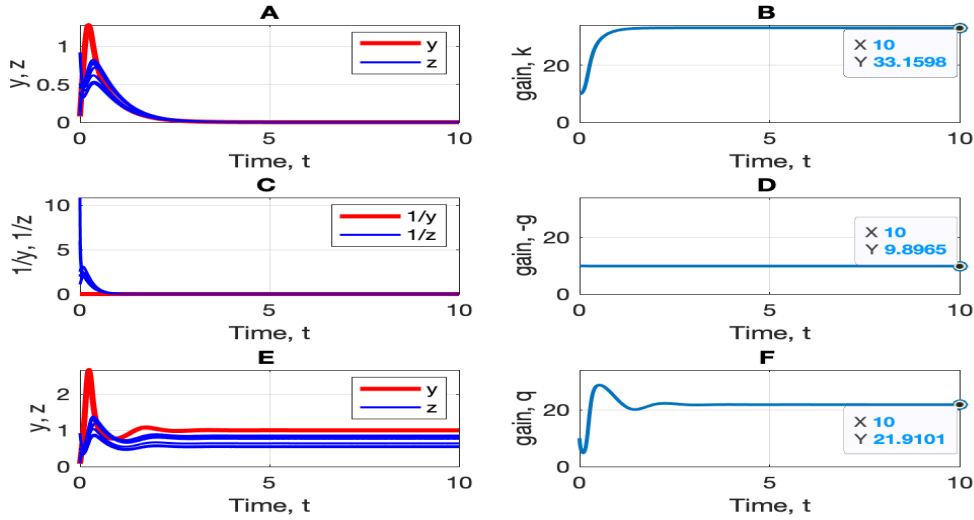


Figure 4.4: 8-dimensional simulation with  $A$  matrix given by  $M_8$  in (4.16) for the three adaptive controllers: A and B for controller (4.3); C and D for controller 4.6; E and F for controller (4.12).

**Remark 4.18.** Table 4.1 shows the limit value for Theorems 4.4, 4.8 and bifurcation value in the cases of systems with different dimensions, showing that  $k_\infty(x_0) > k_c$ ,  $-g_\infty(x_0) < k_c$  and  $q_\infty(x_0) = k_c$ .

Matrices	$k_\infty(x_0)$	$-g_\infty(x_0)$	$q_\infty(x_0)$	$k_c$
$M_3$	10.9090	3.2257	6.2500	6.2500
$M_4$	26.0913	9.8858	18.0625	18.0625
$M_6$	16.0027	3.5982	6.5164	6.5164
$M_8$	33.1598	9.8965	21.9101	21.9101

Table 4.1: The values of  $k_\infty(x_0)$ ,  $-g_\infty(x_0)$ ,  $q_\infty(x_0)$  and  $k_c$  for Simulation Result 4.17.

The simulations in Figures 4.1 , 4.2 , 4.3 and 4.4, show that the arms race controller (4.13) con-

verges to the bifurcation value irrespective of the randomly generated initial conditions and system/system dimension. Further higher dimensional systems are given in the Appendix, Section A.4. These various and numerous simulations suggest that the bifurcation algorithm achieves global stability even though the proof above is only local. In particular,  $q$  always learns  $k_c$ . Notice also the extent to which:  $k_\infty(x_0)$  and  $-g_\infty(x_0)$  over/underestimate  $k_c$ .

**Remark 4.19.** Additive noise on the output measurement  $y(t)$  breaks the simple Byrnes-Willems controller

$$\begin{aligned} u(t) &= -k(t)y(t) \\ \dot{k}(t) &= y^2(t). \end{aligned}$$

in that depending on the “fix”, by either saturating the measurement or the control below by zero, causes either the system to violate the positivity of the state or else produces a divergent gain. On the other hand, the “arms race” controller has inherent robustness to noise because of the convergence to an underlying exponentially stable equilibrium. This is further developed in Section 4.5.

## 4.5 Set point control with a proportional controller

Set-point control or tracking is an exemplar problem in control theory/engineering. It is ubiquitous in many applications from domestic central heating systems to trans-atlantic navigation for supertankers [31]. The aim is to design a controller so that the output of a system tracks, asymptotically, a constant set-point,  $r$ , say. The standard solution to the problem is to use integral control

$$\dot{u}(t) = k(r - y(t)), \quad u(0) = u_0. \quad (4.17)$$

For a stable, linear system

$$\dot{x}(t) = Ax(t) + bu(t), \quad y(t) = c^T x(t)$$

with positive, steady state gain  $-c^T A^{-1} b$ , the integral controller (4.17) achieves set-point control, i.e. asymptotic tracking, if the integral gain  $k$  is small enough. In fact, set-point control can be achieved without knowledge of the system if an adaptive integral controller is used [32]. In this case, we append (4.17) with adaptation of the integrator gain giving an adaptive integral controller

$$u(t) = \frac{1}{\ln k(t)}(r - y(t)), \quad \dot{k}(t) = (r - y(t))^2. \quad (4.18)$$

We can, in fact, use the bifurcation learning controller developed above to provide an alternative solution to this set-point control problem, applicable to Metzler systems as described earlier. We modify the adaptation mechanism in (4.12) so that

$$\begin{aligned} u(t) &= -q(t)y(t) \\ \dot{q}(t) &= \gamma \left( y^2(t) - \rho \frac{1}{y(t)} \right), \end{aligned} \quad (4.19)$$

with  $\gamma$  and  $\rho$  positive. Then we have an equilibrium

$$\left(\rho^{1/3}, -A_2^{-1}\beta, \frac{a - \alpha^T(A_2)^{-1}\beta}{c^T b}\right),$$

with exponentially stable linearisation

$$\dot{w}(t) = \begin{pmatrix} \alpha^T(A_2)^{-1}\beta & \alpha^T & -c^T b \rho^{1/3} \\ \beta & A_2 & 0 \\ 3\gamma\rho^{1/3} & 0 & 0 \end{pmatrix} w(t).$$

We can therefore use (4.19) to control the output  $y(t)$  asymptotically by choosing  $\rho$ . Indeed, we have that

$$\lim_{t \rightarrow \infty} \begin{pmatrix} y(t) \\ z(t) \end{pmatrix} = \rho^{1/3} \begin{pmatrix} 1 \\ -A_2^{-1}\beta \end{pmatrix}.$$

By choosing  $\rho = r^3$ , the proportional adaptive feedback controller achieves asymptotic tracking of the output  $y(t)$  to a set-point  $r$ . Effectively a proportional feedback controller yielding the performance of an integral control action.

**Remark 4.20.** 1. The parameter  $\gamma$  in (4.19) can be used to control the rate of decay.

Choosing  $\gamma\rho^{1/3} = 1$  will standardise the performance for varying set-point  $r = \rho^{1/3}$ .

2. In comparing the adaptive integral controller (4.18) with the modified “arms race” controller (4.19), in a context of set-point control, the former requires the system to be stable whereas the latter does not.
3. We note also that the integral controller (4.17) makes use of the “internal model principle” which says that if a controller can achieve asymptotic tracking of a reference signal, then the controller must contain dynamics that generate the reference signal [33]. In set-point control, the reference is a constant. Such constants are the dynamical consequences of

integrators and so, as expected, the integral controller contains an integrator. In the “arms race” controller, the control is not explicitly an integrated variable - although

$$u = -qy, \quad \dot{q} = y^2 - \frac{1}{y}$$

does contain integration to produce the gain.

4. The adaptive integral controller (4.18) suffers when the output is corrupted by noise so that instead of driving the integrator gain adaptation with an error  $r - y(t)$  we are forced to use  $r - y(t) - d(t)$  for some noise signal  $d(t)$ . Without further modification of the controller, this will cause  $k(t)$  to increase without bound and therefore the integrator gain  $1/\ln k(t)$  to decrease to zero – leading to slower and slower system response. The “arms race” controller (4.19) does not suffer these problems because the set-point corresponds to a locally stable equilibrium.

### Example

Consider the system

$$A = \begin{pmatrix} -7 & 2 & 1 & 1 \\ 2 & -5 & 3 & 1 \\ 2 & 1 & -5 & 1 \\ 3 & 2 & 2 & -6 \end{pmatrix} \quad b = \begin{pmatrix} 1 \\ 0 \\ 0 \\ 0 \end{pmatrix} \quad c^T = [1 \ 0 \ 0 \ 0].$$

The matrix  $A$  is Metzler stable because  $A$  has only positive entries except on the diagonal. The eigenvalue with largest real part is  $\lambda = -0.6704$ . So the assumptions for Theorem 4.13 hold and the “arms race” set-point (4.19) can be used. For the adaptive integral controller (4.18) to work, we additionally need that the steady stage gain  $-c^T A^{-1} b > 0$ . Now

$$-c^T A^{-1} b = \int_0^\infty c^T e^{At} b dt > 0$$

because the exponential of a Metzler matrix is positive. So (4.18) can be used.

We suppose a target set-point  $r = 2$  and compare the set-point control version of our bifurcation learning or “arms race” algorithm (4.19), with  $\gamma = 2$ , to the adaptive integral control algorithm (4.18). We assume that the output  $y(t)$  is corrupted by noise. Specifically, every 5 time unit, the output is disrupted by adding a random number between 0 and 0.2. In this case, the adaptation in the low-gain controller is constantly agitated and so the gain does not converge and performance diminishes as the integral gain  $1/\ln(k)$  is driven towards zero. In contrast, even with noise the adaptive bifurcation algorithm (4.19) will operate close to the exponentially stable equilibrium.

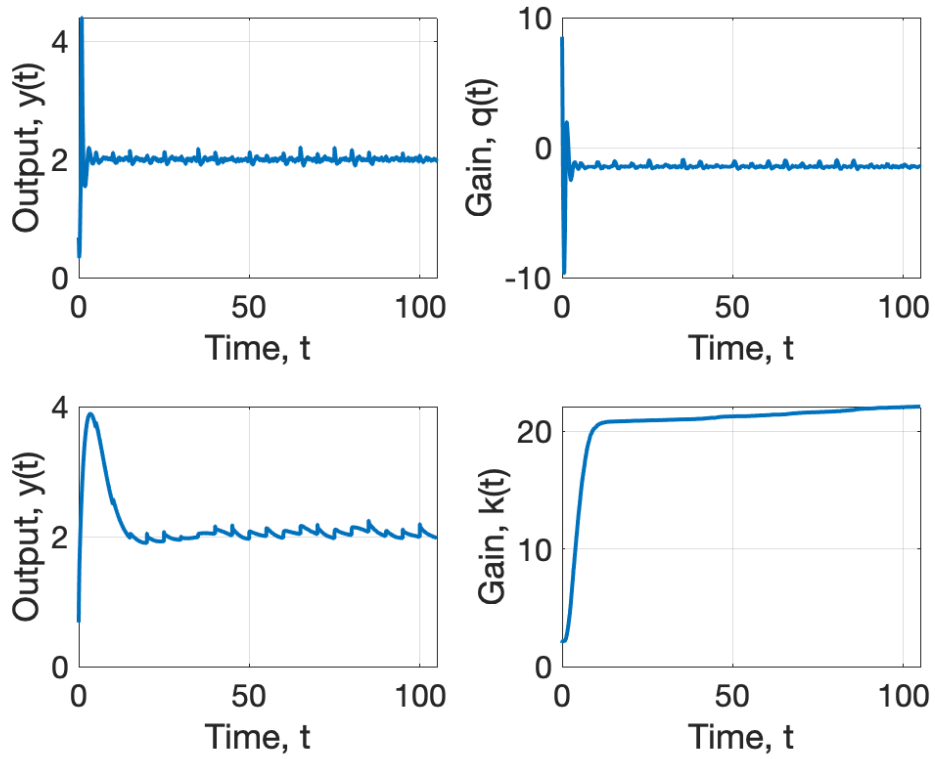


Figure 4.5: Top left and right: Simulations of output and gain for the bifurcation learning algorithm (4.19); Bottom left and right: Simulations for the adaptive integral control algorithm (4.18).

## 4.6 Conclusion

The conclusion of this chapter is:

- We proved, for a class of non-negative Metzler systems, that the Byrnes-Willems adaptive high-gain stabilising controller does indeed learn a (positive enough) stabilising gain – Theorem 4.4.
- We designed an adaptive destabilising controller. Again, for non-negative systems, we proved that the adaptive high-gain destabilising controller did learn a (negative enough) destabilising gain – Theorem 4.8.
- The class of “population-ecology” inspired non-negative systems under consideration admits a simple transition. There is a critical saddle-node bifurcation threshold, so gains above this critical threshold stabilise and gains below destabilise. We found that if the positive high-gain and negative high-gain algorithms are combined, then the saddle-node bifurcation is learnt – Theorem 4.13.
- We used the main result in Theorem 4.13 in terms of developing a novel set-point controller. For a target set-point  $r$ , the new adaptive controller achieves asymptotic tracking of  $r$  without knowledge of system parameters. Because the underpinning nonlinear system has a linearly stable equilibrium, there is guaranteed robustness. This contrasts with adaptive controllers’ that suffer sensitivity and fragility to unmodelled disturbances.

## Chapter 5

# Adaptive Stabilisation and Destabilisation and an Adaptive "Arms Race"

Overview, in the previous chapter, Chapter 4, we revisited the well known Byrnes-Willems adaptive controller. There we combined a high-gain stabilising and a high-gain destabilising adaptive control approach. For classes of relative degree one, minimum phase and Metzler systems, we showed that this combined adaptive controller learns the critical gain - a saddle-node bifurcation. We continue the stabilising-destabilising theme in this chapter, but in a context of discrete-time population projection models. The work is inspired by recent developments of adaptive control in a context of pest management (stabilisation) [1] and population persistence (destabilisation) [24]. As before, there are two competing elements - in essence an arms race - whereby an increasing control parameter ( $v$  say) leads to stabilisation but, perhaps due to acquired resistance, there is an antagonistic destabilising effect with a decreasing parameter ( $r$  say). In contrast to the continuous-time case, where there is a guaranteed convergence to a bifurcation point, in this discrete time case a trio of outcomes is possible which, in a context of

pest management, can be described as: eradication of the pest; uncontrolled outbreak and also possible convergence to a persistent steady state.

The main new results are:

- Adaptive stabilisation for discrete-time populations – Theorem 5.3.
- Adaptive destabilisation for discrete-time populations – Theorem 5.6.
- A simulation study of an adaptive arms race that combines Theorems 5.3 and 5.6.
  - We show that the  $1 + 1$  dimensional arms race model (5.13) results in an unstable spiral – see Proposition 5.11. This is similar to the result in Chapter 4 – see Remark 4.12.
  - We show that the  $2 + 1$  dimensional arms race model (5.16) admits both oscillatory behaviour – see Figure 5.11 – and divergent behaviour – see Figure 5.13. We prove that convergent behaviour is not possible.
  - We show that the  $3 + 1$  dimensional arms race model (5.26) admits both convergent behaviour – see Figure 5.5 and divergent behaviour – see Figure 5.7. We explore parameter ranges which produce these two behaviour types – see Figure 5.15.

**Remark 5.1.** In the bullet points 5, we mentioned  $1 + 1$ ,  $2 + 1$  and  $3 + 1$  to index the dimensions of the matrix  $A$  in (5.10).

This chapter is organised as follows. Section 5.1 considers adaptive stabilisation of discrete-time populations. We modify system (3.8) from [1] to assume that the control acts multiplicatively as opposed to additively. We construct an adaptive algorithm which achieves stabilisation. This leads to the system (5.2) and the result in Theorem 5.3 and simulations in Figure 5.1. Section 5.2 considers adaptive destabilisation. We modify the approach used by [24], see system (3.11)

with switching, to the system (5.6) with multiplicative action. We construct an adaptive algorithm which achieves destabilisation. This is shown in Theorem 5.6 and simulations Figure 5.1. Section 5.3 explores the interplay between adaptive stabilisation and adaptive destabilisation for  $n$ -dimensional systems. In Section 5.3, we consider the case of  $n = 1$  (5.12). Here the system admits a stable spiral Figure 5.10. In the same Section 5.3 we consider the case of  $n = 2$  see text-colored the system equation (5.16). Here, depending on the system matrix  $A$ , we may see both oscillatory and divergent behaviour. In the same Section 5.3 – we consider the  $n = 3$  case see the system equation (5.26). Again we see both convergent and divergent behaviour see Figure 5.15.

## 5.1 Adaptive stabilisation of discrete-time populations

Recall from Chapter 3, the simple adaptive stabilising control system.

$$\left. \begin{aligned} x(t+1) &= (A - B\phi(u(t))F)x(t), & x(0) &= x_0 \\ y(t) &= Cx(t), \\ u(t+1) &= u(t) + \|y(t)\|^p, & u(0) &= u_0 \end{aligned} \right\} t \in \mathbb{N}_0. \quad (5.1)$$

In (5.1),  $n, m \in \mathbb{N}$ ,  $x(t) \in \mathbb{R}_+^n$  is the population structure,  $A \in \mathbb{R}_+^{n \times n}$  is the projection matrix for the population,  $(B, F) \in \mathbb{R}_+^{n \times m} \times \mathbb{R}_+^{m \times n}$  are control design parameters related to which states are targeted by the pesticide. The parameter  $u(t)$  represents the volume of pesticide applied and  $y = Cx$  with  $C \in \mathbb{R}_+^{p \times n}$  is the measurement or information about  $x(t)$ . The initial pesticide effort in the scheme (5.1) is represented by  $u_0$ . The term  $\|y(t)\|^p$ ,  $p > 1$ , is used to convert measured pest abundance  $\|y(t)\|$  into a change of control effort at the following time step and so determines how quickly the control effort  $u$  rises [1]. The function  $\phi$  is a design parameter, capturing the efficacy of the pesticide action in response to applied pesticide  $u$ .  $\phi : \mathbb{R}_+ \rightarrow \mathbb{R}_+^{m \times m}$  with continuous, strictly increasing components  $\phi_i$  vanishing at zero and satisfying image  $\phi_i \subset [0, 1]$ .

Here we consider a modified version of (5.1) given by the adaptive system:

$$\begin{aligned}x(t+1) &= \Phi(v(t))Ax(t), & x(0) &= x_0, \\v(t+1) &= v(t) + \|Cx(t)\|^2, & e(0) &= e_0,\end{aligned}\tag{5.2}$$

where the control parameter is denoted by  $v$ . This is to suggest, in a context of pesticide applications, that  $v$  is more a “volume” (of pesticide) than a control. In comparing (5.2) with (5.1), the effect of  $v$ , through  $\Phi(v)$ , in (5.2) is multiplicative where as  $u$ , through  $\Phi(u)$ , in (5.1) acts additively, with  $p = 2$ . The idea for this control action is that an applied pesticide would act multiplicatively to reduce population in one or more stages by a proportion determined by the amount or efficacy of the pesticide captured in  $e$  – effectively impacting on population transition rates. The function  $\Phi(v)$  is an  $n \times n$  diagonal matrix with diagonal components  $\phi_i$  that satisfy  $\phi_i$  is continuous and non-increasing with  $\phi(v) > 0$  for all  $v$ . Typically one, or more, of these components will satisfy

$$\phi_i(v) \rightarrow 0 \text{ as } v \rightarrow \infty.$$

**Remark 5.2.** In applications, if the underlying matrix  $A$  in (5.2) does indeed arise from applications to pest management, then we must also be mindful that the matrix  $\Phi(v)A$  does not violate biological constraints, for example with regards to the resulting survival and growth rates. However, it is still of interest to consider the system (5.2) without these biological considerations.

**Theorem 5.3.** *Assume that  $A$  is irreducible and suppose there exists  $v^* > 0$  so that growth rate*

$$\lambda(\Phi(v^*)A) < 1,$$

*that is large enough (but unknown) volume  $v$  stabilises (that is spraying enough pesticide works).*

*Then for all  $x(0) = x_0$  and  $v(0) = v_0$ , there exists  $v^\infty$  so that*

$$\lim_{t \rightarrow \infty} v(t) = v^\infty$$

with growth rate

$$\lambda(\Phi(v^\infty)A) < 1,$$

and consequently

$$x(t) \rightarrow 0 \text{ exponentially for (5.2).}$$

**Proof of Theorem (5.3).**

We follow a contradiction style argument common in adaptive results like this one. Suppose there exists  $t^*$  so that

$$\lambda(\Phi(v(t^*))A) = \gamma < 1.$$

Now, componentwise,  $\Phi(v(t))$  is non-increasing and so for all  $t \geq t^*$ ,

$$x(t+1) = \Phi(v(t))Ax(t) \leq \underbrace{\Phi(v(t^*))A}_{\lambda(\Phi(v(t^*))A)=\gamma < 1} x(t).$$

Then

$$x(k+t^*) \leq M^k x(t^*), \quad M = \Phi(v(t^*))A, \quad \lambda(M) = \gamma < 1.$$

It follows that

$$x(t) \rightarrow 0 \text{ exponentially,}$$

and that the non-decreasing sequence  $\{v(t)\}_0^\infty$  satisfies

$$v(\infty) = v(t^*) + \sum_{t=t^*}^{\infty} (Cx(t))^2 < \infty.$$

So  $\{v(t)\}_0^\infty$  converges, completing the proof.

If there does not exist  $t^*$  so that

$$\lambda(\Phi(v(t^*))A) = \gamma < 1,$$

then  $\{v(t)\}_0^\infty$  is bounded and so  $\{v(t)\}_0^\infty$  converges, that is

$$\lim_{t \rightarrow \infty} v(t) = v^\infty$$

for some  $v^\infty$ . But then

$$\lambda(\Phi(v^\infty)A) < 1$$

since if not, then

$$x(t+1) = \Phi(v(t))Ax(t) \geq \underbrace{\Phi(v^\infty)A}_{\lambda(\Phi(v^\infty)A) \geq 1} x(t) = Mx(t), \quad \lambda(M) \geq 1.$$

Moreover,  $M$  inherits irreducibility from  $A$ . This irreducibility and  $r(M) \geq 1$  implies that  $x(t) \geq w$  for some positive vector  $w$ , meaning that  $v(t)$ , given by (5.2) must diverge, so contradicting the already established convergence of  $v(t)$ .  $\square$

### Illustrative examples

(a) In the following we simulate the system (5.2) with:

$$\left. \begin{aligned} \phi_1(v) &= 0.5\left(1 - \frac{2}{\pi}\tan^{-1}(v)\right), & \phi_i &= 1, \quad i = 2, 3, \\ A &= \begin{pmatrix} 2 & 4 & 3 \\ 0.5 & 0 & 0 \\ 0 & 0.4 & 0 \end{pmatrix}, & C &= [1 \ 0 \ 0], \text{ with random initial values.} \end{aligned} \right\} \quad (5.3)$$

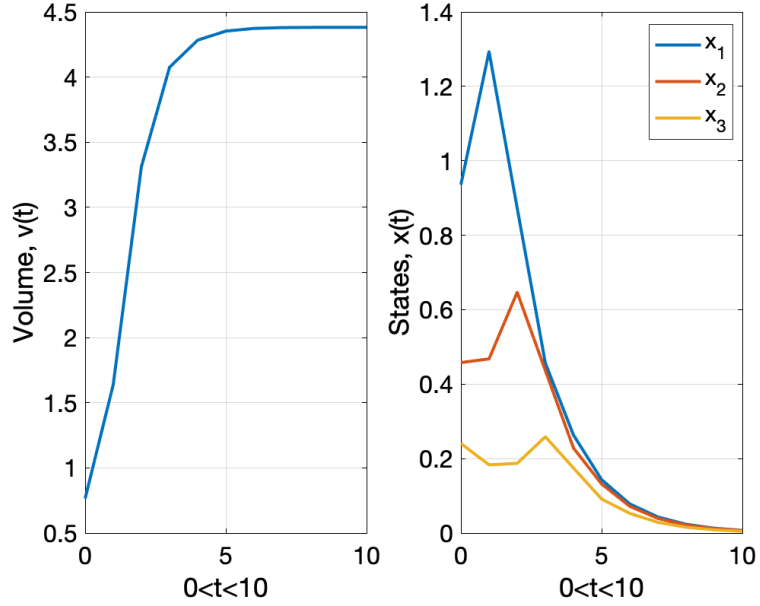


Figure 5.1: Adaptive Stabilisation (5.2) for system (5.3). Left plot: Convergent gain  $v(t)$ . Right plot: Stage structures  $x(t)$  converging to zero.

Figure 5.1 is a simulation of system (5.2) for the example (5.3).

(b) In the following we simulate the system (5.2) with:

$$\left. \begin{aligned}
 \phi_1(v) &= 1 - \tanh(v), & \phi_i &= 1, \quad i = 2, 3, \\
 A &= \begin{pmatrix} 2 & 8 & 3 \\ 0.5 & 0 & 0 \\ 0 & 0.4 & 0 \end{pmatrix}, & C &= [1 \ 0 \ 0], \text{ with random initial values.}
 \end{aligned} \right\} \quad (5.4)$$

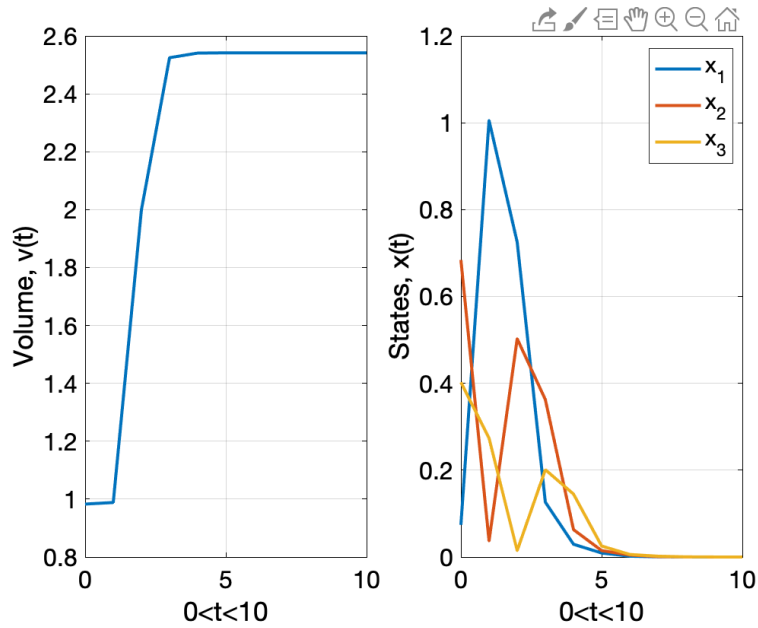


Figure 5.2: Adaptive Stabilisation (5.2) for system (5.4). Left plot: Convergent gain  $v(t)$ . Right plot: Stage structures  $x(t)$  converging to zero.

Figure 5.2 is a simulation of system (5.2) for the example (5.4). In Figure 5.2 the system exhibits faster convergence compared to Figure 5.1 where we used the different function  $\phi(v)$ .

**Remark 5.4.** In the simulations for Figures 5.1 and 5.2, we used different function of  $\phi$ . Our goal is targeting the first stage  $x_1$  of the population projection. The simulations show that both are able to drive the pest to zero. In the first example, see Figure 5.1, the volume converges to almost 4.4. However, in the second example, see Figure 5.2, the volume converges to 2.5.

## 5.2 Adaptive Destabilisation of Discrete-time Populations

Recall from Chapter 3, the system of switching difference equations

$$\begin{aligned} x(t+1) &= A_{s(t)}x(t), \\ u(t+1) &= u(t) + \begin{cases} 0, & M \leq \|u(t)\| \quad \text{or} \quad \|u(t)\|=0 \\ \frac{1}{\|u(t)\|^q}, & \|u(t)\| < M. \end{cases} \end{aligned} \quad (5.5)$$

Here  $A_{s(t)} \in \{A_1, \dots, A_l\} \subset \mathbb{R}_+^{n \times n}$ ,  $n \in \mathbb{N}$ ,  $u(0) = u_0$ ,  $t \in \mathbb{Z}_+$ . In (5.5)  $M$  is positive and represents a design parameter,  $q > 1$ . The key point is that  $A_{s(t)}$  switches through a set of possible matrices. The procedure of picking the switching condition is explained in Chapter 3 more precisely in (3.5) and (3.12).

In the destabilising result, Proposition 3.10, the population projection matrix  $A$  switches through a set of possible population projection matrices, where at least one matrix is unstable<sup>1</sup>. An alternative, and much in the spirit of (5.2), is to assume that the population projecting matrix is determined by some multiplicative scaling factor  $\Phi(-r)$ . This is captured in the following:

$$\begin{aligned} x(t+1) &= \Phi(-r(t))Ax(t) \\ r(t+1) &= r(t) + \frac{1}{\|Cx(t)\|^q}. \end{aligned} \quad (5.6)$$

In (5.6),  $r(t)$  is capturing an acquired resistance so that increasing  $r(t)$  causes population growth rate to increase.  $\Phi(r)$  is an  $n \times n$  diagonal matrix with diagonal components  $\phi_i(r)$  that are continuous, positive and non-increasing. Typically one, or more than one,  $\phi_i$  will be strictly decreasing so that  $\Phi(-r)A$  increases with time as  $r$ , given by (5.6), increases.

**Remark 5.5.** In applications, as with stabilisation above, if the underlying matrix  $A$  in (5.2)

---

<sup>1</sup>Note Proposition 3.10, from [24], was developed concurrently with Theorem 5.6 – developing the same ideas but in a slightly different direction. Our focus was ultimately on the interplay between stabilisation and destabilisation as in Chapter 4.

does indeed arise from population projection applications, then we must also be mindful that the matrix  $\Phi(v)A$  does not violate biological constraints. However, it is still of interest to consider the system (5.2) without these biological considerations.

Later we will introduce an adaptive efficacy  $e(t)$  which combines increasing and decreasing elements, as we did in Chapter 4.

**Theorem 5.6.** *Assume that  $A$  is irreducible and  $C \neq 0$  and suppose there exists  $r^* < \infty$  so that*

$$\lambda(\Phi(-r^*)A) > 1,$$

*so that negative enough (but unknown)  $-r$  destabilises. Then there exists  $r^\infty < \infty$  so that*

$$(i) \lim_{t \rightarrow \infty} r(t) \rightarrow r_\infty < \infty$$

*with*

$$\lambda(\Phi(-r^\infty)A) > 1,$$

*and consequently*

$$x(t) \rightarrow \infty \text{ exponentially for (5.5).}$$

### **Proof of Theorem 5.6**

We argue by contradiction using a similar approach as in the proof of Theorem 5.3. Suppose there exists  $t^*$  so that

$$\lambda(\Phi(-g(t^*))A) = \gamma > 1.$$

Now, componentwise,  $\Phi(-r(t))$  is non-increasing and  $r(t)$  is non-decreasing, so for all  $t \geq t^*$ ,

$$x(t+1) = \Phi(-r(t))Ax(t) \geq \underbrace{\Phi(-r(t^*))A}_{\lambda(\Phi(-r(t^*))A)=\gamma} x(t).$$

Then

$$x(k+t^*) \geq M^k x(t^*), \quad M = \Phi(-r(t^*))A, \quad \lambda(M) = \gamma > 1.$$

It follows that

$$x(t) \rightarrow \infty \text{ exponentially,}$$

and that the non-decreasing sequence  $\{r(t)\}_0^\infty$  satisfies

$$r(\infty) = r(t^*) + \sum_{t=t^*}^{\infty} \frac{1}{\|Cx(t)\|} < \infty.$$

So  $\{r(t)\}_0^\infty$  converges, completing the proof.

If there does not exist  $t^*$  so that the growth rate

$$\lambda(\Phi(-r(t^*))A) = \gamma > 1,$$

then  $\{r(t)\}_0^\infty$  is bounded and so  $\{r(t)\}_0^\infty$  converges, that is

$$\lim_{t \rightarrow \infty} r(t) = r^\infty$$

for some  $r^\infty$ . But then

$$\lambda(\Phi(-r^\infty)A) > 1$$

since if not, then

$$x(t+1) = \Phi(-r(t))Ax(t) \leq \underbrace{\Phi(-r^\infty)A}_{\lambda(\Phi(-r^\infty)A) \leq 1} x(t) = Mx(t), \quad \lambda(M) \leq 1.$$

Moreover,  $M$  inherits irreducibility from  $A$ . This irreducibility and  $\lambda(M) \leq 1$  implies that  $x(t) \leq w$  for some positive vector  $w$ . But then  $1/(Cx(t)) \geq \varepsilon$ , some  $\varepsilon > 0$ , meaning that  $r(t)$  must diverge, so contradicting the already established convergence of  $r(t)$ .  $\square$

### Illustrative examples

(a) In the following we simulate the system (5.6) with:

$$\left. \begin{aligned} \phi_1(r) &= 0.5\left(1 - \frac{2}{\pi}\tan^{-1}(r)\right), & \phi_i &= 1, \quad i = 2, 3, \\ A &= \begin{pmatrix} 0.7013 & 0.3397 & 0.6485 \\ 0.4110 & 0 & 0 \\ 0 & 0.4787 & 0 \end{pmatrix}, & C &= [1 \ 0 \ 0], \text{ with random initial values.} \end{aligned} \right\} \quad (5.7)$$

If  $g_0 < 0$ , then  $\phi(-r_0) < 1/2$  and  $\lambda(\Phi(-r_0A)) < 1$ . So initially, the population is in decline.

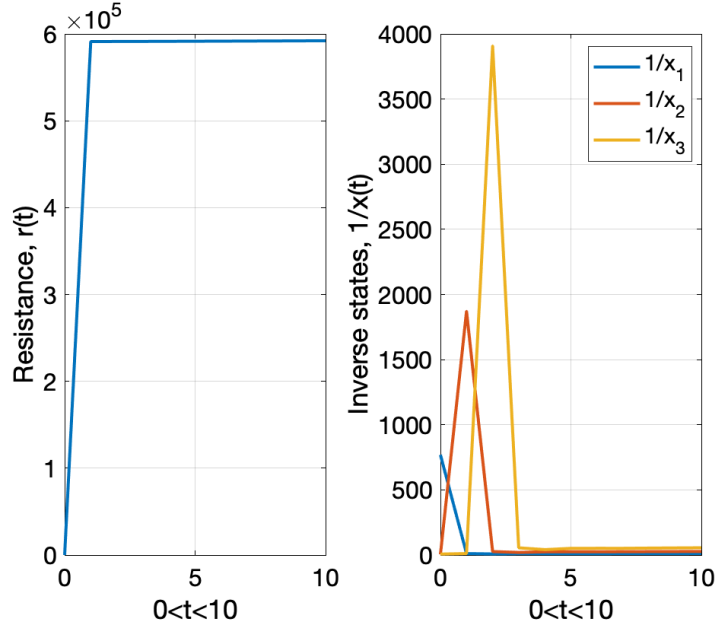


Figure 5.3: Adaptive Destabilisation (population persistence) (5.16). Left plot. Convergent gain  $r(t)$ . Right plot. Divergent (persistent) stage structures  $x(t)$ .

Figure 5.3 is a simulation of system (5.6) for example (5.7).

(b) In the following we simulate the system (5.6) with:

$$\left. \begin{aligned} \phi_1(r) &= 1 - \tanh(r),, & \phi_i &= 1, \quad i = 2, 3, \\ A &= \begin{pmatrix} 0.7013 & 0.3397 & 0.6485 \\ 0.4110 & 0 & 0 \\ 0 & 0.4787 & 0 \end{pmatrix}, & C &= [1 \ 0 \ 0], \text{ with random initial values.} \end{aligned} \right\} \quad (5.8)$$

The outcomes of the simulation, in this case, are depicted in Figure 5.4.

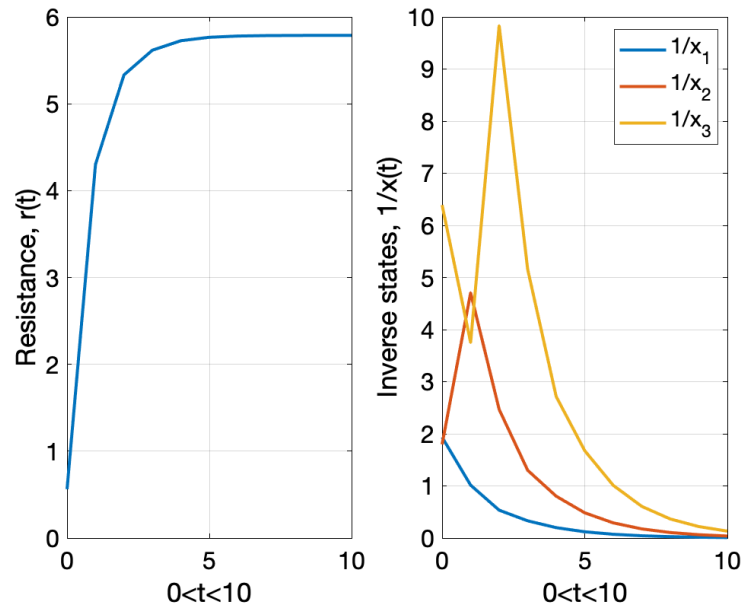


Figure 5.4: Adaptive Destabilisation (population persistence) (5.16). Left plot. Convergent gain  $r(t)$ . Right plot. Divergent (persistent) stage structures  $x(t)$ .

**Remark 5.7.** In the simulations depicted in Figures 5.3 and 5.4, we used different  $\phi$  functions – resulting in different levels of  $r$  and so different values of states. Our goal is targeting the first stage  $x_1$  of the population projection. The simulations show that both choices of  $\phi_1$  result

in a destabilised or persistent population. In the first example Figure 5.3, the “resistance”  $r(t)$  converges to almost  $6 \times 10^5$  . However, in the second example Figure 5.2, “resistance”  $r(t)$  converges to 5.5 , which is smaller than the first example.

**Remark 5.8.** Theorems 5.3 and 5.6, respectively Propositions 3.7 and 3.10, are the discrete-time versions of Theorems (4.4) and 4.8, respectively Propositions 3.4 and 4.8, from Chapter 4. In the next section, we look to explore the discrete-time analogue of Theorem 4.13.

### 5.3 An adaptive arms race

In Chapter 4, we developed an algorithm that could learn a saddle-node bifurcation, in some sense a threshold between population decline and population growth. In this case we find, by adaptation a persistent population. The results depended quite strongly on the underlying system assumptions – especially the minimum phase property which gives strong control of the closed loop eigenvalues with positive or negative high gain. The Metzler assumption also played a role in ensuring a saddle-node transition. We now consider the discrete-time analogue. One motivation is in a context of pest control. Here increasing the amount of pesticide will decrease pest population abundance, but over time, pesticide efficacy may reduce as pests develop resistance. This leads to an “arms race”, similar to that discussed in Chapter 4. The discrete-time analogue of the continuous time “arms race” controller is an adaptive feedback system of the form

$$\begin{aligned} x(t+1) &= \Phi(v(t) - r(t))Ax(t) \\ v(t+1) &= v(t) + \|C_1x(t)\|^p \\ r(t+1) &= r(t) + \frac{1}{\|C_2x(t)\|^q}. \end{aligned} \tag{5.9}$$

Here there are two antagonistic, competing terms:  $v(t)$  is increasing, therefore causing  $v(t) - r(t)$  to increase and so  $\Phi(v(t) - r(t))$  to decrease;  $r(t)$  is increasing, therefore causing  $v(t) - r(t)$

to decrease and so  $\Phi(v(t) - r(t))$  to increase. This combination of adaptive stabilisation and destabilisation is looking to capture that spraying more pesticide will reduce the growth rate of the pest, but an over-spraying may cause the emergence of pesticide resistance and resulting increase in growth rate.

Let  $e = v - r$ . Then

$$\begin{aligned} x(t+1) &= \Phi(e(t))Ax(t) \\ e(t+1) &= e(t) + \|C_1x(t)\|^p - \frac{1}{\|C_2x(t)\|^q} \end{aligned} \quad (5.10)$$

In (5.10),  $A$  is an irreducible  $n \times n$  matrix and  $\Phi(e)$  is an  $n \times n$  diagonal matrix with diagonal components  $\phi_i : \mathbb{R} \mapsto \mathbb{R}_+$  that are continuous, positive and non-increasing. Typically one, or more than one  $\phi_i$  will be strictly decreasing so that  $\Phi(e)A$  increases (decreases). In order to improve (worsens), with time as  $e$ , given by (5.6), decreases (increases). The parameter adaptation in (5.10), driven by observations or measurements  $C_1x(t)$  and  $C_2x(t)$ , allows  $e$  to increase or decrease: as population abundance rises, so  $e$  increases; as population abundance decreases, so  $e$  decreases – so capturing an arms race like behaviour.

**Remark 5.9.** In applications, as with stabilisation and destabilisation above, if the underlying matrix  $A$  in (5.2) does indeed arise from population projection applications, then we must also be mindful that the matrix  $\Phi(v)A$  does not violate biological constraints. However, it is still of interest to consider the system (5.2) without these biological considerations.

Note also, that since  $\Phi$  is a diagonal matrix with entries less than or equal to one, we necessarily need  $\lambda(A) > 1$ , since otherwise  $x(t)$  given by (5.10) will converge to zero and  $e(t)$  will diverge to  $-\infty$  and there is no “arms race”.

**Illustrative examples:** (a) In the first simulation of the system (5.10) we choose the following parameters given in Table 5.1 to populate the PPM (2.13).

$S_1$	$S_2$	
0.8013	0	

Table 5.1: The Parameter values for Example (a).

This gives

$$A = \begin{pmatrix} 0.8013 & 0.3397 & 0.6485 \\ 0.4110 & 0 & 0 \\ 0 & 0.4787 & 0 \end{pmatrix} \text{ with the function of } \phi(e) \text{ as: } \phi(e) = \begin{pmatrix} 1 & 0 & 0 \\ 0 & 0.5(1 - \frac{2}{\pi} \tan^{-1}(e)) & 0 \\ 0 & 0 & 1 \end{pmatrix}. \quad (5.11)$$

The observations are  $C_1 = [0 \ 0 \ 1]$  and  $C_2 = [1 \ 0 \ 0]$ , with random initial values.

The outcomes of the simulation in this case are depicted in Figure 5.5.

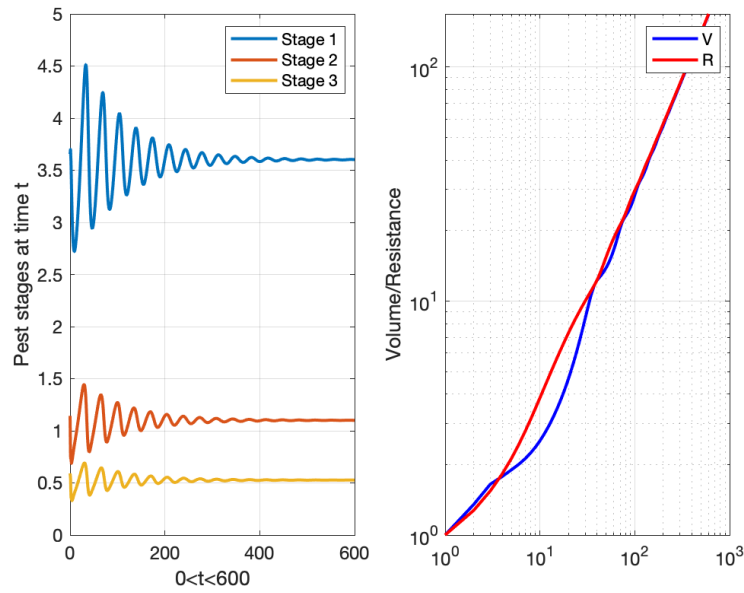


Figure 5.5: Arms race simulation: Left plot – population abundance; Right plot - volume  $v(t)$  and resistance  $r(t)$ .

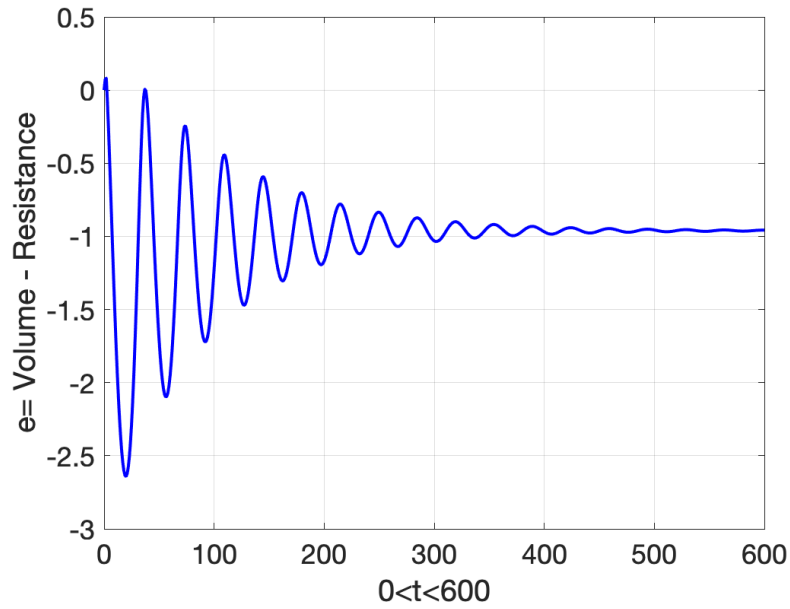


Figure 5.6: Arms race simulation:  $e(t) = v(t) - r(t)$ .

Thus in this simulation with the matrix (5.11) we get  $e_\infty = 0.7436$  and  $\Phi(e_\infty)A = 1.0391$ . In this simulation, we see convergent (or symbiotic) adaptation. In particular  $e(t) = v(t) - g(t)$  converges to  $e_\infty < \infty$ , and the state reaches a positive steady state.

(b) In the second simulation of the system (5.10) we choose the following parameters given in Table 5.2 to populate the PPM (2.13).

$S_1$	$S_2$
0.1373	0

Table 5.2: The Parameter values for Example (b).

This gives

$$A = \begin{pmatrix} 0.1373 & 0.7003 & 1.1082 \\ 0.5843 & 0 & 0 \\ 0 & 0.8905 & 0 \end{pmatrix}$$

We use the same  $\Phi(e)$  in (5.11), with random initial values. The outcomes of the simulation in this case are depicted in Figure 5.7.

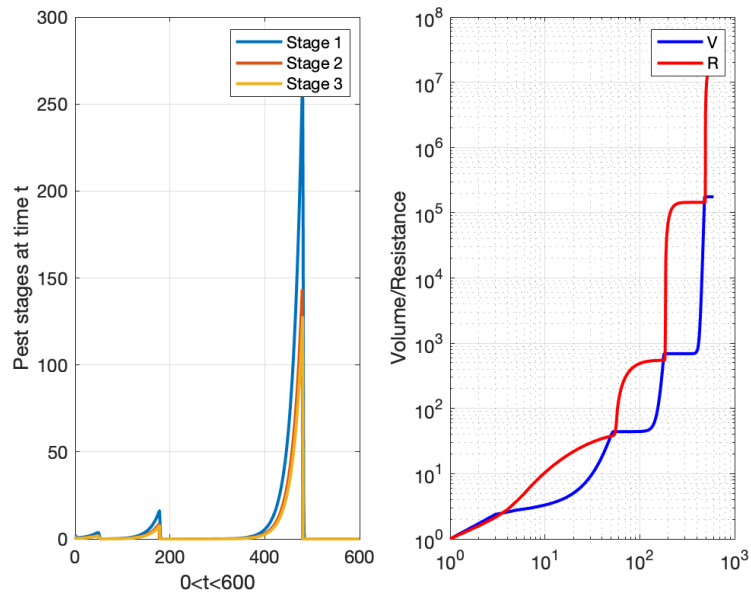


Figure 5.7: Arms race simulation: Left plot – population abundance; Right plot - volume  $v(t)$  and resistance  $r(t)$ .

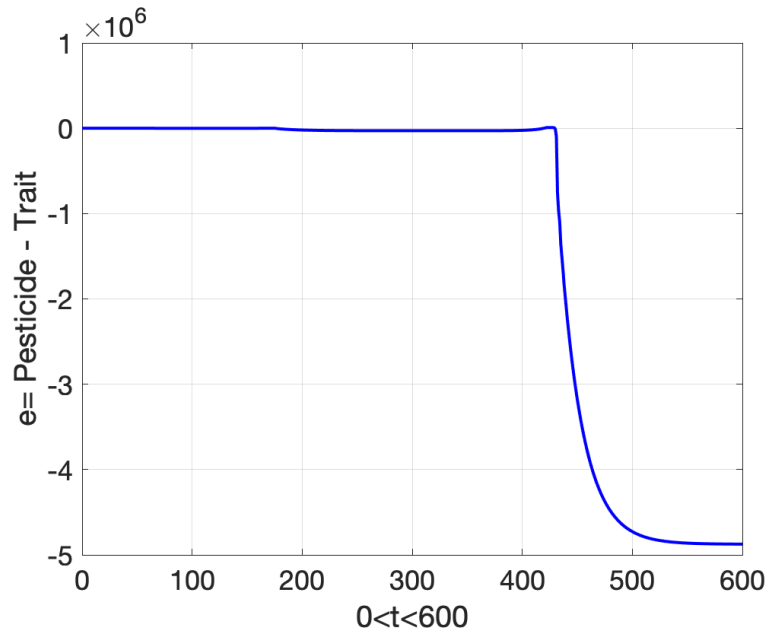


Figure 5.8: Arms race simulation (5.10):  $e(t) = v(t) - r(t)$ .

In this simulation, we see divergent behaviour with  $v(t)$  and  $r(t)$  interweaving and out-doing each other, switching uncontrollably back and forth between increasingly larger positive values. As a result, the population goes through phases of boom and bust.

**Remark 5.10.** The simulations above and Figures 5.5 and 5.7 motivated us to move more deeply in to this system by exploring the dynamics through eigenvalues of linearisations so as to determine when this scheme is convergent versus divergent.

### Adaptive arms race: 1+1 Case

In Chapter 4, (4.10), we have a closed loop system

$$\begin{aligned} \dot{y}(t) &= (a - q(t))y \\ \dot{q}(t) &= y(t)^2 - \frac{1}{y(t)} \end{aligned} \tag{5.12}$$

and

$$\frac{1}{2}(a - q(t))^2 + \frac{1}{2}y^2(t) + \frac{1}{y(t)} = \frac{1}{2}(a - q(0))^2 + \frac{1}{2}y^2(0) + \frac{1}{y(0)} \text{ for all } t \geq 0.$$

So, in the continuous time,  $n = 1$  case,  $y = 0$  and  $q = a$  is an unstable equilibrium of the 1 + 1 arms race. However, as we have seen in Theorem 4.13, for  $n \geq 2$ , and under certain assumptions, there is an adaptive concord, and a learning of a saddle-node bifurcation.

The discrete-time analogue of this 1 + 1 case is the system

$$\begin{aligned} x(t+1) &= \Phi(e(t))ax(t) \\ e(t+1) &= e(t) + |C_1x|^p - \frac{1}{|C_2x|^q}. \end{aligned} \quad (5.13)$$

We seek the equilibria of this system. Let the equilibrium be  $(x^*, e^*)$ . Then

$$\begin{aligned} x^* &= \phi(e^*)ax^* \\ e^* &= e^* + |C_1x^*|^p - \frac{1}{|C_2x^*|^q}. \end{aligned} \quad (5.14)$$

Solving (5.14) gives

$$\phi(e^*)a = 1 \quad \text{and} \quad |C_1x^*|^p |C_2x^*|^q = 1.$$

So

$$x^* = \frac{1}{C_1^p C_2^q}.$$

Linearising the system around  $(x^*, e^*)$  yields a linearisation matrix (or Jacobian)

$$J = \begin{pmatrix} \phi(e^*)a & \phi'(e^*)ax^* \\ p(C_1x^*)^{p-1}C_1 + \frac{qC_2}{(C_2x^*)^{q+1}} & 1 \end{pmatrix} = \begin{pmatrix} 1 & b \\ c & 1 \end{pmatrix}. \quad (5.15)$$

**Proposition 5.11.** *The equilibrium  $(x^*, e^*)$  of (5.13), satisfies*

$$x^* = \phi(e^*)ax^*, \quad e^* = e^* + |C_1x^*|^p - \frac{1}{|C_2x^*|^q}$$

and an unstable spiral.

**Proof** This follows because

$$\phi'(e) < 0 \text{ so that } b = \phi'(e^*)ax^* < 0 \quad \text{and} \quad c = p(C_1x^*)^{p-1}C_1 + \frac{qC_2}{(C_2x^*)^{q+1}} > 0.$$

So the linearisation has eigenvalues  $\lambda_{\pm} = 1 \pm i\sqrt{|cb|}$ , confirming an unstable spiral.  $\square$

**Remark 5.12.** We see that the continuous-time and discrete-time results are matched in the 1 + 1 case. In both cases, the “arms races” is divergent. This similarity is somewhat expected. The key quantities are:

$$r = e^{a-q(t)} \quad \text{continuous-time case} \quad \text{and} \quad \rho = \Phi(e(t))a \quad \text{discrete-time case.}$$

In both cases,  $r$  and  $\rho$  tend to zero or infinity according to whether  $q$  or  $e$  tend to  $-\infty$  or  $+\infty$ . For higher dimensions the parallel is less transparent.

In Figure 5.9 we simulate the system of (5.13) with

$$a = 2, \quad C_1 = 1, \quad C_2 = 1, \quad \text{and} \quad \phi(e) = 0.5\left(1 - \frac{2}{\pi}\tan^{-1}(e)\right).$$

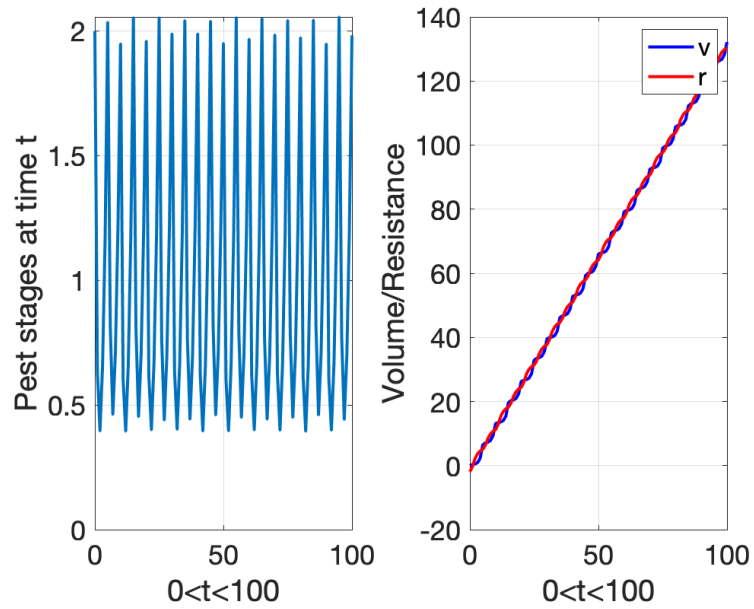


Figure 5.9: Arms race simulation, case 1 + 1 : Left plot – population abundance; Right plot - volume  $v(t)$  and resistance  $r(t)$ .

The Figure 5.10 shows the phase plane to the system (5.13) with spiralling behaviour matching the eigenvalue analysis above.

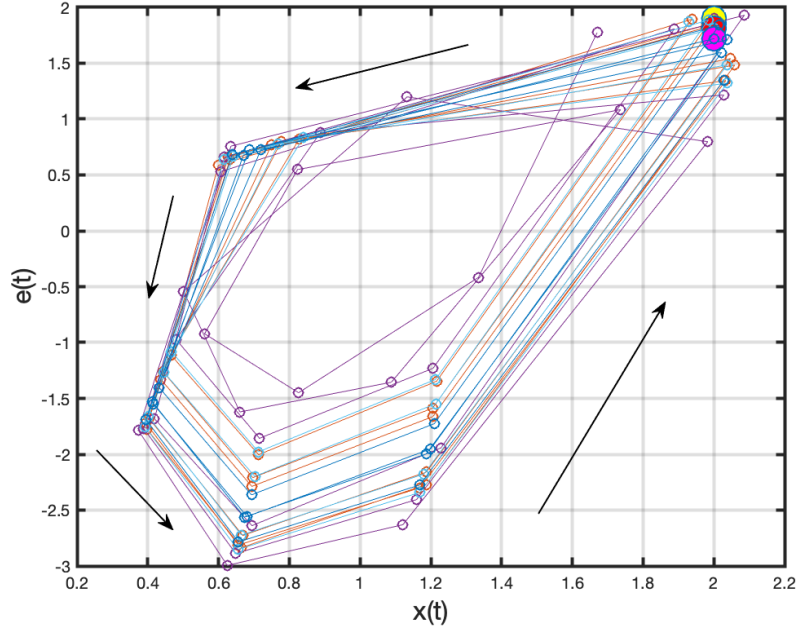


Figure 5.10: Phase plane of (5.14). The black arrows indicate the trajectories direction.

In Figure (5.10), the phase plane has been identified three times to duplicate the behaviours, whereas the dots (red - pink- yellow) are the initial values of the system (5.13).

### Adaptive arms race: 2+1 Case

In this subsection we explore the dynamics of the adaptive arms race on the case  $n = 2$ . This gives a model of the form

$$\begin{aligned} x(t+1) &= \phi(e(t))Ax(t) \\ e(t+1) &= e(t) + |C_1x(t)|^2 - \frac{1}{|C_2x(t)|^2}. \end{aligned} \quad (5.16)$$

Where  $A$  in (5.16) is a 2 by 2 matrix.

### Illustrative examples

(a) In the first simulation of the system (5.16) we choose the following parameters given in Table

5.3 to populate the  $2 \times 2$  PPM.

$S_1$	$S_2$	
0.8530	0	0

Table 5.3: The Parameter values for Example (a).

This gives

$$A = \begin{pmatrix} 0.8530 & 0.2703 \\ 0.8739 & 0 \end{pmatrix} \text{ with the function of } \phi(e) \text{ as: } \phi(e) = \begin{pmatrix} 1 & 0 \\ 0 & 0.5(1 - \frac{2}{\pi} \tan^{-1}(e)) \end{pmatrix} \quad (5.17)$$

The observations are  $C_1 = [1 \ 0]$  and  $C_2 = [0 \ 1]$ , with random initial values. The outcomes of the simulation in this case are depicted in Figure 5.11.

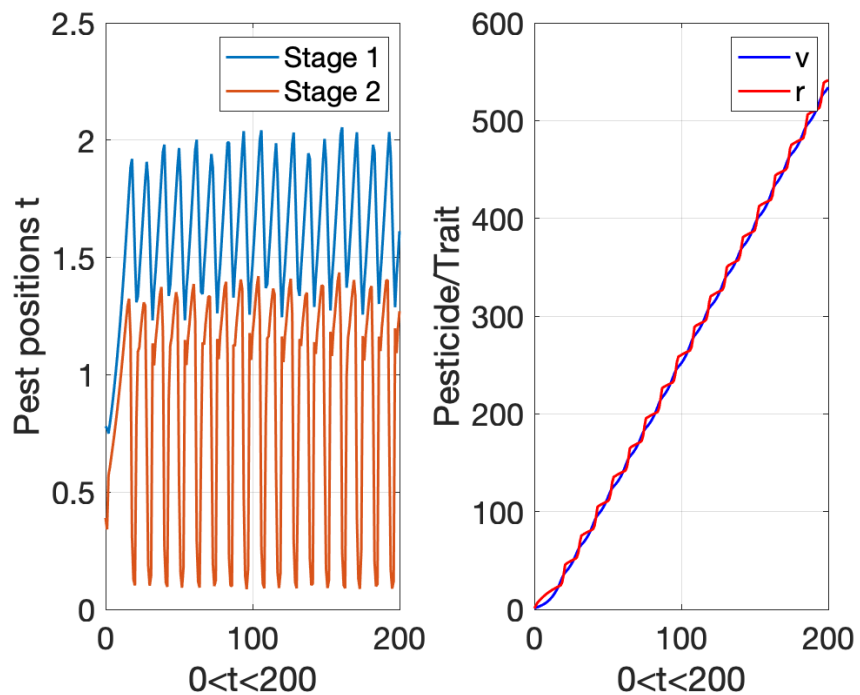


Figure 5.11: Arms race simulation for system (5.16) in 2 dimensions .

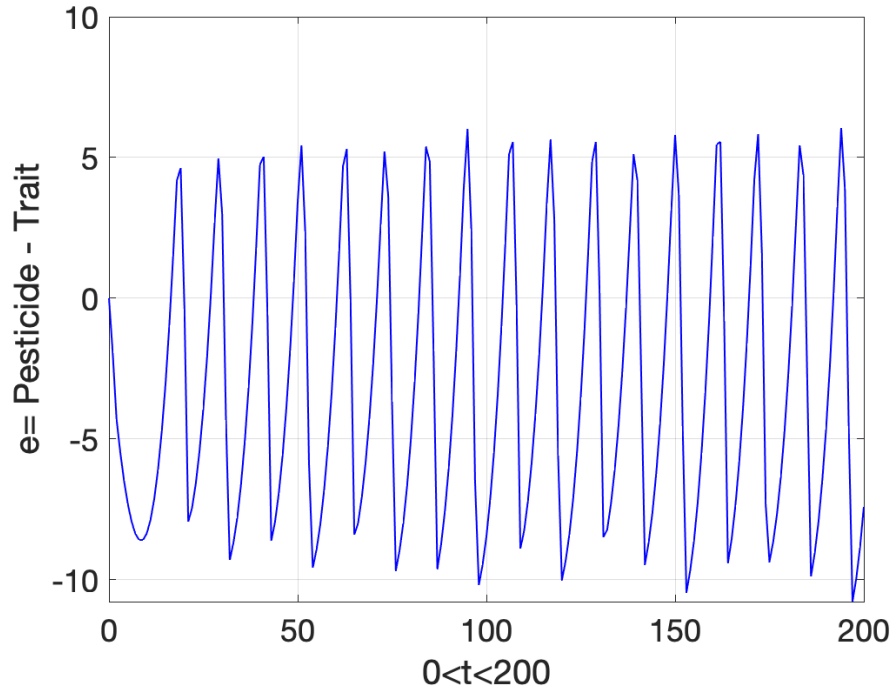


Figure 5.12: Arms race simulation (5.16):  $e(t) = v(t) - r(t)$ .

(b) In the second simulation of the system (5.16) we choose the following parameters given in Table 5.4 the  $2 \times 2$  PPM.

$S_1$	$S_2$	$F_2$
0.5	0	3

Table 5.4: The Parameter values for Example (a).

$$A = \begin{pmatrix} 0.5 & 3 \\ 0.4 & 0 \end{pmatrix} \quad (5.18)$$

We use the same  $\Phi(e)$  in (5.17). The observations are  $C_1 = [1 \ 0]$  and  $C_2 = [0 \ 1]$ , with random initial values.

The outcomes of the simulation in this case are depicted in Figure 5.13.

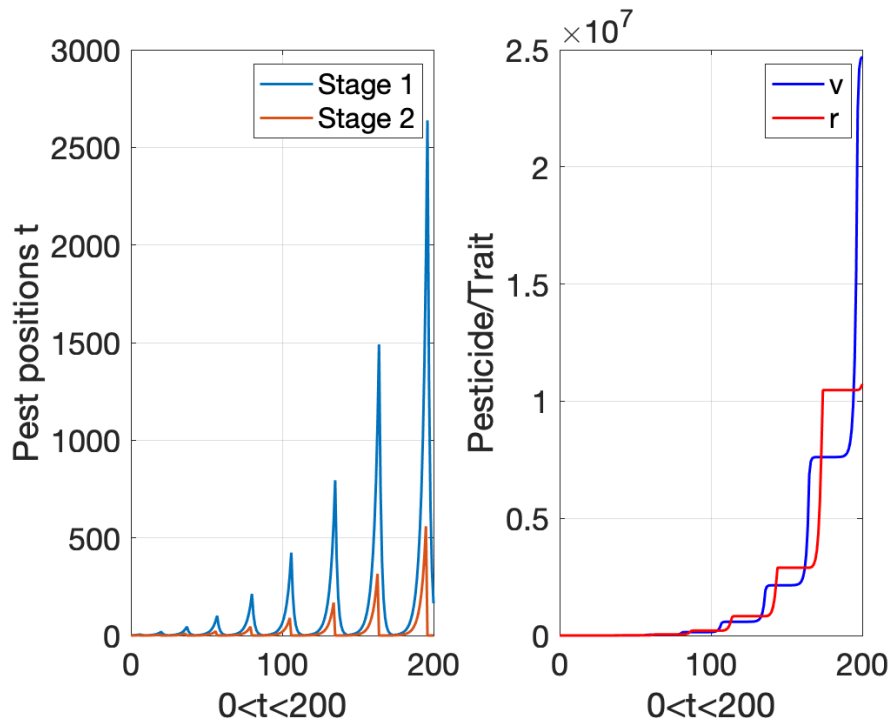


Figure 5.13: Arms race simulation for system (5.16) in 2 dimensions.

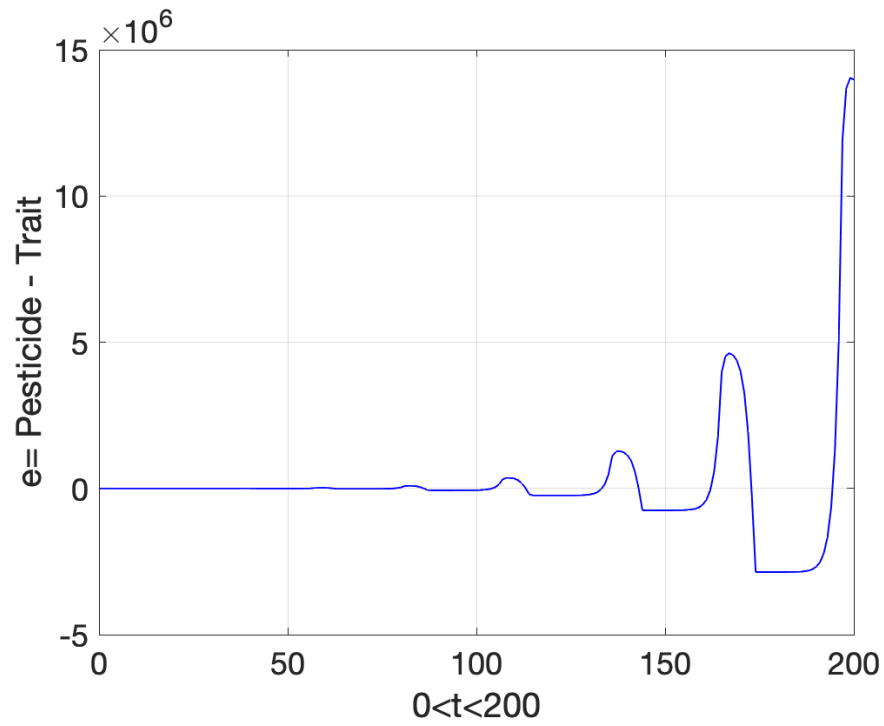


Figure 5.14: Arms race simulation (5.16):  $e(t) = v(t) - r(t)$ .

In these two examples of a  $2 + 1$  arms race we see contrasting behaviour. In one simulation there is an oscillation, in the other a divergence. We will use an equilibrium/linearisation approach to try and understand the cause of these different behaviours. We start by finding the equilibria of the system.

Let  $x(t) = x^*$ ,  $e(t) = e^*$ ,  $\implies x^* = \phi(e^*)Ax^*$ .

Assuming:

$$\phi(e) = \begin{bmatrix} \phi_{11}(e) & 0 \\ 0 & \phi_{22}(e) \end{bmatrix}. \quad (5.19)$$

Here

$$A = \begin{bmatrix} a & b \\ c & 0 \end{bmatrix}.$$

that is a PPM with fecundity and growth but no survival.

Since, we are targeting the second stage  $\phi_{11}(e) = 1$  and  $\phi_{22}(e) = \phi$  in (5.19). Let  $A_1 = \Phi(e)A$ .

Then

$$A_1 = \begin{bmatrix} a & b \\ \phi c & 0 \end{bmatrix}.$$

We find  $\phi^*$  by using the characteristic equation for  $A_1$ , which has a form of  $\text{Det}(A_1 - sI) = 0$  and requiring 1 to be a zero. Then

$$s^2 - as - bc\phi = 0 \quad \text{and} \quad s = 1. \quad (5.20)$$

gives

$$1 - a - bc\phi = 0.$$

Which gives the algebraic expression of  $\phi^*$ , as :  $\phi^* = \frac{1-a}{bc}$ . Substituting  $\phi^*$  in  $A_1$  gives:

$$\implies A_1 = \begin{bmatrix} a & b \\ \frac{1-a}{b} & 0 \end{bmatrix}. \quad (5.21)$$

The eigenvector equation for  $A_1$  and eigenvalue  $\lambda = 1$  has the form

$$A_1 \begin{pmatrix} 1 \\ u \end{pmatrix} = \begin{pmatrix} 1 \\ u \end{pmatrix}.$$

for some  $u$ . Solving to find  $u$  gives

$$\begin{aligned} \implies a + bu &= 1. \\ \frac{1-a}{b} &= u. \end{aligned} \tag{5.22}$$

Then  $x^*$  is given by

$$x^* = \alpha \begin{pmatrix} 1 \\ u \end{pmatrix}, \text{ for some } \alpha. \tag{5.23}$$

Then, to find  $\alpha$ , substitute  $x^*$  into the system (5.16). Then

$$(C_1 x^*)^2 = \frac{1}{C_2 x^*} \implies \alpha^2 \left( C_1 \begin{pmatrix} 1 \\ u \end{pmatrix} \right)^2 = \frac{1}{\alpha C_2 \begin{pmatrix} 1 \\ u \end{pmatrix}} \implies \alpha = \left( \left( C_1 \begin{pmatrix} 1 \\ u \end{pmatrix} \right)^2 \left( C_2 \begin{pmatrix} 1 \\ u \end{pmatrix} \right) \right)^{-\frac{1}{3}}.$$

This leads to  $\alpha = \frac{1}{\left(-\frac{a-1}{b}\right)^{1/3}}$ . By substitution  $\alpha$  in (5.23) This gives

$$x^* = \begin{pmatrix} \frac{1}{\left(-\frac{a-1}{b}\right)^{1/3}} \\ \left(-\frac{a-1}{b}\right)^{2/3} \end{pmatrix}.$$

We obtain the linearisation for the system (5.16) by using the Jacobian matrix:

$$J = \begin{pmatrix} \phi(e^*)A & \phi'(e^*)Ax^* \\ 2C_1 x^* C_1 + \frac{1}{(C_2 x^*)^2} C_2 & 1 \end{pmatrix}. \tag{5.24}$$

But  $C_1 = [1 \ 0]$  and  $C_2 = [0 \ 1]$ . Inserting the above calculations in (5.24) we get:

$$J = \begin{pmatrix} a & b & g\alpha \\ \frac{1-a}{b} & 0 & g/\alpha^2 \\ 2\alpha & \alpha^4 & 1 \end{pmatrix}. \quad (5.25)$$

where

$$g = \phi'(e^*), \quad u = \frac{1-a}{b}, \quad \alpha = \left( \frac{b}{1-a} \right)^{1/3}.$$

Using diagonal similarity transformations, the eigenvalues of the linearisation are equal to those of

$$M = \begin{pmatrix} a & 1-a & g \\ 1 & 0 & g \\ 2\alpha^2 & \alpha^2 & 1 \end{pmatrix}.$$

One can show that the matrix  $M$  has a complex conjugate pair of eigenvalues  $\lambda = 1 \pm \sqrt{3|g|}\alpha i$ , using  $g = \phi'(e^*) < 0$ . Therefore, the equilibrium  $x^*$  cannot be linearly stable. This is consistent with the simulation above where we observed either divergent – see Figure 5.13 or oscillatory behaviour – see Figure 5.11.

### Adaptive arms race: 3+1 Case

We are analysing the equilibria of the system:

$$x(t+1) = \begin{pmatrix} 1 & 0 & 0 \\ 0 & \phi(e(t)) & 0 \\ 0 & 0 & 1 \end{pmatrix} Ax(t). \quad (5.26)$$

$$e(t+1) = e(t) + |C_1 x(t)|^2 - \frac{1}{|C_2 x(t)|}.$$

Let the equilibrium be  $(x^*, e^*)$  :

$$x^* = \begin{pmatrix} 1 & 0 & 0 \\ 0 & \phi^* & 0 \\ 0 & 0 & 1 \end{pmatrix} Ax^*$$

$$e^* = e^* + |C_1 x^*|^2 - \frac{1}{C_2 x^*}$$

In (5.26). Hence  $\phi^* = \phi(e^*)$ . Then since we are targeting the second stage of population, we choose  $\phi_{22} = \phi(e)$   $\phi_{11} = 1$  and  $\phi_{33} = 1$ . Where

$$A = \begin{pmatrix} a & b & c \\ d & 0 & 0 \\ 0 & e & 0 \end{pmatrix}.$$

We first note that:  $\begin{pmatrix} 1 & 0 & 0 \\ 0 & \phi^* & 0 \\ 0 & 0 & 1 \end{pmatrix} A = A_0 + \begin{pmatrix} 0 \\ 1 \\ 0 \end{pmatrix} \phi^* a_2^T$ . where  $a_2^T = (d \ 0 \ 0)$  (5.27)

$A_0$  is given by:

$$A_0 = \begin{pmatrix} a_1^T \\ 0 & 0 & 0 \\ a_3^T \end{pmatrix}, \text{ where } a_i^T \text{ is the } i^{\text{th}} \text{ row of } A.$$

Then,

$$x^* = \left( A_0 + \phi^* \begin{pmatrix} 0 \\ 1 \\ 0 \end{pmatrix} a_2^T \right) x^*$$

Solving this equation we get:

$$(I - A_0)x^* = \phi^* \begin{pmatrix} 0 \\ 1 \\ 0 \end{pmatrix} a_2^T x^*$$

Multiplying both sides by  $(I - A_0)^{-1}$  leads to:

$$x^* = \phi^* (I - A_0)^{-1} \begin{pmatrix} 0 \\ 1 \\ 0 \end{pmatrix} \underbrace{a_2^T x^*}_{\in \mathbb{R}} \quad (5.28)$$

By multiplying  $a_2^T$  and then dividing both sides by  $a_2^T x^*$  gives:

$$1 = \phi^* a_2^T (I - A_0)^{-1} \begin{pmatrix} 0 \\ 1 \\ 0 \end{pmatrix} \quad (5.29)$$

To solve (5.29) we first solve

$$\begin{pmatrix} 1-a & -b & -c \\ 0 & 1 & 0 \\ 0 & -e & 1 \end{pmatrix}^{-1} \begin{pmatrix} 0 \\ 1 \\ 0 \end{pmatrix} = \begin{pmatrix} x \\ y \\ z \end{pmatrix} \implies y=1, z=e \quad \text{and} \quad x = \frac{b+ec}{1-a}.$$

Thus,

$$(I-A_0)^{-1} \begin{pmatrix} 0 \\ 1 \\ 0 \end{pmatrix} = \begin{pmatrix} \frac{b+ce}{1-a} \\ 1 \\ e \end{pmatrix} \quad (5.30)$$

Multiplying the previous by  $a_2^T$  from the left and taking the inverse gives  $\phi^*$ .

$$\implies \phi^* = \frac{1-a}{bd+dec}$$

From (5.28), we have

$$x^* = m \begin{pmatrix} \frac{b+ce}{1-a} \\ 1 \\ e \end{pmatrix}$$

Now,  $|C_1 x^*|^2 = \frac{1}{C_2 x^*}$ . But  $C_1 = [0 \ 0 \ 1]$  and  $C_2 = [1 \ 0 \ 0]$ . Thus  $m$  is given by:

$$m = \left( \frac{1-a}{e^2(b+ce)} \right)^{\frac{1}{3}}.$$

Finally,

$$\phi^* = \phi(e^*) \implies e^* = \left( \frac{1-a}{bd+dec} \right)^{-1}$$

The linearisation of

$$x(t+1) = \begin{pmatrix} 1 & 0 & 0 \\ 0 & \phi(e(t)) & 0 \\ 0 & 0 & 1 \end{pmatrix} Ax(t)$$

$$e(t+1) = e(t) + |C_1 x(t)|^2 - \frac{1}{|C_2 x(t)|}.$$

Around  $(x^*, e^*)$  the linearisation matrix is

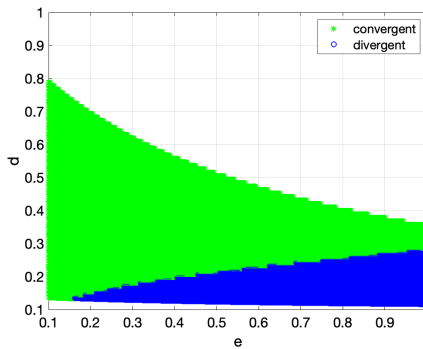
$$J = \begin{pmatrix} A_0 + \phi^* \begin{pmatrix} 0 \\ 1 \\ 0 \end{pmatrix} a_2^T & \phi'(e^*) \begin{pmatrix} 0 \\ 1 \\ 0 \end{pmatrix} a_2^T x^* \\ 2C_1 x^* C_1 + \frac{C_2}{(C_2 x^*)^2} & 1 \end{pmatrix}.$$

Using the above formulas for  $x^*, e^*, m$  and  $\phi^*$ , can be written as:

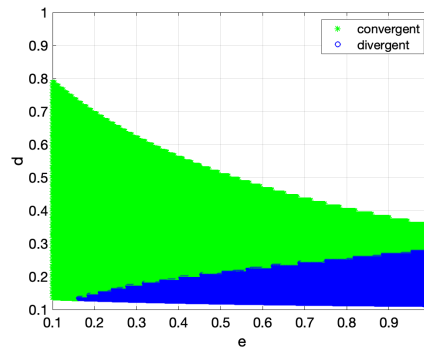
$$\Rightarrow J = \begin{pmatrix} a & b & c & 0 \\ \frac{1-a}{dbce} & 0 & 0 & \frac{-(dg(b-a+ce))}{(e^2(a^2-1)(b+ce))} \\ 0 & e & 0 & 0 \\ \frac{(e^4(a^2-1)^2(b+ce)^2)}{(b-a+ce)^2} & 0 & \frac{-2}{(e(a^2-1)(b+ce))} & 1 \end{pmatrix} \quad (5.31)$$

In the 3 + 1 case, the linearisation matrix is more complicated than in the 2 + 1 case. So we cannot make such a definitive statement as we did in the 2 + 1 case. Instead we resort to some numerical exploration. In the above simulations 5.15, we consider a variety of possibilities:

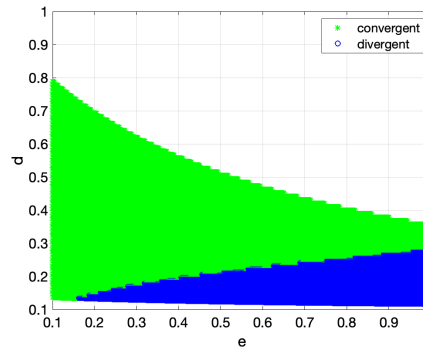
- Solving  $a$  and equating it with the other parameters.
- Varying two parameters  $d$  and  $e$ .



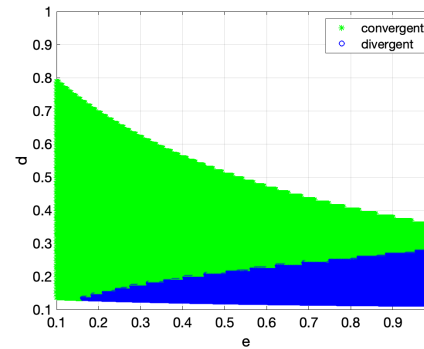
(a) Stability analysis, with  $b = 1.2$  and  $c = 2$ .



(b) Stability analysis, with  $b = 0.8$  and  $c = 6$ .



(c) Stability analysis, with  $b = 1.3$  and  $c = 0.6$ .



(d) Stability analysis, with  $b = 0.3$  and  $c = 10$ .

Figure 5.15: Some Simulations for the above calculation while Convergence "green" as well when is Divergence "blue" with a size step =0.001.

- Fixing the other parameters  $b$  and  $c$ .

The system (5.26) has been adapted by a value to control the matrix  $A$ . The dominate eigenvalue has condition which if the absolute value of the dominate eigenvalue is less than 1 then the system is convergence and if it is greater than 1 it leads to diverge the system.

**Remark 5.13.** In the  $2 + 1$  and  $3 + 1$  simulation studies, we targeted stage 2. We could also consider targeting other stages, or even multiple stages. However, without a clear pattern this would just be yet more speculative simulation without shedding light on what is going on. So this is omitted for brevity.

**Remark 5.14.** As we can see from the simulations in the  $2 + 1$  and  $3 + 1$  cases, we have not found a parallel discrete-time result that mirrors the bifurcation learning algorithm of Chapter 4, except in the  $1 + 1$  case. Theorem 4.13 drew significantly on the relative degree one, minimum phase structure which does not really exist for discrete-time systems. This might explain why we do not find a similar pattern. We did try to match the set-ups – so additive feedback in continuous-time and multiplicative feedbacks in discrete-time. But there are many other subtleties at play. Unravelling the situation is the topic of future work.

## 5.4 Conclusion

This chapter attempts to complement the developments of Chapter 4 in continuous-time with discrete-time counterparts. In Theorems 5.3 (adaptive stabilisation) and 5.6 (adaptive destabilisation or persistence) we prove discrete-time analogues of Theorems 4.4 and 4.8, respectively. As in those continuous-time results, the underlying non-negativity of the system plays a significant role. So far we have not been able to find the discrete-time analogue of the bifurcation learning algorithm described in Theorem 4.13. We find that the  $1 + 1$  system oscillates, agreeing with the continuous-time analogue. The  $2 + 1$  systems oscillates or diverges. The  $3 + 1$  systems

may converge, oscillate or diverge. But in general there is no obvious systematic pattern. This is the subject of future work.

## Chapter 6

# Adaptive Control Inspired Habitat Renewal

Overview, in the final theme we revisit one of the classical paradigms of population ecology - the so called “Principle of Competitive Exclusion”. This principle asserts that *“two species which compete for the same limited resource cannot coexist at constant population values. When one species has even the slightest advantage over another, the one with the advantage will dominate in the long term. This leads either to the extinction of the weaker competitor or to an evolutionary or behavioural shift toward a different ecological niche.”* The principle has been paraphrased in the maxim “complete competitors can not coexist”, see [34]. It is often referred to as the Gause principle. The first mathematical treatment of this principle is due to Volterra [35]. Alongside competition exclusion, using a bounded resource causes the depletion of resource [34].

Whilst competitive exclusion may lead to a shift in population behaviour (and therefore also a change in intra-specific parameters) over evolutionary time scales, the principle is based on an

assumption that parameters do not change on ecological time scales. However, in contrast to mechanical and electrical systems - the mainstay of control theory - natural systems will be subject to degradation over short, ecological time scales. To clarify this point, in an electrical circuit under some feedback control, we can assume that the electrical components, and the corresponding resistance, inductance and capacitance parameters, are not changed by the control action - at least not on reasonable time scales. However, in natural systems, for example in a model of competitive interaction, over (under) abundance of one species may undermine (improve) that species own habitat, manifested as a reduction (increase) in carrying capacity parameters - suggesting the possibility for self-regulation by habitat renewal. By habitat renewal, we mean some mechanism, natural or man-made, which will increase the carrying capacity of a species, so “renewing its habitat”. Borrowing from adaptive control, we propose a simple mechanism for precisely such self-regulation by habitat renewal. The main results are:

- Simulation Result 6.1: We find a simple mechanism for the renewal of otherwise degrading habitats that “stabilises” the interacting population to a co-existence equilibrium. The habitat renewal provides a stabilising mechanism in a way similar to Watt’s Flyball Governor [9] .
- Simulation Result 6.2: If the habitat renewal dynamics are frozen or switched off, then the system reverts back to competitive exclusion. Crucially, which species persists (or is driven to extinction) in resulting the exclusion, is sensitive to the timing of the switching off. Simulations are depicted in Figures 6.3, 6.4 and 6.5.

This chapter is organised as follows: In Section 6.1 we recall the basic modelling framework for two competing species. In Section 6.2 we develop a model which captures the idea of an adaptive habitat that changes (renews or depletes) as a response to decreasing or increasing

population densities. In Section 6.3 we describe the main finding – that this simple adaptive habitat renewal mechanism regulates a system to competitive co-existence that would otherwise exhibit competitive exclusion in the absence of this regulation. The idea is illustrated in a number of examples in Section 6.4. Here we also show the sensitivity of the dynamics to the timing of the termination or freezing of the habitat renewal mechanism.

## 6.1 Habitat renewal and interspecific competition model

Recall from Chapter 2, the competitive interaction of two populations described by the coupled system

$$\frac{dN_1}{dt} = r_1 N_1 \left[ 1 - \frac{N_1}{K_1} - b_{12} \frac{N_2}{K_1} \right] \quad (6.1a)$$

$$\frac{dN_2}{dt} = r_2 N_2 \left[ 1 - \frac{N_2}{K_2} - b_{21} \frac{N_1}{K_2} \right] \quad (6.1b)$$

In equation (6.1),  $N_1$  and  $N_2$  are the abundances of species in competition. The parameters<sup>1</sup>  $r_1$ ,  $K_1$ ,  $b_{12}$ ,  $r_2$ ,  $K_2$  and  $b_{21}$   $> 0$ . The presence of each population inhibits the growth of the other. The parameters  $K_1$  and  $K_2$  capture the intrinsic carrying capacity of each population.

As discussed in Chapter 2, the system 6.1 exhibits competitive exclusion when the parameters satisfy:

$$K_2 b_{12} > K_1 \quad \text{and} \quad K_1 b_{21} > K_2. \quad (6.2)$$

See Figure 6.1

---

<sup>1</sup>We do not apply the standard scaling or non-dimensionalisation (see e.g. [10]) because later we will vary or adapt  $K_1$  and  $K_2$ . Scaling would confuse the situation.

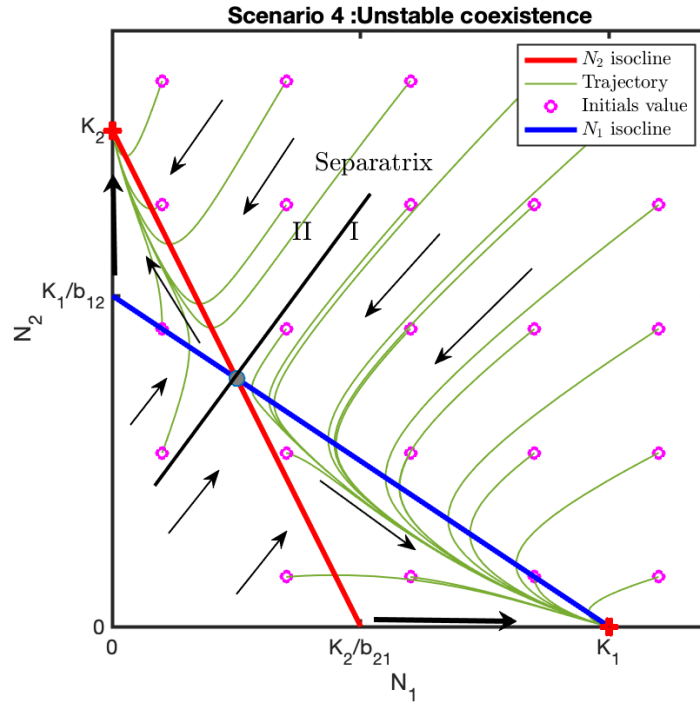


Figure 6.1: Competitive exclusion when  $K_2 > \frac{K_1}{b_{12}}$  and  $K_1 > \frac{K_2}{b_{21}}$  in (6.1).

Within this parameter regime, there is a separatrix made up from the stable manifold of the co-existent hyperbolic equilibrium – for initial conditions on the lower right side of the separatrix, the population  $N_1$  tends to carrying capacity and  $N_2$  tends to zero; for initial conditions on the upper left side, the population  $N_2$  tends to carrying capacity and  $N_1$  tends to zero. This is the so-called “Principle of Competitive Exclusion” [10].

Note that in this simple framework, the carrying capacities are assumed to be fixed, i.e. constant in time. Such an assumption of fixed parameters is a reasonable assumption, especially in a context of mechanical or electrical systems whereby, over reasonable time scales, the stiffness of a spring or the resistance of a resistor would not change significantly over timescales of the velocities or currents. But for natural ecological systems, this assumption can be challenged.

Indeed, it is reasonable to suppose that the parameters, for example the carrying capacities, do change with time – perhaps degraded by anthropogenic factors such as land-use change. Moreover, in a context of management or control, the parameters may be forced to change – for example by some conservation action. Of course this second way in which parameters change will also apply in mechanical and electrical systems where a variable resistance or moment of inertia may play an important role (e.g. Watt’s flyball governor [9]).

## 6.2 A habitat-population feedback mechanism for habitat renewal

Here we investigate the dynamical consequences of carrying capacities that change with time. We are motivated by habitat degradation/renewal which here we take to mean a decrease/increase in the respective carrying capacities. These increases/decreases are tied to the population abundances as follows:

1. if  $N_1 > N_2$ , so that population 1 is relatively over abundant compared to population 2, then carrying capacity  $K_2$  increases;
2. if  $N_2 > N_1$ , so that population 2 is relatively over abundant compared to population 1, then carrying capacity  $K_1$  increases;
3. in the absence of recovery driven by these relative abundances, both habitats degrade over time, that is both  $K_1$  and  $K_2$  would decrease.

These properties can be captured in various ways by making the carrying capacities “dynamical”. One approach is to append to the competitive interaction described by (6.1) the “habitat renewal” dynamics

$$\frac{dK_1}{dt} = -K_1 + \varepsilon \left( \frac{N_2}{N_1} \right)^2, \quad \frac{dK_2}{dt} = -K_2 + \varepsilon \left( \frac{N_1}{N_2} \right)^2. \quad (6.3)$$

These rates of change of  $K_1$  and  $K_2$  contain two parts: the  $-K_i$  term in each equation forces  $K_i$  to decrease (degrade) exponentially over time; the terms  $(N_2/N_1)^2$ , respectively  $(N_1/N_2)^2$  are non-negative “relative abundance” terms. If population 1 is more abundant than population 2, then  $N_1 > N_2$ . In this case, the  $N_2$  dynamics are driven by a positive term, greater than 1 in magnitude and habitat 2 recovers, i.e. “renews”. If, vice-versa, population 2 is more abundant than population 1, then  $N_2 > N_1$ . In this case, the  $N_1$  dynamics are driven by a positive term, greater than 1 in magnitude and habitat 1 recovers, i.e. “renews”. The parameter  $\varepsilon > 0$  in (6.3) is used to control the strength of the habitat renewal process.

The addition of dynamical carrying capacities driven by relative over/under abundances of respective populations leads to a four-dimensional system:

$$\begin{aligned}
 \frac{dN_1}{dt} &= r_1 N_1 \left[ 1 - \frac{N_1}{K_1} - b_{12} \frac{N_2}{K_1} \right] \\
 \frac{dN_2}{dt} &= r_2 N_2 \left[ 1 - \frac{N_2}{K_2} - b_{21} \frac{N_1}{K_2} \right] \\
 \frac{dK_1}{dt} &= -K_1 + \varepsilon \left( \frac{N_2}{N_1} \right)^2 \\
 \frac{dK_2}{dt} &= -K_2 + \varepsilon \left( \frac{N_1}{N_2} \right)^2 .
 \end{aligned} \tag{6.4}$$

### 6.3 Habitat-population feedback and competitive co-existence

System (6.4) includes the new simple feedback whereby  $\dot{K}_1$  and  $\dot{K}_2$  depend on population density. These are the mechanisms for habitat renewal that we use to force a coexistence stable point in the competitive-exclusion system. Otherwise, the parameters in (6.4) have a similar explanation as with the parameters in system (6.1), with the addition of the extra parameter  $\varepsilon > 0$  that controls the strength of habitat renewal.

Our findings are summarised as follows:

**Simulation Result 6.1.** Remarkably we find that the simple mechanism (6.3) for the renewal of otherwise degrading habitats “stabilises” the interacting population to a co-existence equilibrium. This stabilising mechanism acts like Watt’s Flyball Governor [9].

**Simulation Result 6.2.** If the habitat renewal dynamics (6.3) are frozen, (i.e.  $K_1(t)$  and  $K_2(t)$  are constant for  $t \geq t_s$ , some  $t_s$ ) then the system reverts back to competitive exclusion.

So how does this stabilising mechanism work. Suppose that the system dynamics are tending towards excluding population 1, so that  $N_1$  is relatively much smaller than  $N_2$ . In this case,  $(N_2/N_1)^2$  is very large and  $K_1$  will increase meaning that  $N_1$  can now recover. If instead, the system dynamics are tending towards excluding population 2, so that  $N_2$  is relatively much smaller than  $N_1$ . In this case,  $(N_1/N_2)^2$  is very large and  $K_2$  will increase meaning that  $N_2$  can now recover. This counter-balancing process leads to the 4-dimensional system (6.4) admitting an equilibrium

$$E_{\text{coexist}} = (N_1^*, N_2^*, K_1^*, K_2^*)$$

with  $N_1^* > 0$  and  $N_2^* > 0$ . In our simulations we also find that:

- the equilibrium values  $K_1^*$  and  $K_2^*$  are such that

$$K_2^* b_{12} > K_1^* \quad \text{and} \quad K_1^* b_{21} > K_2^*,$$

meaning that the equilibrium values of the adaptive carrying capacities would support competitive exclusion;

- the linearisation of (6.4) at equilibrium  $E_{\text{coexist}}$  has only eigenvalues with negative real part, ensuring local stability of the equilibrium. In addition, two eigenvalues are non real which produces a spiralling behaviour of  $N_1$  and  $N_2$ .

- in the simulation,  $E_{\text{coexist}}$  appears to be a globally asymptotically stable for all positive initial conditions  $N_1(0)$  and  $N_2(0)$ ;
- if we switch off, i.e. freeze, the habitat renewal mechanism at time  $t = t_S$ , with  $t_S \gg 1$ , large enough so that  $K_1(t_S)$  and  $K_2(t_S)$  will be close enough to  $K_1^*$  and  $K_2^*$  to make

$$K_2(t_S)b_{12} > K_1(t_S) \quad \text{and} \quad K_1(t_S)b_{21} > K_2(t_S).$$

Then the frozen system reverts back to competitive exclusion. In particular, to a competitive exclusion system with its own separatrix;

- Because the nonlinear system (6.4) has a spiralling behaviour for  $N_1$  and  $N_2$  around  $(N_1^*, N_2^*)$ , which sits very close to the separatrix of a competitive system, then the timing of  $t = t_S$  at which the habitat renewal is frozen will determine on which side of the separatrix  $(N_1(t_S), N_2(t_S))$  sits. This leads to a sensitivity, with respect to the timing  $t_S$ , of which population is excluded.

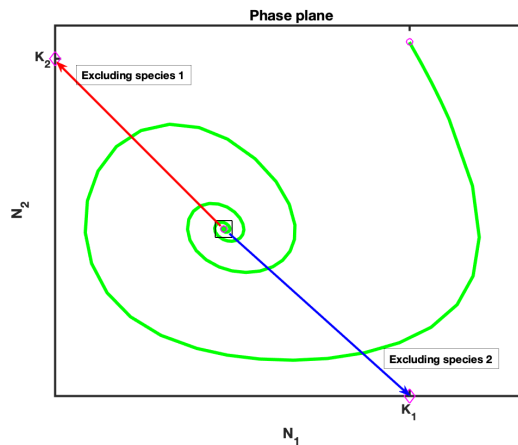


Figure 6.2: A cartoon explaining the sensitivity process; with respect to the timing  $t_S$ , of which population is excluded.

The sensitivity process, with respect to the timing  $t_S$ , of which population is excluded is illustrated in Figure 6.2. In Figure 6.2 the green trajectory represents the phase diagram of  $N_1$  and  $N_2$  for (6.4). The black square shows a new co-existence stable point. The black line is the separatrix for the frozen system, effectively passing through the co-existence equilibrium when  $t_S \gg 1$ . The blue and red lines are trajectories heading towards respective exclusions  $N_1 = K_1(t_S)$  and  $N_2 = K_2(t_S)$ , indicated by pink diamonds. Because of the spiralling dynamics, which side of the separatrix  $(N_1(t_S), N_2(t_S))$  sits depends sensitively on the timing  $t_S$ .

## 6.4 Examples

In this section we illustrate the co-existence by habitat renewal for a number of examples with different parameters.

**Remark 6.3.** In each example, we will use two pairs of initial values  $K_1(0)$  and  $K_2(0)$  that without habitat renewal would produce competitive exclusion.

### Example 1

The table (6.1) shows the parameter values used in the first example.

$r_1$	$r_2$	$b_{12}$	$b_{21}$	$\varepsilon$
5	4	1.5	1.15	3

Table 6.1: The Parameter values for Example 1.

In this case, system (6.4) admits a coexistence equilibrium point at:

$$(N_1^*, N_2^*, K_1^*, K_2^*) = (1.2636, 1.3203, 3.2607, 2.7578).$$

In the first simulation, the initial values are  $K_1(0) = 9$  and  $K_2(0) = 7$ . These initial values of

$K_1(0)$  and  $K_2(0)$  satisfy

$$K_2(0)b_{12} = 10.5 > K_1(0) = 9 \quad \text{and} \quad K_1(0)b_{21} = 10.35 > K_2(0) = 7.$$

In the second simulation, the initial values are  $K_1(0) = 10$  and  $K_2(0) = 10$ . These initial values of  $K_1(0)$  and  $K_2(0)$  satisfy

$$K_2(0)b_{12} = 15 > K_1(0) = 10 \quad \text{and} \quad K_1(0)b_{21} = 11.5 > K_2(0) = 10.$$

So both pairs of initial conditions for  $K_1$  and  $K_2$  would lead to competitive exclusion.

We also check competitive exclusion for the equilibrium values  $K_1^* = 3.2607$  and  $K_2^* = 2.7578$ .

In this case

$$K_2^*b_{12} = 4.1367 > K_1^* = 3.2607 \quad \text{and} \quad K_1^*b_{21} = 3.7498 > K_2^* = 2.7578.$$

These inequalities hold for  $K_1(t)$  and  $K_2(t)$  when  $t = t_S$  and  $t_S$  is large enough, leading to competitive exclusion in the frozen system .

The Jacobian matrix of the system (6.4) is expressed as:

$$\begin{pmatrix} -\frac{r_1}{k_1} & -\frac{b_{12}r_1}{k_1} & \frac{r_1(N_1 + N_2 b_{12})}{k_1^2} & 0 \\ -\frac{b_{21}r_2}{k_2} & -\frac{r_2}{k_2} & 0 & \frac{r_2(N_2 + N_1 b_{21})}{k_2^2} \\ -\frac{2N_2^2 \epsilon}{N_1^3} & \frac{2N_2 \epsilon}{N_1^2} & -1 & 0 \\ \frac{2N_1 \epsilon}{N_2^2} & -\frac{2N_1^2 \epsilon}{N_2^3} & 0 & -1 \end{pmatrix}. \quad (6.5)$$

Substituting the parameters of 6.1 in the Jacobian matrix (6.5) at the equilibrium  $(N_1^*, N_2^*, K_1^*, K_2^*) =$

(1.2636, 1.3203, 3.2607, 2.7578). Leads to a linearisation:

$$J|_{(N_1^*, N_2^*, K_1^*, K_2^*)} = \begin{pmatrix} -1.5334 & -2.3001 & 1.5256 & 0 \\ -1.6680 & -1.4504 & 0 & 1.4587 \\ -5.1840 & 4.9614 & -1 & 0 \\ 4.3493 & -4.1625 & 0 & -1 \end{pmatrix} \quad (6.6)$$

The linearisation has eigenvalues

$$\lambda_1 = -0.2717 + 3.6618i, \quad \lambda_2 = -0.2717 - 3.6618i, \quad \lambda_3 = -3.4405, \quad \lambda_4 = -1. \quad (6.7)$$

All the eigenvalues in (6.7) have a negative real part. So

$$(N_1^*, N_2^*, K_1^*, K_2^*) = (1.2636, 1.3203, 3.2607, 2.7578).$$

is a stable coexistence equilibrium of the nonlinear system with habitat renewal. Note also, that there is a pair of non-real eigenvalues in (6.7) which produce a spiralling behaviour and resulting sensitivity with respect to the “switching off” time  $t = t_S$ .

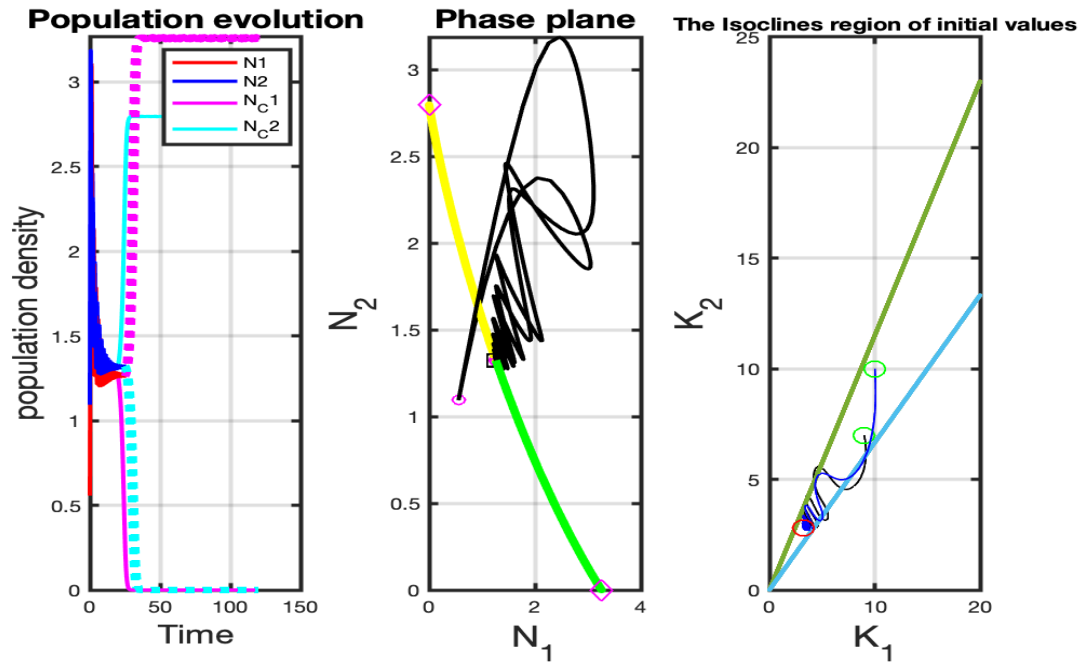


Figure 6.3: Simulation results for habitat renewal (6.4) using the parameters 6.1.

In the simulation presented in Figure 6.3, the left figure indicates the population evolution over time for the system with Habitat renewal feedback (6.4) the red colour for species  $N_1$  and the blue one for  $N_2$ . The cyan dots represent  $N_1$ , and the magenta dots show  $N_2$  in the system of competitive exclusion (6.1). The trajectories of the evolution of the population densities  $N_1$  and  $N_2$  depend on when the habitat renewal switch off. So this is a sensitivity concerning switching off; we switch off slightly later, and the trajectory, we get cyan dots exclusion in one case and pink exclusion in the other. In the middle Figure of (6.3), the trajectory is tending the stable spiral point  $(N_1^*, N_2^*)$  and then the feedback switches off near the stable spiral point. Thus it has switched off twice on the left of the spiral point, which leads to excluding  $N_1$  'Yellow trajectory' and then switched off again on the right of the spiral point with the 'green trajectory' to exclude  $N_2$ . The right figure shows  $K_1$  and  $K_2$  space. The initial values of  $K_1$  and  $K_2$  are in

the wedge between the blue and green lines, with a green circle for the initial values. Each time, we simulate  $K_1$  and  $K_2$ , tending the trajectories to the red circle in the wedge, as shown in the figure. Thus the two spaces within the wedge lead to competitive exclusion, hence our initial conditions in both spaces.

### Example 2

Table 6.2 shows the parameter values used in this example.

$r_1$	$r_2$	$b_{12}$	$b_{21}$	$\varepsilon$
8	7	1.3571	1.125	19

Table 6.2: The Parameter values for Example 2.

In this case, system (6.4) admits a coexistence equilibrium point at:

$$(N_1^*, N_2^*, K_1^*, K_2^*) = (8.4465, 8.5336, 19.8808, 18.1730).$$

In the first simulation, the initial values are  $K_1(0) = 10$  and  $K_2(0) = 10$ . These initial values of  $K_1(0)$  and  $K_2(0)$  satisfy

$$K_2(0)b_{12} = 13.5714 > K_1(0) = 10 \quad \text{and} \quad K_1(0)b_{21} = 11.25 > K_2(0) = 10.$$

In the second simulation, the initial values are  $K_1(0) = 25$  and  $K_2(0) = 20$ . These initial values of  $K_1(0)$  and  $K_2(0)$  satisfy

$$K_2(0)b_{12} = 27.1429 > K_1(0) = 25 \quad \text{and} \quad K_1(0)b_{21} = 28.125 > K_2(0) = 20.$$

So both pairs of initial conditions for  $K_1$  and  $K_2$  would lead to competitive exclusion.

We also check competitive exclusion for the equilibrium values  $K_1^* = 19.8808$  and  $K_2^* = 18.1730$ .

In this case

$$K_2^*b_{12} = 24.6634 > K_1^* = 19.8808 \quad \text{and} \quad K_1^*b_{21} = 22.3659 > K_2^* = 18.1730.$$

These inequalities hold for  $K_1(t)$  and  $K_2(t)$  when  $t = t_S$  and  $t_S$  is large enough, leading to competitive exclusion in the frozen system . Using (6.5) we obtain the eigenvalues of the linearisation

$$\lambda_1 = -0.4537 + 1.7974i, \quad -0.4537 - 1.7974i, \quad \lambda_3 = -0.8803, \quad \lambda_4 = -1. \quad (6.8)$$

All the eigenvalues in (6.8) have a negative real part. So

$$(N_1^*, N_2^*, K_1^*, K_2^*) = (8.4465, 8.5336, 19.8808, 18.1730).$$

Is a stable coexistence equilibrium of the nonlinear system with habitat renewal. Note also, that there is a pair of non-real eigenvalues in (6.8) which produce a spiralling behaviour and resulting sensitivity with respect to the “switching off” time  $t = t_S$ .

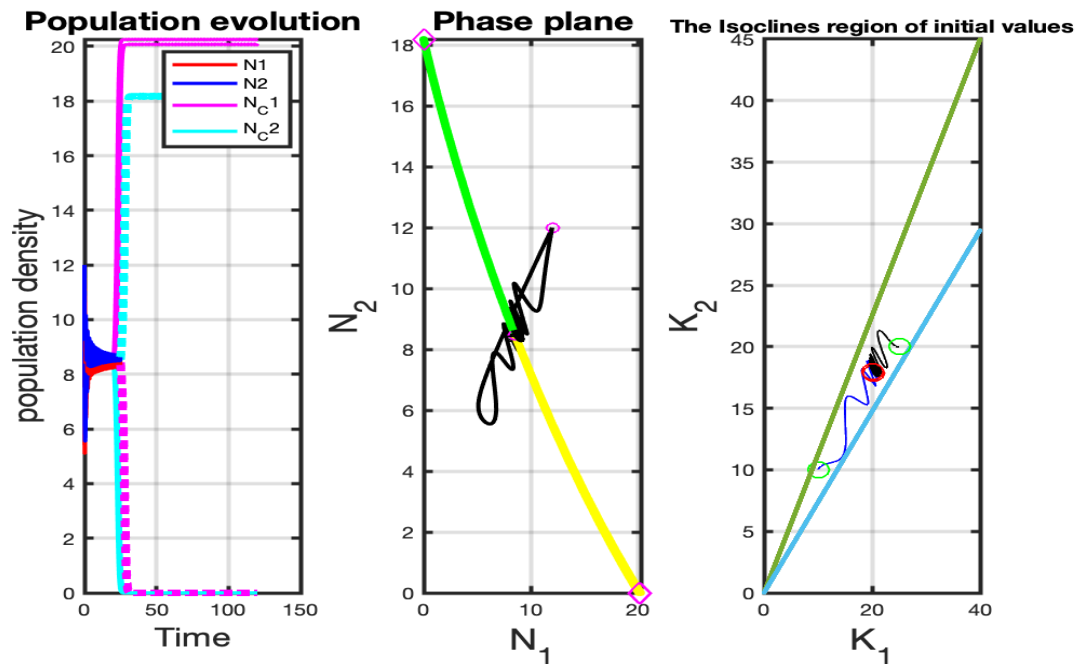


Figure 6.4: Simulation results for habitat renewal (6.4) using the parameters 6.2.

In the simulation presented in Figure 6.4, the left figure indicates the population evolution over

time for the system with Habitat renewal feedback (6.4) the red colour for species  $N_1$  and the blue one for  $N_2$ . The cyan dots represent  $N_1$ , and the magenta dots show  $N_2$  in the system of competitive exclusion (6.1). The trajectories of the evolution of the population densities  $N_1$  and  $N_2$  depend on when the habitat renewal switch off. We switch off slightly later, and the trajectory, we get cyan dots exclusion in one case and pink exclusion in the other. In the middle Figures of 6.4, the trajectory is tending the stable spiral point  $(N_1^*, N_2^*)$  and then the feedback switches off near the stable spiral point. Thus it has switched off twice on the left of the spiral point, which leads to excluding  $N_1$  'Yellow trajectory' and then switched off again on the right of the spiral point with the 'green trajectory to exclude  $N_2$ . The right figure shows  $K_1$  and  $K_2$  space. The initial values of  $K_1$  and  $K_2$  are in the wedge between the blue and green lines, with a green circle for the initial values. Each time, we simulate  $K_1$  and  $K_2$ , tending the trajectories to the red circle in the wedge, as shown in the figure. Thus the two spaces within the wedge lead to competitive exclusion, hence our initial conditions in both spaces.

### Example 3

Table 6.3 shows the parameter values used in this example.

$r_1$	$r_2$	$b_{12}$	$b_{21}$	$\varepsilon$
3	2	1.125	1.0882	12

Table 6.3: The Parameter values for Example 3.

In this case, system (6.4) admits a coexistence equilibrium point at:

$$(N_1^*, N_2^*, K_1^*, K_2^*) = (5.6848, 5.7067, 12.0881, 11.91140).$$

In the first simulation, the initial values are  $K_1(0) = 20$  and  $K_2(0) = 20$ . These initial values of

$K_1(0)$  and  $K_2(0)$  satisfy

$$K_2(0)b_{12} = 22.5 > K_1(0) = 20 \quad \text{and} \quad K_1(0)b_{21} = 21.7647 > K_2(0) = 20.$$

In the second simulation, the initial values are  $K_1(0) = 5$  and  $K_2(0) = 5$ . These initial values of  $K_1(0)$  and  $K_2(0)$  satisfy

$$K_2(0)b_{12} = 5.625 > K_1(0) = 5 \quad \text{and} \quad K_1(0)b_{21} = 5.4412 > K_2(0) = 5.$$

So both pairs of initial conditions for  $K_1$  and  $K_2$  would lead to competitive exclusion.

We also check competitive exclusion for the equilibrium values  $K_1^* = 12.0881$  and  $K_2^* = 11.91140$ .

In this case

$$K_2^*b_{12} = 13.4003 > K_1^* = 12.0881 \quad \text{and} \quad K_1^*b_{21} = 13.1547 > K_2^* = 11.91140.$$

These inequalities hold for  $K_1(t)$  and  $K_2(t)$  when  $t = t_S$  and  $t_S$  is large enough, leading to competitive exclusion in the frozen system . Using (6.5) we obtain the eigenvalues of the linearisation

$$\lambda_1 = -0.4989 + 1.2237i, \quad -0.4989 - 1.2237i, \quad \lambda_3 = -0.4182, \quad \lambda_4 = -1. \quad (6.9)$$

All the eigenvalues in (6.9) have a negative real part. So

$$(N_1^*, N_2^*, K_1^*, K_2^*) = (5.6848, 5.7067, 12.0881, 11.91140).$$

is a stable coexistence equilibrium of the nonlinear system with habitat renewal. Note also, that there is a pair of non-real eigenvalues in (6.9) which produce a spiralling behaviour and resulting sensitivity with respect to the “switching off” time  $t = t_S$ .

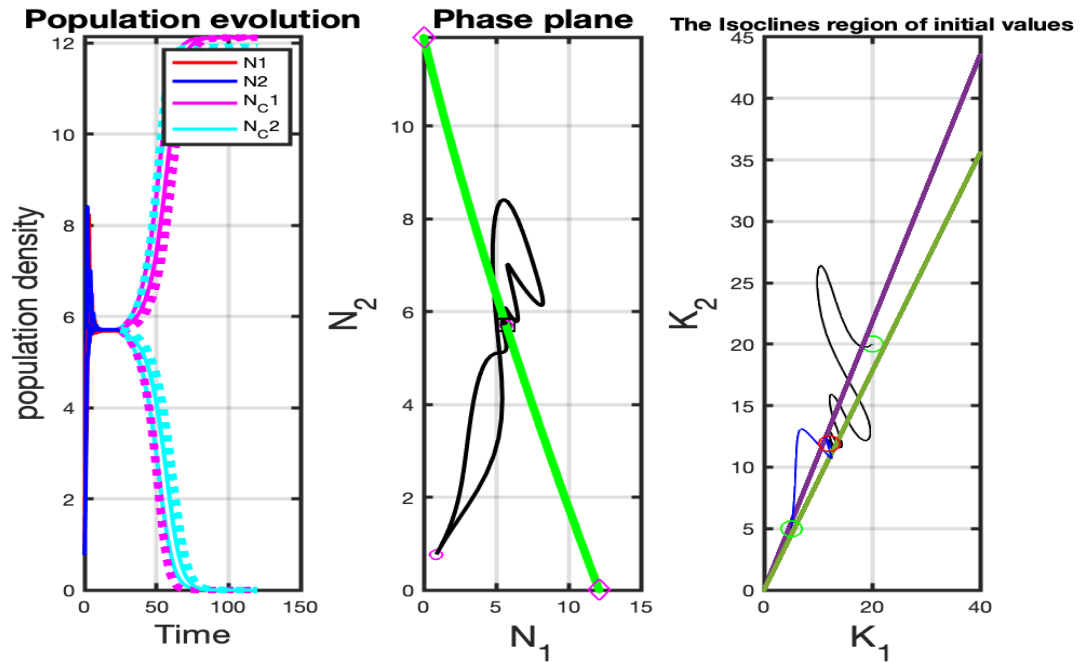


Figure 6.5: Simulation results for habitat renewal (6.4) using the parameters 6.3.

In the simulation presented in Figure 6.5, the left figure indicates the population evolution over time for the system with habitat renewal feedback (6.4) the red colour for species  $N_1$  and the blue one for  $N_2$ . The cyan dots represent  $N_1$ , and the magenta dots show  $N_2$  in the system of competitive exclusion (6.1). The trajectories of the evolution of the population densities  $N_1$  and  $N_2$  depend on when the habitat renewal switch off. So this is a sensitivity concerning switching off; we switch off slightly later, and the trajectory, we get cyan dots exclusion in one case and pink exclusion in the other. In the middle Figures of 6.5, the trajectory is tending the stable spiral point  $(N_1^*, N_2^*)$  and then the feedback switches off near the stable spiral point. Thus it has switched off twice on the left of the spiral point, which leads to excluding  $N_1$  'Yellow trajectory' and then switched off again on the right of the spiral point with the 'green trajectory' to exclude  $N_2$ . The right figure shows  $K_1$  and  $K_2$  space. The initial values of  $K_1$  and  $K_2$  are in the wedge

between the mauve and green lines, with a green circle for the initial values. Each time, we simulate  $K_1$  and  $K_2$ , tending the trajectories to the red circle in the wedge, as shown in the figure. Thus the two spaces within the wedge lead to competitive exclusion, hence our initial conditions in both spaces.

**Simulation Result 6.4.** In simulations 6.3, 6.4 and 6.5- we have this system (6.1), and we deploy the habitat renewal feedback. But while running the system (6.4), the habitat renewal feedback switches off, and then the system reverts to competitive exclusion (6.1). The timing depends on the timing of the switch off, and since the trajectory of the phase plane tends to a stable spiral point. When we switch off the habitat renewal feedback, it depends on which side it is switched off on since the system without the habitat renewal has an existing separatrix line. Thus, if it is stopped at the right of the spiral point, the system will exclude  $N_2$  species, and if it switches off at the left of the point, the phase plane provides an exclusion for  $N_1$  species. In the third picture, We run the simulations from those two initial conditions. And we arrive at the red circle still in the wedge. The initial conditions and the final conditions all satisfy how competitive exclusion. But the adaptive system is got competitive coexistence.

**Simulation Result 6.5.**

- Adaptation (6.3) active produces a stable equilibrium  $(N_1^*, N_2^*, K_1^*, K_2^*)$  of the 4D system;
- So without an active adaptive habitat renewal in play, we will revert to competitive exclusion;
- So freezing  $K_1 = K_1(t_f)$  and  $K_2 = K_2(t_f)$  with  $t_f$  large enough will freeze  $K_1$  and  $K_2$  at carrying capacity values that lead to competitive exclusion;
- Because  $(N_1^*, N_2^*, K_1^*, K_2^*)$  is a stable spiral of the 4D system, the frozen  $N_1(t_f)$  and  $N(t_f)$

will be on one side or the other side of the separatrix of the frozen system depending on the freezing time  $t_f$  – freezing later will swap the side of the separatrix;

- This means that the freezing time will determine which population goes extinct.

These simulations 6.3, 6.4 and 6.5 lead to a conjecture, summarised in the following theorem.

**Conjecture 6.1.** *The system (6.4) admits a stable equilibrium  $(N_1^*, N_2^*, K_1^*, K_2^*)$  in which*

- $N_1^*, N_2^* > 0$ , *that means we have co-existence.*
- $K_2^* b_{12} > K_1^*$  and  $K_1^* b_{21} > K_2^*$ , *that means we have competitive exclusion in the absence of habitat renewal.*
- *In the  $N_1, N_2$  plane, the dynamics around  $(N_1^*, N_2^*)$  are a stable spiral.*

## 6.5 Conclusion

In this chapter we revisited the classical paradigm of population ecology, the so called “Principle of Competitive Exclusion”. We adopted the simplest model of two species in a competitive interaction and exhibiting competitive exclusion. We then combined these population dynamics with a simple mechanism for habitat depletion/renewal. Here, habitats deplete over time, so that the corresponding carrying capacities reduce, but the habitat of the relatively least abundant species is renewed (its corresponding carrying capacity increases). With a parsimonious mechanism to capture this depletion/renewal, we find that the system is stabilised to co-existence. When the depletion/renewal mechanism is switched off, the system reverts back to competitive exclusion but with high sensitivity to the timing of the switch. This simple study scratches the surface of a much deeper study in to how adaptation - both natural or man-made - made significantly alter the prevailing population dynamics.

# Chapter 7

## Conclusion

The thesis is rooted in ideas from adaptive control but looks to take these ideas in novel directions. Our starting point are simple direct adaptive control schemes exemplified by the Byrnes-Willems adaptive controller (3.6) of Chapter 3. These are significantly developed in a context of non-negative Metzler systems in Theorem 4.4 and Theorem 4.8 from Chapter 4. The highly novel development is in Theorem 4.13 where direct adaptive stabilising and destabilising effects are combined. This leads to a brand new bifurcation learning algorithm. As a by-product of this learning algorithm we find a new solution to the classical set-point control problem, see Chapter 4, Section 4.5. Our new solution significantly out-performs existing approaches, such as adaptive integral controllers, in terms of robustness to un-modelled output disturbances. The adaptive stabilising and destabilising controllers are further explored in Chapter 5 as an adaptive “arms race” in a context of discrete-time systems. Here we find both convergent and divergent (escalating) behaviours. Finally, in Chapter 6 we use adaptive control-like mechanisms for habitat renewal. These habitat renewal mechanisms force competitive coexistence on a competitive exclusion system.

# Appendix A

## Preliminaries

In the following appendices I collect together various pieces of background theory and information.

### A.1 Continuous vs. discrete time systems

In my research, I will be switching between continuous and discrete-time models, depending on context and which might be easiest to control.

- 1- Continuous-time

Here the state of the system moves continuously (or in infinitesimal jumps) [36]

- 2- Discrete

Here the state of the system moves between points by jumping, [36]. In other words, to move from time  $t_n$  to  $t_{n+1}$

Here is an example showing the difference between continuous vs discrete dynamics, or in other words between a flow and a map systems. I use the logistic growth equation introduced by

Verhulst 1845 [37]

$$\frac{dX}{dt} = rX\left(1 - \frac{X}{K}\right) \quad (\text{A.1})$$

In (A.1),  $X$  represents the size of the species,  $r$  is the reproduction rate and  $K$  carrying capacity. In computing the dynamics of this system, one would use an ODE solver such as ODE45 due to the accuracy. In discrete time the same system (A.1) is modelled as

$$X_{t+1} = rX_t\left(1 - \frac{X_t}{K}\right) \quad (\text{A.2})$$

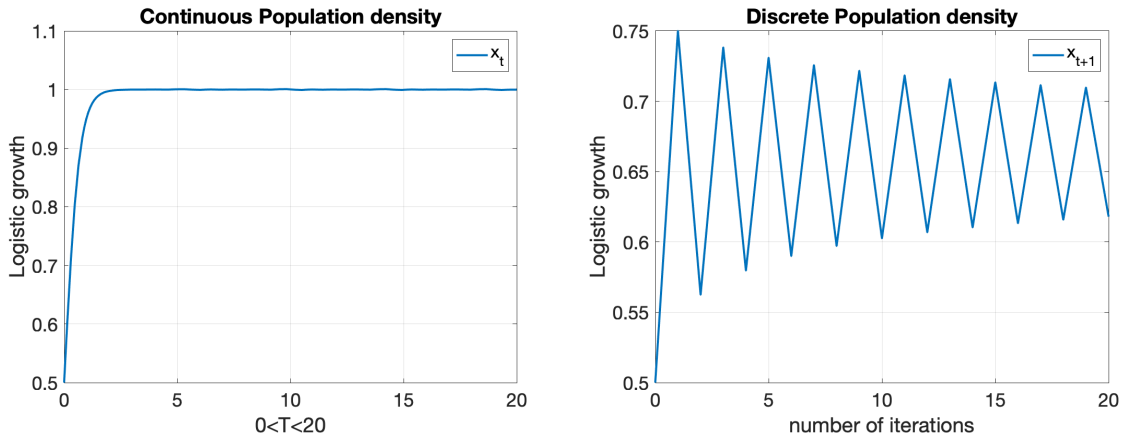


Figure A.1: The difference among the ODE of the logistic growth model.

The dynamical behaviours of the ecological systems, build from the flow and map time models. In discrete-time systems within a one-dimensional model there is a rich dynamic behaviour. On the other hand, where the time is continuous the execution of the dynamics are specified and unsurprising when the system is lower than three dimensions [38]. Here both of the systems are logistic growth the only difference being one of them is continuous in the left of figure A.1 the other discrete in A.1 . Hence both models are run where the parameters are fixed  $r = 3, K = 1$  and

the start point  $X = 0.5$ . The left figure of A.1 explains the dynamics meanwhile using equation A.1. Here the population density of  $X$  grows smoothly and continuously until being stabilising in value 1. The right figure in A.1. provides more dynamics that are complicated in discrete time. There is no growth among the time steps of the model, and the population density changes with the time by a jump between steps.

## **A.2 Pest Management**

### **A.2.1 What is a pest?**

A Pest is any damaging or troublesome being like as insect,an animal,a weed otherwise might be a disease etc [39].

### **A.2.2 What is a pesticide?**

A pesticide describes the treatment that is used for controlling the pest and/or exterminating the population of the pest [40].

#### **Goals of pest Management**

- Preventing: Keep pest societies bugs hidden [41] .
- Suppression: Minimising the pest population to reasonable amount [42].
- Eradication: Exterminating the pest completely [43].
- Avoidance: Trying to make the environmental atmosphere not favourable for the pest [44].

#### **What is Integrated Pest Management**

The idea of integrated pest management,an 'IPM' is facilitated use of features to minimise damage to a reasonable level that is justified with the control tactics. [42]

## pesticide Resistance

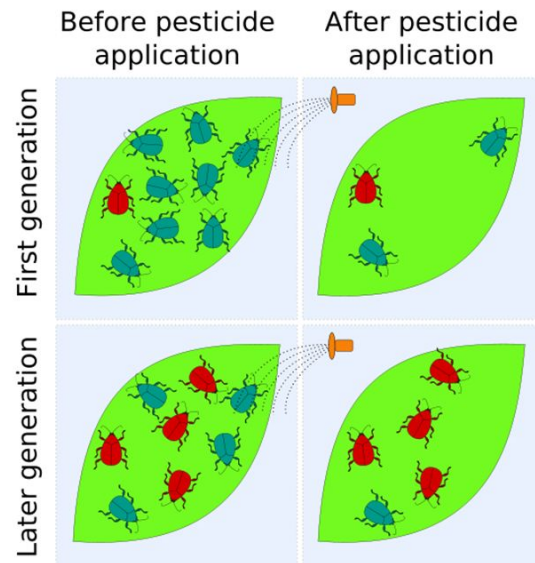


Figure A.2: individuals resistance Pesticide Credit [https://upload.wikimedia.org/wikipedia/commons/8/85/Pesticide\\_resistance.svg](https://upload.wikimedia.org/wikipedia/commons/8/85/Pesticide_resistance.svg).

An example of pesticide when applying a chemical one, there are some individuals have a genetic trait which gives them the allowance to avoid the pesticide for survival. The problem is shown when the reproduction' new generation' happens. The individual will inherit their ability to resist the pesticide. As long as the pesticide is kept applied frequently that leads to pest population sooner will be mostly is pesticide-resistant.

### A.3 Linearisation

In this part, consider linearisation of the system (A.3) around the equilibrium point to study the stability and check the topological of the neighbourhood behaviour around the steady states to

classify this fixed points with phase plane, a saddle, a node or a spiral. Consider the system:

$$\frac{du}{dt} = f(u, v) \text{ and } \frac{dv}{dt} = g(u, v) \quad (\text{A.3})$$

Since already shown above the steady state at  $(u_s, v_s)$  can be founded by solving  $f(u, v) = g(u, v) = 0$ . Setting  $\tilde{u} = u - u_s$  and  $\tilde{v} = v - v_s$  then, we can re arrange the system of two equations above and extending the right hand said terms as Taylor series.

$$\begin{aligned} \frac{d\tilde{u}}{dt} &= f_u \tilde{u} + f_v \tilde{v} \\ \frac{d\tilde{v}}{dt} &= g_u \tilde{u} + g_v \tilde{v} \end{aligned}$$

where,  $f_u$  described the partial derivative of  $u$  at  $(u_s, v_s)$ . In addition  $f_v$ ,  $g_u$  and  $g_v$  are the same of  $f_u$ . [45]

Expressing that in terms of matrices can be done as,

$$\frac{d}{dt} \begin{pmatrix} \tilde{u} \\ \tilde{v} \end{pmatrix} = \begin{pmatrix} f_u & f_v \\ g_u & g_v \end{pmatrix} \begin{pmatrix} \tilde{u} \\ \tilde{v} \end{pmatrix} = A \begin{pmatrix} \tilde{u} \\ \tilde{v} \end{pmatrix}$$

The stability matrix represented by  $A$ , which is called the Jacobian matrix. Sorting out the general solution for the linearised system above can be dealt with it by the next formula:

$$(\tilde{u}, \tilde{v}) \sim \alpha \underline{w}_1 e^{\lambda_1 t} + \beta \underline{w}_2 e^{\lambda_2 t}$$

Where  $\alpha$  and  $\beta$  are constants,  $\lambda_1$  and  $\lambda_2$  are the eigenvalues,  $\underline{w}_1$  and  $\underline{w}_2$  are the eigenvectors for  $A$ . The Steady state can be classified under conditions to be weather stable or unstable. if the system at the steady state is stable that means the solution decrease in time that happens at  $Re\lambda_1 < 0$  AND  $Re\lambda_2 < 0$ . In the other hand if the system is unstable at the steady state that means the solution increase under these two conditions:  $Re\lambda_1 > 0$  AND/OR  $Re\lambda_2 > 0$ . For instant and

more simplicity assume

$$A = \begin{pmatrix} a & b \\ c & d \end{pmatrix} \text{ then, } Tr(A) = a + d \text{ and } Det(A) = ad - bc$$

Eigenvalues for A, can be founded by the characteristic polynomial of A, which as follow:

$$\lambda^2 - (a + d)\lambda + ad - cb = 0$$

Hence we have  $Tr(A) = a + d$  and  $Det(A) = ad - cb$  that leads to,

$$\lambda_{1,2} = \frac{1}{2} \left( Tr(A) \pm \sqrt{(Tr(A))^2 - 4Det(A)} \right)$$

To finalise that and summarise it in three points and to show the all the situations and meaning of classification of the points. [10]

- Stable (node of focus)  $\Leftrightarrow Det(A) > 0$  and  $Tr(A) < 0$ .
- Unstable (Node of focus)  $\Leftrightarrow Det(A) > 0$  and  $Tr(A) > 0$ .
- Unstable (Saddle)  $\Leftrightarrow Det(A) < 0$ .

Here is a picture of the classifications by Murray in appendix A.

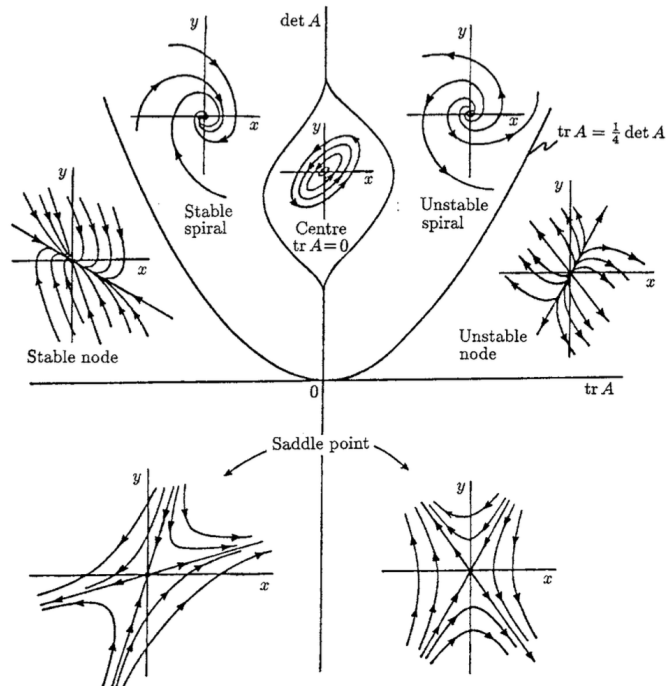


**Figure A.2.** Summary diagram showing how  $\text{tr } A$  and  $\det A$ , where  $A$  is the linearisation matrix given by (A.4), determine the type of phase plane singularity for (A.1). Here  $\det A = f_x g_y - f_y g_x$ ,  $\text{tr } A = f_x + g_y$ , where the partial derivatives are evaluated at the singularities, the solutions of  $f(x, y) = g(x, y) = 0$ .

Figure A.3: An explanation about the phase plane analysis within the linearisation shows above.

## A.4 High dimensional simulation For Bifurcation algorithms

In this section we used high dimensional simulation for the adaptive controllers 4.4, 4.8 and 4.13.

$$M_9 = \begin{pmatrix} 9 & 1 & 4 & 4 & 2 & 3 & 3 & 2 & 2 \\ 4 & -24 & 4 & 4 & 2 & 4 & 2 & 4 & 2 \\ 4 & 3 & -27 & 2 & 2 & 2 & 3 & 1 & 2 \\ 3 & 3 & 1 & -26 & 3 & 3 & 3 & 4 & 3 \\ 2 & 2 & 3 & 1 & -27 & 3 & 1 & 2 & 3 \\ 1 & 1 & 3 & 2 & 1 & -27 & 3 & 2 & 4 \\ 3 & 2 & 1 & 2 & 3 & 1 & -27 & 2 & 4 \\ 3 & 1 & 3 & 2 & 3 & 2 & 3 & -25 & 2 \\ 2 & 2 & 4 & 4 & 1 & 1 & 3 & 2 & -27 \end{pmatrix};$$

$$M_{13} = \begin{pmatrix} 1 & 4 & 1 & 3 & 2 & 3 & 1 & 1 & 4 & 1 & 2 & 3 & 1 \\ 3 & -34 & 1 & 3 & 2 & 3 & 4 & 1 & 1 & 3 & 4 & 4 & 2 \\ 4 & 2 & -31 & 2 & 4 & 2 & 2 & 2 & 4 & 4 & 1 & 2 & 3 \\ 3 & 1 & 2 & -33 & 3 & 3 & 2 & 3 & 3 & 2 & 4 & 1 & 1 \\ 4 & 3 & 1 & 3 & -34 & 4 & 3 & 1 & 3 & 3 & 3 & 4 & 3 \\ 1 & 3 & 1 & 1 & 4 & -33 & 1 & 4 & 4 & 1 & 3 & 2 & 1 \\ 2 & 1 & 4 & 1 & 2 & 1 & -34 & 3 & 4 & 2 & 4 & 2 & 4 \\ 2 & 1 & 4 & 2 & 1 & 2 & 1 & -33 & 2 & 1 & 3 & 2 & 3 \\ 3 & 2 & 3 & 3 & 4 & 2 & 1 & 4 & -34 & 1 & 1 & 2 & 2 \\ 1 & 2 & 1 & 3 & 1 & 2 & 4 & 2 & 1 & -33 & 4 & 4 & 1 \\ 1 & 1 & 2 & 1 & 3 & 3 & 1 & 4 & 4 & 2 & -31 & 1 & 4 \\ 2 & 4 & 2 & 4 & 4 & 3 & 4 & 2 & 2 & 1 & 2 & -32 & 3 \\ 1 & 3 & 1 & 4 & 3 & 2 & 3 & 4 & 2 & 3 & 2 & 4 & -31 \end{pmatrix}. \quad (\text{A.4})$$

$$M_{15} = \begin{pmatrix} 9 & 3 & 2 & 1 & 1 & 3 & 3 & 2 & 2 & 2 & 1 & 1 & 1 & 3 & 1 \\ 1 & -39 & 4 & 1 & 2 & 4 & 2 & 1 & 2 & 2 & 4 & 1 & 4 & 1 & 1 \\ 1 & 4 & -39 & 3 & 4 & 3 & 4 & 4 & 3 & 2 & 1 & 3 & 4 & 4 & 1 \\ 3 & 1 & 1 & -40 & 1 & 2 & 4 & 2 & 2 & 2 & 1 & 1 & 1 & 3 & 2 \\ 3 & 2 & 3 & 4 & -38 & 3 & 1 & 1 & 1 & 3 & 2 & 2 & 4 & 4 & 4 \\ 3 & 1 & 3 & 4 & 4 & -40 & 2 & 1 & 4 & 2 & 3 & 4 & 4 & 1 & 2 \\ 3 & 4 & 4 & 2 & 3 & 1 & -37 & 1 & 3 & 1 & 2 & 1 & 2 & 4 & 3 \\ 4 & 2 & 1 & 2 & 4 & 1 & 1 & -40 & 3 & 3 & 4 & 4 & 1 & 2 & 2 \\ 2 & 1 & 4 & 1 & 2 & 4 & 4 & 4 & -39 & 2 & 1 & 1 & 1 & 1 & 4 \\ 1 & 1 & 2 & 2 & 3 & 1 & 1 & 2 & 1 & -37 & 4 & 2 & 1 & 4 & 4 \\ 1 & 1 & 4 & 2 & 4 & 3 & 4 & 3 & 4 & 2 & -38 & 4 & 4 & 3 & 1 \\ 3 & 4 & 4 & 2 & 1 & 1 & 3 & 4 & 2 & 2 & 3 & -39 & 2 & 2 & 1 \\ 3 & 1 & 3 & 3 & 4 & 3 & 4 & 1 & 3 & 3 & 1 & 1 & -37 & 3 & 3 \\ 1 & 4 & 1 & 4 & 1 & 3 & 4 & 3 & 3 & 3 & 1 & 3 & 1 & -39 & 2 \\ 2 & 2 & 1 & 3 & 2 & 3 & 1 & 2 & 4 & 4 & 3 & 3 & 3 & 1 & -40 \end{pmatrix} .$$

(A.5)

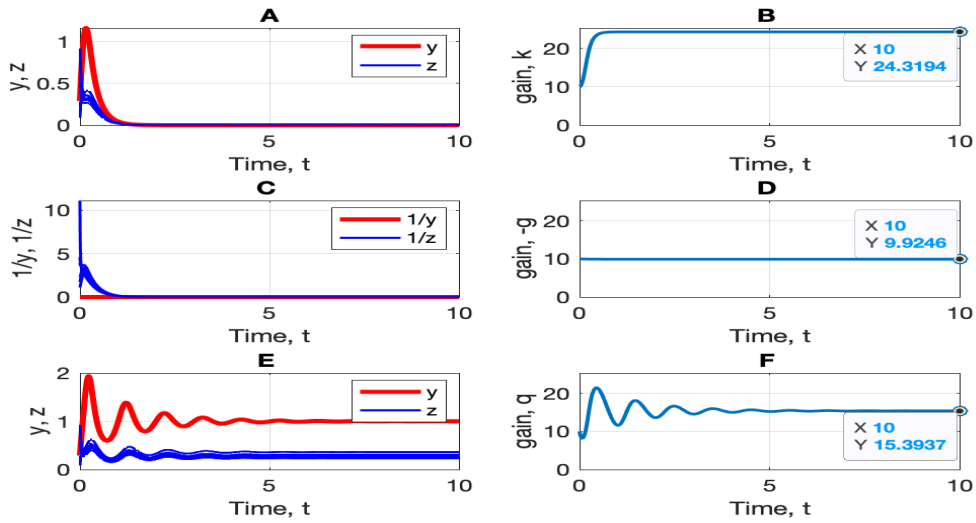


Figure A.4: 9 -dimensional simulation for the adaptive controllers 4.4, A and B, 4.8, C and D, 4.13, E and F. A matrix given by  $M_9$  in (4.16).

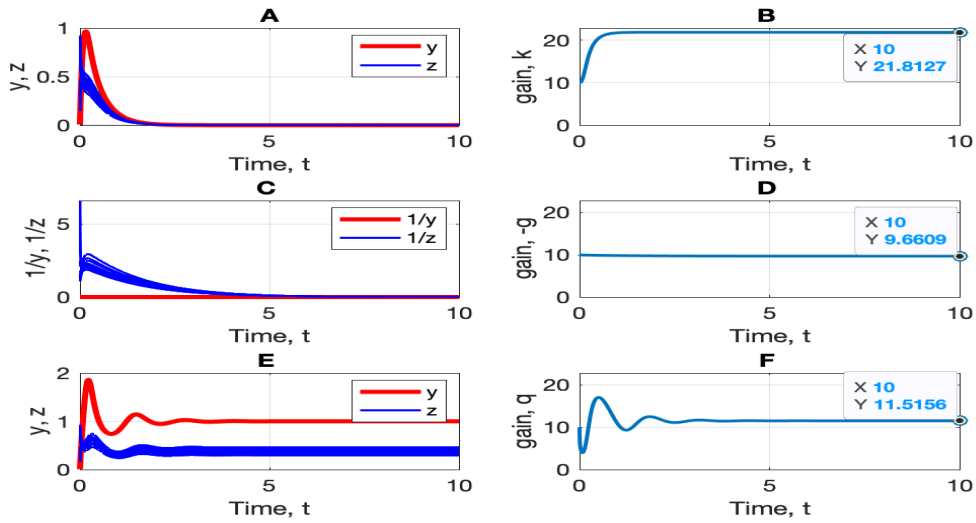


Figure A.5: 13 -dimensional simulation for the adaptive controllers 4.4, A and B, 4.8, C and D, 4.13, E and F. A matrix given by  $M_{13}$  in (4.16).

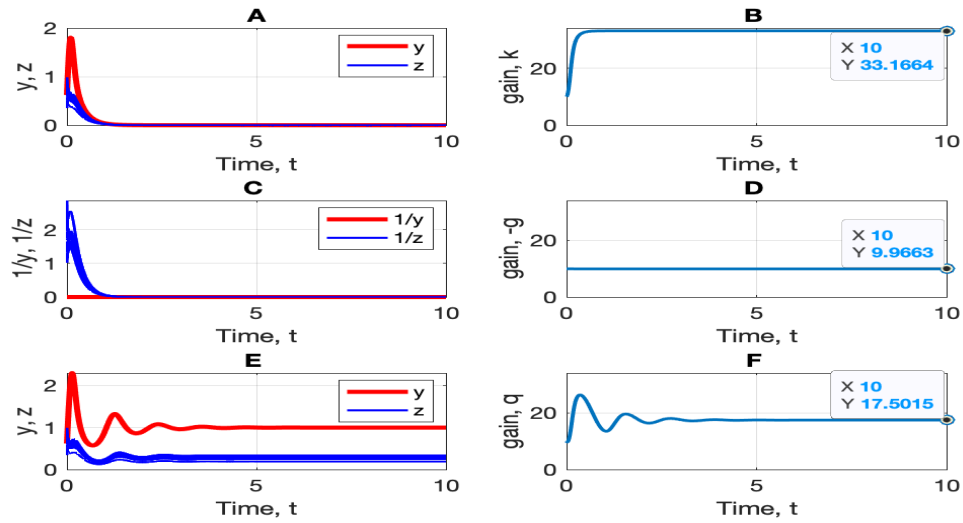


Figure A.6: 15 -dimensional simulation for the adaptive controllers 4.4, A and B, 4.8, C and D, 4.13, E and F. A matrix given by  $M_{15}$  in (A.5).

Matrices	$k_{\infty}(x_0)$	$-g_{\infty}(x_0)$	$q_{\infty}(x_0)$	$k_c$
$M_9$	24.3194	9.9246	15.3973	15.3973
$M_{13}$	21.8127	9.6609	11.5156	11.5156
$M_{15}$	33.1664	9.9663	17.5015	17.5015

Table A.1: The values of  $k_{\infty}(x_0)$ ,  $-g_{\infty}(x_0)$ ,  $q_{\infty}(x_0)$  and  $k_c$ . Resulting of 4.17.

# Bibliography

- [1] Chris Guiver, Christina Edholm, Yu Jin, Markus Mueller, Jim Powell, Richard Rebarber, Brigitte Tenhumberg, and Stuart Townley. Simple adaptive control for positive linear systems with applications to pest management. *SIAM Journal on Applied Mathematics*, 76(1):238–275, 2016.
- [2] Sebastian J Schreiber, Reinhard Bürger, and Daniel I Bolnick. The community effects of phenotypic and genetic variation within a predator population. *Ecology*, 92(8):1582–1593, 2011.
- [3] Gerhard Kreisselmeier and Brian Anderson. Robust model reference adaptive control. *IEEE Transactions on Automatic Control*, 31(2):127–133, 1986.
- [4] Belinda Barnes and G R Fulford. *Mathematical modelling with case studies: a differential equations approach using Maple and MATLAB*. Chapman and Hall/CRC, 2011.
- [5] Andrej Fischer, Ignacio Vázquez-García, and Ville Mustonen. The value of monitoring to control evolving populations. *Proceedings of the National Academy of Sciences*, 112(4):1007–1012, 2015.

- [6] Lance Gunderson and Stephen S Light. Adaptive management and adaptive governance in the everglades ecosystem. *Policy Sciences*, 39(4):323–334, 2006.
- [7] Pooja D Gupta and Tannaz J Birdi. Development of botanicals to combat antibiotic resistance. *Journal of Ayurveda and integrative medicine*, 8(4):266–275, 2017.
- [8] Christopher I Byrnes and Jan C Willems. Adaptive stabilization of multivariable linear systems. In *The 23rd IEEE conference on decision and control*, pages 1574–1577. IEEE, 1984.
- [9] Gennady A Leonov. *Mathematical problems of control theory: an introduction*, volume 6. World Scientific, 2001.
- [10] James D Murray. Mathematical biology: I. an introduction. interdisciplinary applied mathematics. *Mathematical Biology*, Springer, 17, 2002.
- [11] Nicolas Bacaër. *A short history of mathematical population dynamics*. Springer Science & Business Media, 2011.
- [12] Jeffrey L Edmunds. Multiple attractors in a discrete competition model. *Theoretical population biology*, 72(3):379–388, 2007.
- [13] Garrett Hardin. The competitive exclusion principle: An idea that took a century to be born has implications in ecology, economics, and genetics. *science*, 131(3409):1292–1297, 1960.
- [14] Robert MacArthur and Richard Levins. The limiting similarity, convergence, and divergence of coexisting species. *The american naturalist*, 101(921):377–385, 1967.

- [15] Jonathan M Chase, Peter A Abrams, James P Grover, Sebastian Diehl, Peter Chesson, Robert D Holt, Shane A Richards, Roger M Nisbet, and Ted J Case. The interaction between predation and competition: a review and synthesis. *Ecology letters*, 5(2):302–315, 2002.
- [16] O. Gilad. Competition and competition models. In Sven Erik Jørgensen and Brian D. Fath, editors, *Encyclopedia of Ecology*, pages 707–712. Academic Press, Oxford, 2008.
- [17] Michael Begon and Colin R Townsend. *Ecology: from individuals to ecosystems*. John Wiley & Sons, 2020.
- [18] K.C. Burns and P.J. Lester. Competition and coexistence in model populations. In Sven Erik Jørgensen and Brian D. Fath, editors, *Encyclopedia of Ecology*, pages 701–707. Academic Press, Oxford, 2008.
- [19] Hal Caswell. Matrix population models. *Encyclopedia of Environmetrics*, 3, 2006.
- [20] Karl J Åström and Björn Wittenmark. *Adaptive control*. Courier Corporation, 2013.
- [21] Achim Ilchmann. *Non-identifier-based high-gain adaptive control*. Springer Berlin, Heidelberg, 1993.
- [22] Nhan T Nguyen. Model-reference adaptive control. In *Model-Reference Adaptive Control*, pages 83–123. Springer, 2018.
- [23] H Charles J Godfray and Tara Garnett. Food security and sustainable intensification. *Philosophical transactions of the Royal Society B: biological sciences*, 369(1639):20120273, 2014.

- [24] Daniel Franco, Chris Guiver, Phoebe Smith, and Stuart Townley. A switching feedback control approach for persistence of managed resources. *Discrete and Continuous Dynamical Systems - B*, 27(3):1765–1787, 2022.
- [25] Miroslav Krstic. Invariant manifolds and asymptotic properties of adaptive nonlinear stabilizers. *IEEE Transactions on Automatic Control*, 41(6):817–829, 1996.
- [26] Stuart Townley. An example of a globally stabilizing adaptive controller with a generically destabilizing parameter estimate. *IEEE Transactions on Automatic Control*, 44(11):2238–2241, 1999.
- [27] GR Rokni Lamooki, Stuart Townley, and Hinke M Osinga. Bifurcations and limit dynamics in adaptive control systems. *International Journal of Bifurcation and Chaos*, 15(05):1641–1664, 2005.
- [28] Stuart Townley. Topological aspects of universal adaptive stabilization. *SIAM journal on control and optimization*, 34(3):1044–1070, 1996.
- [29] Adam Bill, Chris Guiver, Hartmut Logemann, and Stuart Townley. Stability of nonnegative lur’e systems. *SIAM Journal on Control and Optimization*, 54(3):1176–1211, 2016.
- [30] Robert Shorten and Kumpati S Narendra. On a theorem of redheffer concerning diagonal stability. *Linear algebra and its applications*, 431(12):2317–2329, 2009.
- [31] B Wayne Bequette. *Process control: modeling, design, and simulation*. Prentice Hall Professional, 2003.
- [32] Hartmut Logemann and Stuart Townley. Low-gain control of uncertain regular linear systems. *SIAM journal on control and optimization*, 35(1):78–116, 1997.

- [33] Bruce A Francis and Walter Murray Wonham. The internal model principle of control theory. *Automatica*, 12(5):457–465, 1976.
- [34] Jitka Polechová and David Storch. Ecological niche. *Encyclopedia of ecology*, 2:1088–1097, 2008.
- [35] Aldo Rescigno and Irvin W Richardson. On the competitive exclusion principle. *The bulletin of mathematical biophysics*, 27:85–89, 1965.
- [36] Steven Smith. *Digital signal processing: a practical guide for engineers and scientists*. Elsevier, 2013.
- [37] Richard L. Wyman. *Bios*, 56(4):236–238, 1985.
- [38] Gary William Flake. *The computational beauty of nature: Computer explorations of fractals, chaos, complex systems, and adaptation*. MIT press, 1998.
- [39] Shahamat U Khan. *Pesticides in the soil environment*. Elsevier, 2016.
- [40] Isra Mahmood, Sameen Imadi, Kanwal Shazadi, Alvina Gul, and Khalid Hakeem. *Effects of Pesticides on Environment*. 12 2015.
- [41] David Dent. *Insect pest management*. Cabi, 2000.
- [42] Marcos Kogan. Integrated pest management: historical perspectives and contemporary developments. *Annual review of entomology*, 43(1):243–270, 1998.
- [43] Aurelio Ciancio and KG Mukerji. *Integrated management of arthropod pests and insect borne diseases*, volume 5. Springer Science & Business Media, 2010.
- [44] Cyril Ehi-Eromosele. *Integrated Pest Management*, pages 105–115. 02 2013.

[45] John Michael Tutiil Thompson and H Bruce Stewart. *Nonlinear dynamics and chaos*. John Wiley & Sons, 2002.